

**Reevaluation of the *Ouranopithecus macedoniensis*
paradigm, using Virtual Anthropology and Geometric
Morphometrics**

Melania Ioannidou

Dissertation



Tübingen, 2021

[Artwork by © William Daniel Snyder]

Reevaluation of the *Ouranopithecus macedoniensis* paradigm, using Virtual Anthropology and Geometric Morphometrics

Dissertation

der Mathematisch-Naturwissenschaftlichen Fakultät
der Eberhard Karls Universität Tübingen
zur Erlangung des Grades eines
Doktors der Naturwissenschaften
(Dr. rer. nat.)

vorgelegt von

Melania Ioannidou

aus Thessaloniki, Griechenland

Tübingen

2021

Gedruckt mit Genehmigung der Mathematisch-Naturwissenschaftlichen Fakultät der
Eberhard Karls Universität Tübingen.

Tag der mündlichen Qualifikation:

21.07.2021

Dekan:

Prof. Dr. Thilo Stehle

1. Berichterstatterin:

Prof. Dr. Katerina Harvati

2. Berichterstatter:

Prof. Dr. Christopher Miller

To my grandfather & aunt

Table of Contents

Acknowledgments	xi
Abstract.....	xiii
Zusammenfassung.....	xv
List of Abbreviations.....	xvii
List of Figures	xviii
List of Tables.....	xxiii
CHAPTER 1	1
1 Introduction	3
1.1 Introducing the Hominoids	4
1.1.1 Definitions	4
1.1.2 Extant great apes	4
1.1.3 Miocene hominoids.....	6
1.2 <i>Ouranopithecus macedoniensis</i>	9
1.2.1 History of the fossiliferous sites (Northern Greece).....	9
1.2.2 Findings of <i>Ouranopithecus macedoniensis</i>	10
1.2.3 Stratigraphy and dating of the localities.....	12
1.2.4 Paleoenvironment and paleodiet.....	14
1.2.5 Characteristics of <i>O. macedoniensis</i>	14
1.2.6 The place of <i>O. macedoniensis</i>	16
1.2.7 Beyond <i>O. macedoniensis</i>	17
1.3 Objectives and research questions.....	18
CHAPTER 2	23
2 Materials and Methods.....	25
2.1 Comparative Sample.....	25
2.2 Methodology	25
CHAPTER 3	29
3.1 Introduction	33
3.2 Materials and Methods	33
3.3 Results.....	43
3.4 Discussion	53
Supplementary Material.....	63
CHAPTER 4	69
4.1 Introduction	74
4.2 Materials and Methods	75
4.3 Results.....	82
4.4 Discussion	94
Supplementary Material.....	105
CHAPTER 5	109
5.1 Introduction	113
5.2 Materials and Methods	115
5.3 Results.....	117
5.4 Discussion	127
Supplementary Material.....	135

CHAPTER 6	139
6 General discussion	141
6.1 Key results and discussion	141
6.1.1 Study 1	141
6.1.2 Study 2	143
6.1.3 Study 3	145
6.2 Concluding remarks and future perspectives	148
REFERENCES	153
APPENDICES	169
DECLARATION	171

Acknowledgments

First and foremost, I would like to thank my supervisors, Prof. Katerina Harvati (University of Tübingen) and Prof. George Koufos (Aristotle University of Thessaloniki), for their tremendous support during my PhD journey. I want to express my deepest gratitude for your guidance, patience and for giving me the opportunity to work on such important fossil material. Your work, each of you in your field, has been an inspiration for me, and I feel honored working with you. Σας ευχαριστώ πολύ και τους δύο από καρδιάς. Moreover, I would like to thank Prof. Louis de Bonis (University of Poitiers) for his help and support during these years. You are always so kind to me. Merci beaucoup. A huge thank you to my EVEREST committee, Prof. Christopher Miller (University of Tübingen) and Dr. Nils Anthes (University of Tübingen), for their help and fruitful discussions during our TAC meetings. Your insights were valuable, thank you!

Further thanks go to the following persons and institutions that provided access to comparative sample: Dr. C. Hemm and Dr. O. Kullmer, Senckenberg Museum of Natural History in Frankfurt; Dr. S. Merker and C. Leidenroth, Natural History Museum in Stuttgart; Prof. D. Begun and K. Pitiri, University of Toronto; Prof. M. Brunet, Dr. F. Guy, and Dr. D. Neaux, University of Poitiers; Dr. K. Helgen and Dr. M. Tocheri, Smithsonian National Museum of Natural History in Washington, D.C.; Prof. N. Lynnerup, University of Copenhagen; Dr. F. Mayer and C. Funk, Museum für Naturkunde - Leibniz Institute for Evolution and Biodiversity Science in Berlin; and Prof. E. Delson, City University of New York.

I also want to thank ALL my colleagues at INA who helped me through these years. A big thank you to the awesome girls of room 519 (Annabelle, Judith, Laura, and Nina) for their support and friendship. You were always there to help me not only with proofreading my manuscripts or with German bureaucracy, but also listening to my drama(s) almost every day! Special thanks to Caro and Laura for their help, especially during the last steps of my PhD. You are both amazing! Thanks to the statistics freaks Alexandros, Abel, and (again) Caro for their help when I felt lost with R or SPSS or just numbers... I don't want to continue naming, as I think each of you - people of the Paleoanthropology group - have a special place in my heart. However, I should thank Karin Kießling and Dr. Monica Doll for the countless times you both saved me from the German bureaucracy or "emergency" situations.

Herzlichen Dank an euch beide. I would also like to thank William D. Snyder for his wonderful artwork on the cover of my dissertation.

Special thanks to my besties from Thessaloniki/Tübingen/Jena/Berlin/Greifswald/the US (you all know who you are!) for your endless support and love. Thank you, ευχαριστώ, mulțumesc, Danke, teşekkürler, gracias...Also, I cannot thank enough my boyfriend, Atheer, for his understanding. You gave me so much power to continue doing what I love! Moreover, I want to thank Katerina and Lucia for their much appreciated help during the writing process of this dissertation. Saying thank you is not enough - I am grateful for your efforts!

Last but not least, I would like to thank my family, especially my mom, my dad, and my sister, for all the love and support. You always believed in me (well, Despoina, you are always yanking my chain, but I know you love me)! Thank you for letting me follow my dream. How can I not mention my beloved grandparents, Despoina and Achilleas, for their unconditional love... Grandpa, I may have lost you recently, but I know that you are still my number one fan. You were telling everybody that your granddaughter is working with "rocks" and you were so proud of me. This dissertation is dedicated to you. This dissertation is also dedicated to my beloved aunt, Theodora, whom we have unexpectedly lost recently. I promise to make you both proud. Please, keep an eye on me and guide me through life. I always remember your words and have them close to my heart.

Abstract

Ouranopithecus macedoniensis from Greece belongs to the hominoids that flourished during the Miocene epoch (~23-6 Ma) in Africa and Eurasia. The hominoids are our distant relatives, and their emergence represents the beginning of the long path that led to humans. Although their appearance was plentiful, their fossil record is fragmentary and scarce.

This dissertation aims to reconstruct and analyze fragmentary fossil specimens belonging to *O. macedoniensis* and explore craniodental similarities (or dissimilarities) between this Miocene ape and primarily extant great apes. Research questions addressed in this dissertation include: (1) What are the morphological affinities of the reconstructed facial area of *O. macedoniensis* in relation to the extant great apes?, (2) Does male-female mandibular shape vary within *O. macedoniensis*?, (3) How do mandibular shape, size, and sexual dimorphism in *O. macedoniensis* compare to the extant great apes?, and (4) Is the study of the internal root morphology the key to resolving the debatable phylogenetic position of *O. macedoniensis*?. These research questions are explored by applying virtual techniques and utilizing advanced statistical analyses.

Study 1 presents the virtual reconstruction of the facial anatomy of *O. macedoniensis*, that of the XIR-1 cranium and RPI-128 maxilla; the only cranial fossils found heretofore belonging to this species. This study aimed to quantify, using advanced geometric morphometrics, shape variation between the virtual reconstructions of *O. macedoniensis* and a comparative sample of other fossil hominoids, extant great apes (*Gorilla*, *Pan*, and *Pongo*), and humans. The results showed that *O. macedoniensis* groups phenetically with *Gorilla*, rather than *Pan*, *Pongo*, or *Homo*. In the principal component analyses, *O. macedoniensis* falls within or close to the *Gorilla* convex hull. Both specimens, face and maxilla, are classified as *Gorilla* based on discriminant function analyses.

Study 2 presents the 3D analysis of four partial mandibles (RPI-54; 56; 75; 79) and a ramus (RPI-391) belonging to *O. macedoniensis*. This study aimed to explore mandibular shape similarities between *O. macedoniensis* and a comparative sample of extant great apes and assess mandibular shape variation and homogeneity within *O. macedoniensis*. Additionally, the degree of mandibular sexual dimorphism was explored in *O. macedoniensis* and

compared to that of extant great apes. The results indicated that mandibular shape could differentiate *O. macedoniensis* from the extant great apes, although it showed some shape similarities to the larger great apes (*Gorilla* and *Pongo*). The PCA results suggested that the male and female specimens of *O. macedoniensis* have mandibular shapes that are quite similar. The analyses of the Procrustes distances suggested, however, that there is more shape variation in *O. macedoniensis* than in the extant great apes. Moreover, the degree of sexual dimorphism in *O. macedoniensis* was found to be greater than in any of the great apes.

Study 3 is a case study and presents a 3D analysis of the mandibular dentition of *O. macedoniensis*. Two mandibular fragments (RPI-54 and 75) and an isolated lower molar (RPI-237) from this species are studied and compared with the literature. This study aims to observe and characterize the root morphology and length in the lower post-canine dentition of *O. macedoniensis*, and compare it to extant and extinct taxa (including *Graecopithecus freybergi*). The results showed that the lower dentition of the two mandibular specimens used exhibits a similar mandibular root morphology to each other, implying homogeneity in this species. *O. macedoniensis* shares several dental traits with the African great apes and *Pongo*. However, the results did not indicate a clear relationship of *O. macedoniensis* with any of the great apes in particular. Additionally, the results showed that *O. macedoniensis* differs from *G. freybergi* in the root and pulp canal configuration. This supports the hypothesis that *O. macedoniensis* is taxonomically distinct from *G. freybergi*.

This dissertation emphasizes the importance of applying advanced techniques in the investigation of the fragmentary fossil record. It also highlights the need for unity among people working on Miocene materials, providing more robust comparative analyses and offering more decisive findings on very debated specimens.

Zusammenfassung

Die Hominoidea, einschließlich der Art *Ouranopithecus macedoniensis* aus Griechenland, erlebten in Afrika und Europa eine Blütezeit während des Miozän (~23-6 Ma). Sie gehören zu unseren entfernten Verwandten und ihr in Erscheinung treten war der Beginn einer langen Evolutionslinie, die bis zu uns Menschen reicht. Obwohl die Hominoidea im Miozän sehr zahlreich waren, sind ihre Fossilien selten und stark fragmentiert.

Ziel dieser Doktorarbeit ist es fragmentarische Fossilien der miozänen Art *O. macedoniensis* zu rekonstruieren und diese in Bezug auf kraniale und dentale Gemeinsamkeiten (oder Unterschiede) mit vor allem rezenten Menschenaffen zu vergleichen. Dabei steht die folgenden vier Forschungsfragen im Focus: (1) Welche morphologischen Affinitäten weist der rekonstruierte Gesichtsbereich von *O. macedoniensis* im Vergleich zu rezenten Menschenaffen auf; (2) Gibt es geschlechtsspezifische Unterschiede in der Unterkieferform innerhalb von *O. macedoniensis*; (3) Wie verhalten sich Unterkieferform und -größe, sowie Geschlechtsdimorphismus am Unterkiefer im Vergleich zu rezenten Menschenaffen; und (4) Bildet die interne Morphologie der Zahnwurzeln im Unterkiefer einen Schlüssel, um die umstrittene phylogenetische Position von *O. macedoniensis* aufzuklären? Zur Beantwortung dieser Forschungsfragen wurden virtueller Techniken und höherer Statistik angewendet.

Die virtuelle Rekonstruktion der Gesichtsanatomie von *O. macedoniensis* bildeten den Schwerpunkt der ersten in dieser Doktorarbeit eingeschlossenen Studie. Dies geschah auf Basis der einzigen zwei bisher gefunden Gesichtsschädelteile, des XIR-1 Schädels und dem RPI-128 Oberkiefer. Mit Hilfe der geometrischen Morphometrie wurde die Form der beiden virtuell rekonstruierten mit der von anderen fossilen Hominoidea, rezenten Menschenaffen (*Gorilla*, *Pan* und *Pongo*) sowie Menschen verglichen. Die Ergebnisse gruppieren *O. macedoniensis* phänetisch näher zu *Gorilla* als zu *Pan*, *Pongo* oder *Homo*. In der Hauptkomponentenanalyse fällt *O. macedoniensis* entweder in die oder nahe der Variation von *Gorilla* und beide Individuen, Gesicht und Oberkiefer, werden mittels Diskriminanzanalyse als *Gorilla* klassifiziert.

In der zweiten Studie standen vier Unterkieferfragmente (RPI-54; 56; 75; 79) sowie ein Ramus mandibularis (RPI-391) der Art *O. macedoniensis* im Mittelpunkt. Deren

Unterkieferform wurde auf Gemeinsamkeiten und Unterschiede zu rezenten Menschenaffen sowie der Variation und Einheitlichkeit innerhalb von *O. macedoniensis* untersucht. Zusätzlich wurde der Grad des beobachteten Geschlechtsdimorphismus zwischen *O. macedoniensis* und rezenten Menschenaffen verglichen. Die Ergebnisse weisen darauf hin, dass die Unterkieferform *O. macedoniensis* von rezenten Menschenaffen unterscheidet, auch wenn einige Aspekte denen der größeren Menschenaffenarten (*Gorilla* und *Pongo*) ähneln. In der Hauptkomponentenanalyse weisen sowohl männliche als auch weibliche *O. macedoniensis* eine ähnliche Unterkieferform auf. Bei Betrachtung der Procrustes Distanzen zeigt *O. macedoniensis* eine größere Variation an Form und damit einhergehend einen größeren Grad an Geschlechtsdimorphismus auf als alle rezenten Menschenaffen.

Die dritte Studie ist eine Fallstudie über das untere Dauergebiss von *O. macedoniensis*. Zwei Unterkieferteilstücke (RPI-54 und 75) sowie ein einzelner Molar (RPI-237) wurden hierfür analysiert und zusätzlich mit veröffentlichtem Material verglichen. Ziel dieser Studie war die Beschreibung der internen Zahnwurzelmorphologie und -länge der kleinen und großen Backenzähne in *O. macedoniensis* und deren Vergleich zu rezenten und ausgestorbenen Taxa (inklusive *Graecopithecus freybergi*). Die zwei Unterkieferteilstücke weisen eine zueinander ähnliche Zahnwurzelmorphologie auf, was auf eine gewisse Homogenität in dieser Art hindeutet. In Relation zu den Menschenaffen waren keine Hinweise auf eine nähere Verwandtschaftsbeziehung zu einer der Arten erkennbar, jedoch teilt *O. macedoniensis* einige Zahnmerkmale mit afrikanischen Menschenaffen und *Pongo*. Darüber hinaus zeigen die Ergebnisse eine unterschiedliche Zahnwurzel- sowie Zahnwurzelkanalanordnung zwischen *O. macedoniensis* und *G. freybergi*, was die Hypothese zweier taxonomisch verschiedener Arten bekräftigt.

Diese Doktorarbeit unterstreicht die Wichtigkeit neuer und vor allem zerstörungsfreier Methoden bei der Erforschung fragmentarischer Fossilien zu verwenden. Darüber hinaus deutlich wie nötig die Zusammenarbeit von Wissenschaftlern, welche an Material aus dem Miozän arbeiten, deutlich. Nur so sind umfangreichere und robustere vergleichende Analysen möglich, die zu aussagekräftigen Ergebnissen über strittige Fossilien führen können.

List of Abbreviations

CT	Computed Tomography
DFA	Discriminant Function Analysis
DIT	Dytiko 2
DTK	Dytiko 1
DKO	Dytiko 3
GM	Geometric Morphometrics
Ma	Million Years
MN	Mammal Neogene
NKT	Nikiti
PC	Principal Component
PCA	Principal Component Analysis
PNT	Pentalofos
RPI	Ravin de la Pluie
PXM	Prochoma 1
RZ-1	Ravin des Zouaves
RZO	Ravin des Zouaves 5
VA	Virtual Anthropology
VAT	Vathylakkos 3
VLO	Vathylakkos 1
VTK	Vathylakkos 2
XIR-1	Xirochori 1
3D	Three Dimensions
4D	Four Dimensions

List of Figures

Chapter 1

- Fig. 1:** Basic phylogenetic tree of the great apes. After Brooks and McLennan, 2003. 5
- Fig. 2:** Examples of cladograms (simplified) supporting either an (a.) African or (b.) European origin of the hominine. Modified after Cote, 2004. 9
- Fig. 3:** The *O. macedoniensis* localities in northern Greece. 11
- Fig. 4:** Excavations in the PPI (a.) and XIR (b.) localities. Photographs by G.D. Koufos. 13
- Fig. 5:** Maxillary fragments (RPI-128, RPI-775, RPI-80) and partial mandibles (RPI-88, RPI-89, RPI-79) of *O. macedoniensis* from the RPI locality. Photographs by G. D. Koufos. 16

Chapter 3

- Fig. 1:** a. *O. macedoniensis* (XIR-1): face and maxilla with an almost complete dentition and b. *O. macedoniensis* (RPI-128): maxilla with an almost complete dentition. Photographs by G. D. Koufos. 35
- Fig. 2:** The 56 registered three-dimensional landmarks used in the analysis on a surface scan of a female *Pan troglodytes* cranium. 38
- Fig. 3:** PCA in shape space (full landmark dataset). PC 1 explains 55.93 % and PC 2 11.21 % of total variance. Convex hulls are drawn for *Homo* (purple for females and olive green for males), *Gorilla* (blue for females and brown for males), *Pan* (aqua blue for females and black for males) and *Pongo* (fuchsia for females and green for males). a: mean shape at the negative end of PC 1 in frontal and lateral view, b: mean shape at the positive end of PC 2 in frontal and lateral view, c: mean shape at the positive end of PC 1 in frontal and lateral view, d: mean shape at the negative end of PC 2 in frontal and lateral view. 45
- Fig. 4:** PCA in shape space including the RPI-128 maxilla (maxillary landmark dataset). PC 1 explains 46.85 % and PC 2 16.72 % of total variance. Convex hulls are drawn for *Homo*, *Gorilla*, *Pan* and *Pongo*. 47

- Fig. 5:** Correlation between the second PC and centroid size a. in full landmark dataset and b. in maxillary landmark dataset. Density ellipses are drawn for *Homo* (purple for females and olive green for males), *Gorilla* (blue for females and brown for males), *Pan* (aqua blue for females and black for males) and *Pongo* (fuchsia for females and green for males). 49
- Fig. 6:** Discriminant Function Analysis (DFA) using the first six components of shape space (full landmark dataset). Convex hulls are drawn for *Homo* (purple for females and olive green for males), *Gorilla* (blue for females and brown for males), *Pan* (aqua blue for females and black for males) and *Pongo* (fuchsia for females and green for males). 51
- Fig. 7:** Discriminant Function Analysis (DFA) using the first eight components of shape space (maxillary landmark dataset). Convex hulls are drawn for *Homo* (purple for females and olive green for males), *Gorilla* (blue for females and brown for males), *Pan* (aqua blue for females and black for males) and *Pongo* (fuchsia for females and green for males). 52
- Fig. S1:** The final result of the XIR-1 cranium reconstruction after merge in (a) frontal, (b) occipital, (c) right lateral, (d) left lateral, (e) basal view, and (f) superior view 63
- Fig. S2:** The final result of the RPI-128 maxilla reconstruction after merge in (a) frontal, (b) occipital, (c) right lateral, (d) left lateral, (e) basal view, and (f) superior view. 64
- Fig. S3:** PCA in shape space (full landmark dataset). PC 3 explains 7.39 % of total shape variation, while PC 4 explains 3.76 % of total shape variation. Convex hulls are drawn for *Homo*, *Gorilla*, *Pan* and *Pongo*. 65
- Fig. S4:** PCA in shape space including the RPI-128 maxilla (maxillary landmark dataset). PC 3 explains 5.80 % of total shape variation, while PC 4 explains 4.10 % of total shape variation. Convex hulls are drawn for *Homo*, *Gorilla*, *Pan* and *Pongo*. 66
- Fig. S5:** PCA in shape space, excluding the landmarks around the nasal area. PC 1 explains 57.39 % of total shape variation, while PC 2 explains 10.78 % of total shape variation. Convex hulls are drawn for *Homo*, *Gorilla*, *Pan* and *Pongo*. 67

Chapter 4

- Fig. 1:** The four *O. macedoniensis* partial mandibles (RPI-54, RPI-75, RPI-79 and RPI-56) and the RPI-391 ramus. Photographs by G. D. Koufos and M. Ioannidou. 76
- Fig. 2:** Three-dimensional (3D) landmarks used in the analysis, registered on a surface scan of a female *Pan troglodytes* mandible. a. corpus and symphysis (for the hemimandible analysis landmarks 1-3 and 12-20 were used); b. ramus. 79
- Fig. 3:** PCA results of the bilateral (a.) and hemimandible (b.) analyses in shape space: a. PC 1 (37.89 %) vs PC 2 (19.86 %). i-iv: Shape changes, in frontal and lateral view, for negative and positive extreme values associated with PC 1 (i. and ii.) and PC 2 (iii. and iv.); and b. PC 1 (32.61 %) vs PC 2 (18.06 %). Convex hulls for *Gorilla* - green circle; male (filled symbol), female (open symbol), *Pan* - red triangle; male (filled symbol), female (open symbol) and *Pongo* - blue square; male (filled symbol), female (open symbol). 85
- Fig. 4:** PCA results of the ramus dataset in shape space: PC 1 (51.42 %) vs PC 2 (17.82 %). i-iv: Shape changes, in lateral view, for negative and positive extreme values associated with PC 1 (i. and ii.) and PC 2 (iii. and iv.) 86
- Fig. 5:** Boxplots of the intra-specific Procrustes distances pairs of the great apes and *O. macedoniensis*, a. bilateral and b. hemimandible analyses. a: *Gorilla-Gorilla*, b: *Pongo-Pongo*, c: *Pan-Pan*, d: *Ouranopithecus-Ouranopithecus*. 88
- Fig. 6:** Distribution and density curve of pairwise intra-specific distances within species in extant great apes and *Ouranopithecus* (bilateral analysis). a. *Gorilla* and *Ouranopithecus*, b. *Pan* and *Ouranopithecus*, and c. *Pongo* and *Ouranopithecus*. 90
- Fig. 7:** Distribution and density curve of pairwise intra-specific distances within species in extant great apes and *Ouranopithecus* (hemimandible analysis). a. *Gorilla* and *Ouranopithecus*, b. *Pan* and *Ouranopithecus*, and c. *Pongo* and *Ouranopithecus*. 91
- Fig. 8:** Boxplots of the pairwise male-female centroid size differences of *Ouranopithecus macedoniensis* and each of the extant great apes, a. bilateral and b. hemimandible analyses. 93

Fig. S1: Boxplots of the male-female centroid size differences in *Ouranopithecus*, *Gorilla*, *Pan*, and *Pongo* (bilateral analysis) 105

Fig. S2: Boxplots of the male-female centroid size differences in *Ouranopithecus*, *Gorilla*, *Pan*, and *Pongo* (hemimandible analysis). 105

Chapter 5

Fig. 1: a. Partial mandible of the young adult female holotype of *Ouranopithecus macedoniensis* (RPI-54), b. Partial mandible of the male adult *O. macedoniensis* (RPI-75), and c. isolated first lower molar of *O. macedoniensis* (RPI-237). Photographs by G. D. Koufos. 116

Fig. 2: Box-plot diagrams comparing the absolute root lengths of the lower premolars (P_3 and P_4) of *Ouranopithecus macedoniensis*, extant great apes (*Gorilla gorilla*, *Pan troglodytes*, *Pongo pygmaeus*), *Homo sapiens*, and a few other Miocene hominoids/hominids: *Sahelanthropus tchadensis* (Emonet et al., 2014) and *Graecopithecus freybergi* (Fuss et al., 2017). a: *O. macedoniensis* – female, b: *O. macedoniensis* – male, c: *G. freybergi* – male, d: *S. tchadensis* – male, e: *P. pygmaeus* – female, f: *P. pygmaeus* – male, g: *G. gorilla* – female, h: *G. gorilla* – male, i: *P. troglodytes* – female, j: *P. troglodytes* – male, k: *H. sapiens* – female, l: *H. sapiens* – male. 120

Fig. 3: Box-plot diagrams comparing the absolute root lengths of the lower molars (M_1 and M_2) of *Ouranopithecus macedoniensis*, extant great apes (*Gorilla gorilla*, *Pan troglodytes*, *Pongo pygmaeus*), *Homo sapiens*, and a few other Miocene hominoids/hominids: *Sahelanthropus tchadensis* (only M_1 ; Emonet et al., 2014) and *Graecopithecus freybergi* (Fuss et al., 2017). a: *O. macedoniensis* – female, b: *O. macedoniensis* – male, c: *G. freybergi* – male, d: *S. tchadensis* – male, e: *P. pygmaeus* – female, f: *P. pygmaeus* – male, g: *G. gorilla* – female, h: *G. gorilla* – male, i: *P. troglodytes* – female, j: *P. troglodytes* – male, k: *H. sapiens* – female, l: *H. sapiens* – male. 121

Fig. 4: Virtual reconstructions of the *Ouranopithecus macedoniensis* specimens used in this study. a. RPI-54 (i. buccal view, ii. occlusal view), b. RPI-75 (i. buccal view, ii. occlusal view), and c. RPI-237 (i. buccal and ii. lingual view). 122

Fig. 5: Result of the virtual segmentation of the lower dentition of RPI-54 (right P_3 to M_2). i. lingual view, ii. buccal view, iii. occlusal view, and iv. ventral view. 124

- Fig. 6:** Result of the virtual segmentation of the lower dentition of RPI-75 (right P₃ and M₂, and left P₄) including the whole teeth and the subsequent isolation of the pulp canal. a. right P₃ b. left P₄ and c. right M₂. In all, a to c: i. lingual view, ii. buccal view, iii. occlusal view, and iv. ventral view. 125
- Fig. S1:** Cross-sectional depiction of the four canals present in the M₁ of RPI-75. 135
- Fig. S2:** Cross-sectional depiction of the P₄ of RPI-54, where it can be observed that the mesial pulp canals are entirely connected with a secondary dentine layer. 136
- Fig. S3:** Cross-sectional depiction of the P₄ of RPI-75, where it can be observed that the mesial pulp canals are entirely connected with a secondary dentine layer. 137

List of Tables

Chapter 3

Table 1:	List of fossils used for the comparative analysis.	37
Table 2:	Extant great apes and humans used in the analysis.	37
Table 3:	List of landmarks used for the comparative analysis.	39
Table 4:	Classification and cross validation results of the discriminant function analysis (full landmark dataset).	41
Table 5:	Classification and cross validation results of the discriminant function analysis (maxillary landmark dataset).	42
Table 6:	Mean Procrustes shape distances among <i>Ouranopithecus</i> specimen (XIR-1) and the represented extant taxa (full landmark dataset).	48
Table 7:	Mean Procrustes shape distances among <i>Ouranopithecus</i> specimen (XIR-1) and the represented extant taxa (maxillary landmark dataset).	48
Table 8:	Mean Procrustes shape distances among <i>Ouranopithecus</i> specimen (RPI-128) and the represented extant taxa (maxillary landmark dataset).	48
Table 9:	Classification and cross validation results of the discriminant function analysis (full landmark dataset).	51
Table 10:	Classification and cross validation results of the discriminant function analysis (maxillary landmark dataset).	52

Chapter 4

Table 1:	Number of extant great apes and <i>Ouranopithecus macedoniensis</i> fossils used in this study.	78
Table 2:	List of landmarks, definitions, and intra-observer error: bilateral and ramus analyses. For the hemimandible analysis the landmarks used are: 1-3 and 12-20.	81
Table 3:	Intra-specific distance statistics of <i>Ouranopithecus</i> and the extant great apes.	87

Table 4:	Inter-individual variability among <i>Ouranopithecus</i> and the extant great apes (one-way ANOVA).	87
Table 5:	Mean centroid sizes and results of independent-samples t-tests of males and females of the extant great apes and <i>O. macedoniensis</i> .	92
Table S1:	Values within the 95% probability interval – bilateral analysis.	106
Table S2:	Values within the 95% probability interval – hemimandible.	106
Table S3:	Procrustes distances between RPI-391 and the extant great apes used in this study – ramal analysis.	106
Table S4:	Number of pairwise M/F centroid size comparisons in the extant species that exceeded the values in <i>Ouranopithecus</i> .	107
 Chapter 5		
Table 1:	<i>Ouranopithecus macedoniensis</i> and other Miocene extinct species used in the study.	115
Table 2:	Dental root measurements of the lower dentition of the <i>Ouranopithecus macedoniensis</i> specimens used in this study.	118
Table 3:	RPI-54 - root and pulp canal configuration.	123
Table 4:	RPI-75 - root and pulp canal configuration.	123
Table 5:	Mandibular root and pulp canal number in <i>Ouranopithecus macedoniensis</i> and comparative sample.	126

CHAPTER 1

1 Introduction

The origin of the **hominoids**, our distant relatives, represents the start of the long path that led to us, humans. A big challenge that arises after a paleoanthropological discovery is the proper placement of any new fossil(s) to the already known fossil record. Understanding and reconstructing the phylogenetic relationships of the extinct groups with the extant ones is essential to solve the puzzles of the human lineage. However, our knowledge about the past is constantly changing due to discoveries and the reexamination of known fossils with improved techniques.

One of the most significant improvements nowadays is the growing knowledge and emergence of new technologies, e.g., the use of hyper-computers and specialized software programs that offer new approaches to studying the past. As a result of the scientific advancement, new fields of science develop, such as virtual anthropology (VA) and geometric morphometrics (GM). Virtual anthropology refers to the multidisciplinary perspective of analyzing morphology in three or four dimensions (3 or 4D), combining knowledge from different fields, including anthropology, paleontology, mathematics, and statistics (Weber et al., 2001; Weber and Bookstein, 2011; Weber, 2015). The power of virtual anthropology lies in the preservation of the geometry throughout analyses, access to internal anatomical regions, and reproducibility of carried out studies (Weber et al., 2001; Weber, 2015). Geometric morphometrics, specifically, refers to the advanced statistical and analytical analysis of form (shape and size) (Bookstein, 1991). During the last decades, GM has been used extensively in a variety of studies focused on taxonomy, ontogenetic variation, population history, and habitual behaviors (e.g., Rolf and Marcus; 1993; Nicholson and Harvati, 2006; von Cramon-Taubadel et al., 2007; Mitteroecker and Gunz, 2009; Karakostis et al., 2018; Harvati et al., 2019). Various digital imaging techniques, e.g., computed tomography (CT) and surface scanning, are needed for such studies. In this dissertation, a combination of virtual anthropology, advanced geometric morphometrics, and various scanning techniques was used to answer the research questions related to the much-discussed *Ouranopithecus macedoniensis* (cf. Chapter 1.3).

1.1 Introducing the Hominoids

1.1.1 Definitions

To this day, the usage of terms defining hominoids varies among authors. This variation can lead to misunderstandings and confusion. Therefore, the terminology used in this dissertation is outlined in detail in the following paragraph.

In a broad frame, **hominoids**, belonging to the superfamily **Hominoidea** (Gray, 1825), refer to Hylobatidae (gibbons), **great apes** (*Gorilla*, *Pan*, and *Pongo*), *Homo* and their ancestors. Under current conception, great apes and humans form the **Hominidae** or **hominids**, which can be further divided into two subfamilies: **Homininae** or **hominine** (*Gorilla*, *Pan*, and humans) and **Ponginae** (*Pongo*). *Gorilla* and *Pan* are also referred to as **African apes**, while **hominin** refers to humans and their ancestors (non-ape).

In the rest of this dissertation, I will focus on the **great apes** and the **Miocene hominoids**. When tracing the evolutionary path of a taxon, it is helpful to start from extant relatives and go back in time along with the (known) fossil record. Yet, having only the extant great apes as models restricts our image of what might have been present in the past, as variability (of any kind) could have been different (cf. Chapter 6). Nonetheless, studying various aspects of the extant great apes, such as morphology, systematics, and behavior, can help us better understand the extinct taxa, like *Ouranopithecus macedoniensis*.

1.1.2 Extant great apes

Great apes are our closest living relatives, although molecular and morphological studies have separated *Pongo* from *Gorilla*, *Pan*, and humans (e.g., Eastal and Hembert, 1997; Lockwood et al., 2002; Glazko and Nei, 2003; Fig. 1). Many efforts have been undertaken to estimate divergence times between the great apes and humans, while new sequencing techniques in recent years have provided updated insights into their history (e.g., Hobolth et al., 2011; Langenraber et al., 2012; Scally et al., 2012; Hara et al., 2012; Venn et al., 2014). Among African great apes, *Pan* is closest to humans, while *Gorilla* is more distant (Ruvolo, 1997; Diogo et al., 2017). Prüfer et al. (2012) suggest that almost 99 % of our genome is shared with *Pan*.

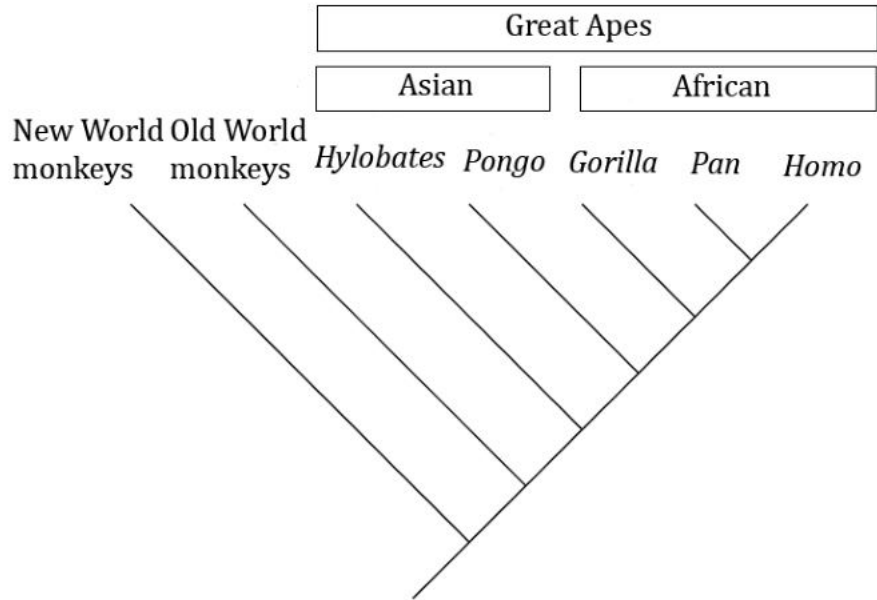


Fig. 1: Basic phylogenetic tree of the great apes. After Brooks and McLennan, 2003.

The genus *Pan* includes chimpanzees (*Pan troglodytes*) and bonobos (*Pan paniscus*), with the former occupying regions across central Africa and living in isolated populations, while the latter is limited to the forests of Congo (previously Zaire) (Grooves, 2001; Kulhwilm et al., 2016). The latest studies suggest a geological time of 6-9 million years ago (Ma) for the split between *Pan* and *Homo* (Hara et al., 2012; Moorjani et al., 2016). Besides *Pan*, *Gorilla* is primarily divided into two species, *Gorilla gorilla* (western gorillas) and *Gorilla beringei* (eastern gorillas). Western gorillas can be found mainly in the Congo basin, while eastern gorillas are found in Uganda, Rwanda, and the Democratic Republic of Congo (DCR; Schaller, 1963; Taylor and Grooves, 2003; Kulhwilm et al., 2016). The geological time of the divergence between *Gorilla* from *Pan-Homo* is proposed to be between 8-19 Ma (Wilkinson et al., 2011; Langenraber et al., 2012). In contrast to the other great apes, *Pongo* is the only genus found in Asia. It includes primarily two species, the Bornean (*Pongo pygmaeus*) and Sumatran (*Pongo abelii*) orangutans (Locke, 2011; Kulhwilm et al., 2016). Recent studies suggest a timeframe between 15-21 Ma for the last common ancestor of *Pongo* and the other great apes (Perelman et al., 2011; Schrago and Voloch, 2013).

1.1.3 Miocene hominoids

Based on the current fossil record, the African continent is the place of the origin of the Miocene hominoids. Until now, more than 35 species are known from Africa but and Eurasia (Fleagle, 2013; Harrison, 2010a; Andrews, 2020). Most scientists agree that the hominoids flourished during the Miocene epoch (roughly 23-6 Ma), during which many geological events took place, shaping the evolutionary rise and fall of the hominoids. Recent findings, however, showed that *Rukwapithecus fleaglei* from the Oligocene (~25 Ma), in Tanzania could be the earliest known (stem¹) hominoid found (Stevens et al., 2013).

The age of abundance of the hominoids starts in East Africa at around 20 Ma (Early Miocene) with the families of Proconsulidae, Afropithecidae, and Nyanzapithecidae (including among others the taxa *Proconsul*, *Ekembo*, *Afropithecus*, *Nyanzapithecus*) (Pilbeam, 1982a; Harrison, 2010a; Fleagle, 2013; McNulty et al., 2015; Nengo et al., 2017). These first (stem) hominoids preserved a primitive nasomaxillary morphology, which they share with later hominoids (Pilbeam, 1982a). In contrast, their primitive dental traits are not shared with later hominoids (Le Gros Clark and Leakey, 1950; Pilbeam, 2002). They were monkey-like arboreal climbers with variable size (varying from 3 to 80 kg) (Andrews, 2020 and ref. therein). They mostly lived in the forest or woodland environments, while in some larger species, a terrestrial behavior was observed (Andrews, 2020; Gilbert et al., 2020). Despite their abundance in East Africa, no evidence of early Miocene hominoids was found elsewhere.

It appears that in the middle Miocene (17-15 Ma), subtropical forest conditions were expanded, and along with other geological changes (such as the overcome of geographical barriers), set the stage for the radiation of the Miocene hominoids outside Africa. Thus, as the hominoids appeared all over Eurasia, their geographical expansion led to adaptation and speciation (de Bonis and Koufos, 2001; Alba, 2012; Begun, 2015), which lasted until the late

¹ The terms stem (basal) group and crown (modern) group are used to explain and classify the relationships of extant and extinct organisms.

Miocene (around 8 Ma). In Eurasia, among the first family taxa found was *Griphopithecus* in early middle Miocene deposits of Turkey and Central Europe (Germany and Slovakia) (Abel, 1903; Tekkaya, 1974; Casanovas-Vilar et al., 2011), while Kenyapithecidae were found in Western Africa (Pickford, 1985). There were many taxa present in the European region, during the middle to late Miocene, including *Dryopithecus*, *Pierolapithecus*, *Anoiapithecus*, and *Hispanopithecus* in Spain (Moyà-Solà and Köhler, 1993; Pose, 1993; Moyà-Solà et al., 2004); *Rudapithecus* in Hungary (Kordos and Begun, 2002); *Danuvius* in Germany (Böhme et al., 2019); *Ouranopithecus* and *Graecopithecus* in the Balkans and Turkey (von Koenigswald, 1972; de Bonis, 1974; Gülec et al., 2007). For some researchers, all the European taxa mentioned above are referred to as "dryopiths" (e.g., Alba, 2012; Begun, 2015; Almécija et al., 2021), while for others, the hominoids from the Balkans/Turkey should be considered separately (e.g., de Bonis and Koufos, 2001; Fuss et al., 2017). Despite this disagreement, the European taxa, in general, show several derived characters in cranial, dental and postcranial features with extant hominoids (e.g., Alba, 2012; Begun, 2015). Because of these derived characters, their phylogenetic implications are somewhat controversial. They are either treated as stem hominoids (e.g., Pilbeam, 1996), stem hominids (e.g., Alba, 2012; Kelley and Gao, 2012), or are considered closer to hominins (de Bonis et al., 1990; Fuss et al., 2017). Miocene taxa present in Asia, include among others: *Sivapithecus* and *Indopithecus* in India and Pakistan (Pilgrim, 1915; Pilbeam, 1982b); *Khoratpithecus* in Thailand and Myanmar (Chaimanee et al., 2006); *Ankarapithecus* in Turkey (Alpagut et al., 1996); and *Lufengpithecus* and *Gigantopithecus* in China (von Koenigswald, 1952; Xu et al., 1978). These Miocene Asian hominoids are hypothesized to be linked with orangutans; thus, they are also referred to as a family taxon of Pongidae (Harrison, 2010b; Zhang and Harrison, 2017; Chaimanee et al., 2019; Andrews, 2020). All the hominoids mentioned above were adapted taxa with monkey-like characteristics and mainly lived in woodland environments and higher terrestrial adaptations (Andrews, 2020).

Late Miocene hominoids found outside of Eurasia, and particularly in Africa, are scarce. These include *Samburupithecus* (Ishida and Pickford, 1997) and *Chororapithecus* (Suwa et al., 2007) from East Africa. Within the proposed timeframe of the emergence of the hominins (6-8 Ma) the African fossil record also includes: *Ardipithecus* from Ethiopia (White et al.,

1994), *Orrorin* from Kenya (Senut et al., 2001), and *Sahelanthropus* from Chad (Brunet et al., 2002). The characterization of the latter fossils as stem hominins is, however, questioned (e.g., Mongle et al., 2019; Macchiarelli et al., 2020).

The end of the late Miocene in Eurasia (around 8 Ma) was characterized by climatic changes due to a change in the oceanic currents in Europe on the one hand and the rising of the Himalayas in Asia on the other (Koufos, 2016; Gilbert, 2020). These climatic changes included drier conditions and the collapse of the subtropical forests all over Eurasia. Consequently, this dramatically decreased the number of hominoids and other mammals and led to a period of extinction (Cachel, 2015; Gilbert et al., 2020). The only exception within the hominoids – with the current data – is *Gigantopithecus*, who survived until the Pleistocene (Harrison et al., 2014; Zhang and Harrison, 2017).

The phylogenetic relationships of the Miocene hominoids among themselves and to extant taxa are complicated and remain a vigorously debated topic in Paleoanthropology (e.g., see Alba, 2012; Begun, 2015; Fuss et al., 2017; Almécija et al., 2021). The fossil hominoids from Asia (Pongidae), such as *Sivapithecus* and *Khoratpithecus*, share craniodental traits connecting them with *Pongo*, who also occupy the same continent (Pilbeam, 1982b; Chaimanee et al., 2006; Cachel, 2015). Tracing the ancestors of the African clade, meaning that of chimpanzees, gorillas, and the human lineage, is complicated because the fossil record of both *Pan* and *Gorilla* is practically unknown. On the one hand, McBrearty and Jablonski (2007) reported the first fossil specimens (teeth) attributed to *Pan* (ca. 0.5 Ma) in Kenya, while on the other hand, it was only recently suggested that *Chororapithecus* (dating to ca. 10-10.5 Ma) from Kenya could be related to the *Gorilla* lineage (Suwa et al., 2007). The origins of the African apes, and therefore the discussion about the emergence of **hominine**, can be summarized in two main hypotheses:

The African origin: The first hominoids emerged in Africa, followed by radiation in Europe and Asia (Fig. 2a). This radiation led to speciation in the European taxa and the rise of gibbons and pongidae in Asia (Andrews and Bernor, 1999; Cote, 2004). Most probably, a series of dispersals between Africa, Europe, and Asia took place during the middle-late Miocene, favored by climatic changes and the appearance of land bridges. Following this, the

African apes would have emerged from the African Miocene taxa (e.g., Coppens, 1994; Suwa et al., 2007), which cannot be directly inferred from the incomplete fossil record.

The European origin: This theory supports a European hominine origin (Fig. 2b), followed by later radiation in Africa (Begun, 2000; 2003; 2015). In this view, the hominoids emerged in Africa while they migrated to Eurasia in the middle Miocene, where they started to diversify until the late Miocene. Synchronously, African taxa became extinct, based on the fact that late Miocene fossils found in Africa are scarce. Therefore, the ancestor of hominine shall be found among the European hominoids present during the late Miocene.

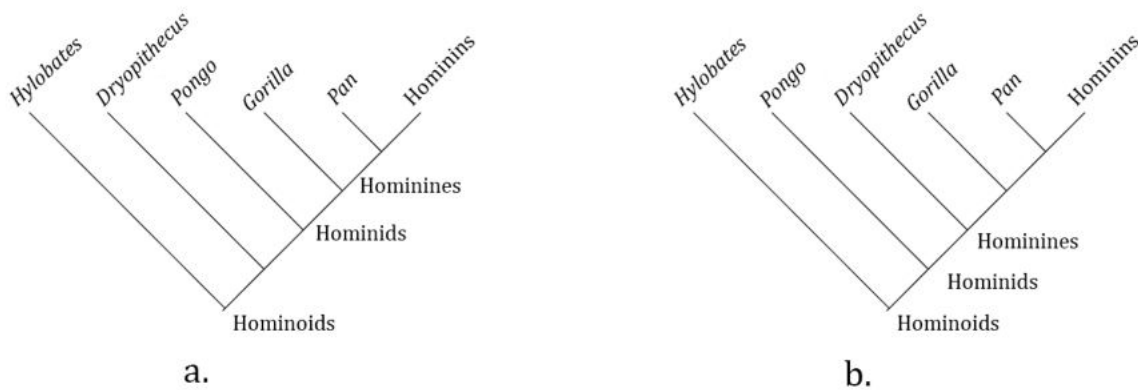


Fig. 2: Examples of cladograms (simplified) supporting either an (a.) African or (b.) European origin of the hominine. Modified after Cote, 2004.

These hypotheses are purely based on the occurrence or absence of late Miocene hominoids in Eurasia or Africa. The reality might have been even more complicated, with numerous dispersals from Africa to Eurasia and vice versa (Cote, 2004; Almécija et al., 2021). Our need to connect all the extinct taxa with extant may bias our understanding of the actual position of these extinct species. While they belong to the complex evolutionary tree that led to us, humans, we shall think of other alternative possibilities and consider more compounded scenarios than a direct connection from the past to the present.

1.2 *Ouranopithecus macedoniensis*

1.2.1 History of the fossiliferous sites (Northern Greece)

The hominoid *Ouranopithecus macedoniensis* was first documented in 1973 in the late Miocene deposits of the Axios Valley in Northern Greece (de Bonis, 1974). Interestingly, the

fossiliferous deposits of this region were discovered during the First World War (1915-1916), more than 100 years ago. The first mammal bones were found in the village of Diavata, 10 km away from Thessaloniki, where British soldiers were digging trenches in the region for military reasons. Without further investigations in situ, the mammal bones were sent to the British Museum and were studied and described by Andrews et al. (1918). During approximately the same period, French soldiers found fossils in bulk deposits, in an area close to the village Vathylakkos and in Axios valley, which is more than 35 km from Thessaloniki. Coincidentally, the military officer was Camille Arambourg, a paleontologist and later a Professor in the Natural History Museum Paris, who started to excavate the area around the Axios valley and found more material. In other regions close by, the excavations came to discover many other fossiliferous localities in Agionerion and Nea Messimvria villages and the western bank of Axios river near the village Dytiko (Arambourg and Piveteau, 1929). After their discovery, the collected fossil material was transferred first in Algeria and later in France and the Natural History Museum in Paris, studied there by Arambourg and Piveteau (1929). This collection of fossils, known as the "Arambourg collection", is still housed in Paris. After that time, the fossiliferous sites around the Axios valley were abandoned. It was only in 1973 where new excavation seasons were started by Aristotle University of Thessaloniki (Laboratory of Geology and Paleontology) and the University of Paris (Laboratory of the Vertebrate and Human Paleontology), which was later continued by the corresponding laboratory of the University of Poitiers. The continued investigation of the area provided numerous mammal localities, and a significant number of fossils have been unearthed. Among them was a hominoid, which was later named *Ouranopithecus macedoniensis* and was firstly found in the fossiliferous locality of Ravin de la Pluie (RPI).

1.2.2 Findings of *Ouranopithecus macedoniensis*

RPI-54 found in the PPI locality in 1973 is the type specimen of *Ouranopithecus macedoniensis*, a mandible of a late adolescent/young adult individual (de Bonis, 1974; Fig. 3). This specimen was published under the name *Dryopithecus macedoniensis* following Simons and Pilbeam (1965), who have published a systematic revision of the Miocene hominoids at that time. However, as additional material was found within the next few years

in the same locality, the new genus *Ouranopithecus* was introduced (de Bonis and Melentis, 1977).

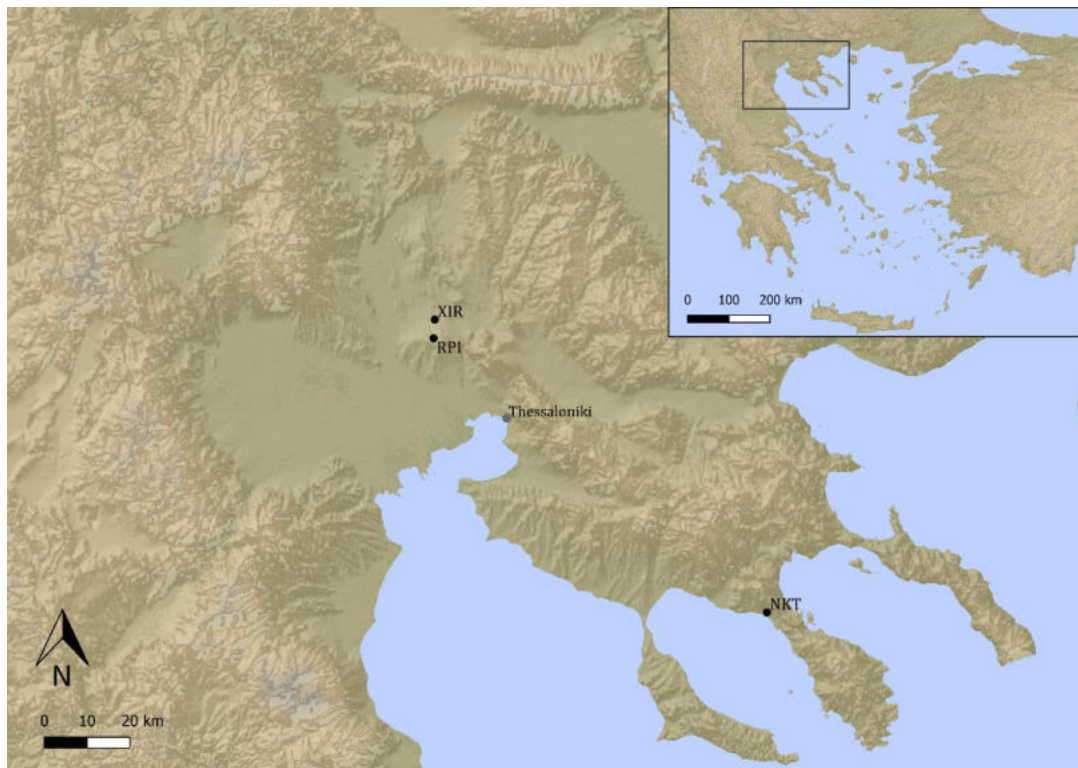


Fig. 3: The *O. macedoniensis* localities in northern Greece.

In 1989 excavations in a new locality, Xirochori 1 (XIR), near the homonymous village about 1.5 Km North of RPI, has brought into light the most important fossil of *Ouranopithecus macedoniensis*, an almost entire face (XIR-1; de Bonis et al., 1990; for a figure see page 35/ Chapter 3). Excavations in this locality were extremely demanding, as the matrix is hard, and the isolation of fossils was difficult. The following year a mandible and later a maxilla of a hominoid were discovered in the new locality Nikiti 1 (NKT), located near the village of Nikiti (Chalkidiki Peninsula), about 100 Km southeast of Thessaloniki (Koufos, 1993; 1995). These fossils were assigned to *Ouranopithecus macedoniensis* (Koufos, 1993; 1995). Continuing excavations have yielded several maxillary and mandibular remains of this hominoid, especially from RPI (de Bonis et al., 1998; Koufos and de Bonis, 2004; 2006); the postcranial remains, on the other hand, are limited and include only two phalanges (de Bonis and Koufos, 2014). In 2016, new isolated teeth of *O. macedoniensis* from the RPI locality were described (Koufos et al., 2016a).

1.2.3 Stratigraphy and dating of the localities

Fossils are significantly relying on their geological context, without which no proper interpretations can be made. As mentioned above, *Ouranopithecus macedoniensis* is currently known from three localities in Macedonia, Northern Greece: Ravin de la Pluie (RPI), and Xirochori (XIR) in Axios valley, and Nikiti-1 (NKT) in the Chalkidiki Peninsula (de Bonis and Koufos, 2001; Fig. 4). The localities of the Axios valley are situated in its lower part, a tectonic depression between the Serbo-Macedonian massif to the East and the Paikon mountains to the West (Mercier, 1973). The late Miocene deposits of Axios Valley are divided into three different formations (Fm): Nea Messimvria Fm, Vathylakkos Fm, and Dytiko Fm (de Bonis and Koufos, 2001), and they are lying unconformably on Mesozoic rocks (Mercier, 1973). The N. Messimvria Fm, the oldest one, outcrops in the eastern bank of Axios river, and it mainly consists of red sandstones mixed with pebbles and red clays (de Bonis and Koufos, 1993; 2001). This formation includes four main fossiliferous localities: Pentalofos 1 (PNT-1), Ravin de la Pluie (RPI), Xirochori 1 (XIR-1), and Ravin des Zouaves 1 (RZ-1). The localities RPI and XIR are situated in the upper part of this formation, while the faunal remains found to suggest a late Vallesian age (MN 10) for these levels (de Bonis and Koufos, 1993; 1994; Appendix I). However, the giraffid remains of XIR indicated that its fauna is more primitive than that of RPI (Koufos, 2013 and ref. therein). The magnetostratigraphic study of the two sections suggested an estimated age of ~9.6 Ma for XIR and ~9.3 Ma for RPI (Sen et al., 2000). Vathylakkos Fm is overlying N. Messimvria Fm and is mainly composed of sands of grey color, marls, and sandstones. Five of the most important fossiliferous localities of this formation are Vathylakkos 1, 2, and 3 (VLO, VTK, VAT); Prochoma 1 (PXM), and Ravin des Zouaves 5 (RZO) (de Bonis and Koufos, 1993; 1994). The basal part of Vathylakkos Fm includes the locality RZO, which is correlated with MN 11 (early Turolian, ~ 8.2 Ma; Koufos, 2013). Dytiko Fm is the last and uppermost stratigraphic layer of Axios valley, consisting of gravels, sands, and grey clays (de Bonis and Koufos, 1993; 1994). It includes three principal localities: Dytiko 1, 2, and 3 (DTK, DIT, DKO). The rich fauna of Dytiko localities is correlated with MN 13 (late Turolian) and is more precise from 7-6 Ma (Koufos and Vasileiadou, 2015). The Nikiti Fm (NKT) is one of the two formations along with Nikolaos Fm that belong to the Sithonia Neogene deposits in the Chalkidiki peninsula (Syrides, 1990). Nikiti Fm includes

two localities, Nikiti 1 and 2, and it overlays the basement unconformably. It mainly consists of cross-bedded conglomerates, including sandy sediments of red color or pebbles coming from the erosion of the basement (Koufos, 2016). As NKT's deposits cannot allow magnetostratigraphy, dating is based on biochronological data. The NKT fauna is more derived than that of RPI, suggesting a younger age. Therefore, a terminal Vallesian age, between 9.3-8.7 Ma, is proposed (Koufos et al., 2016b).

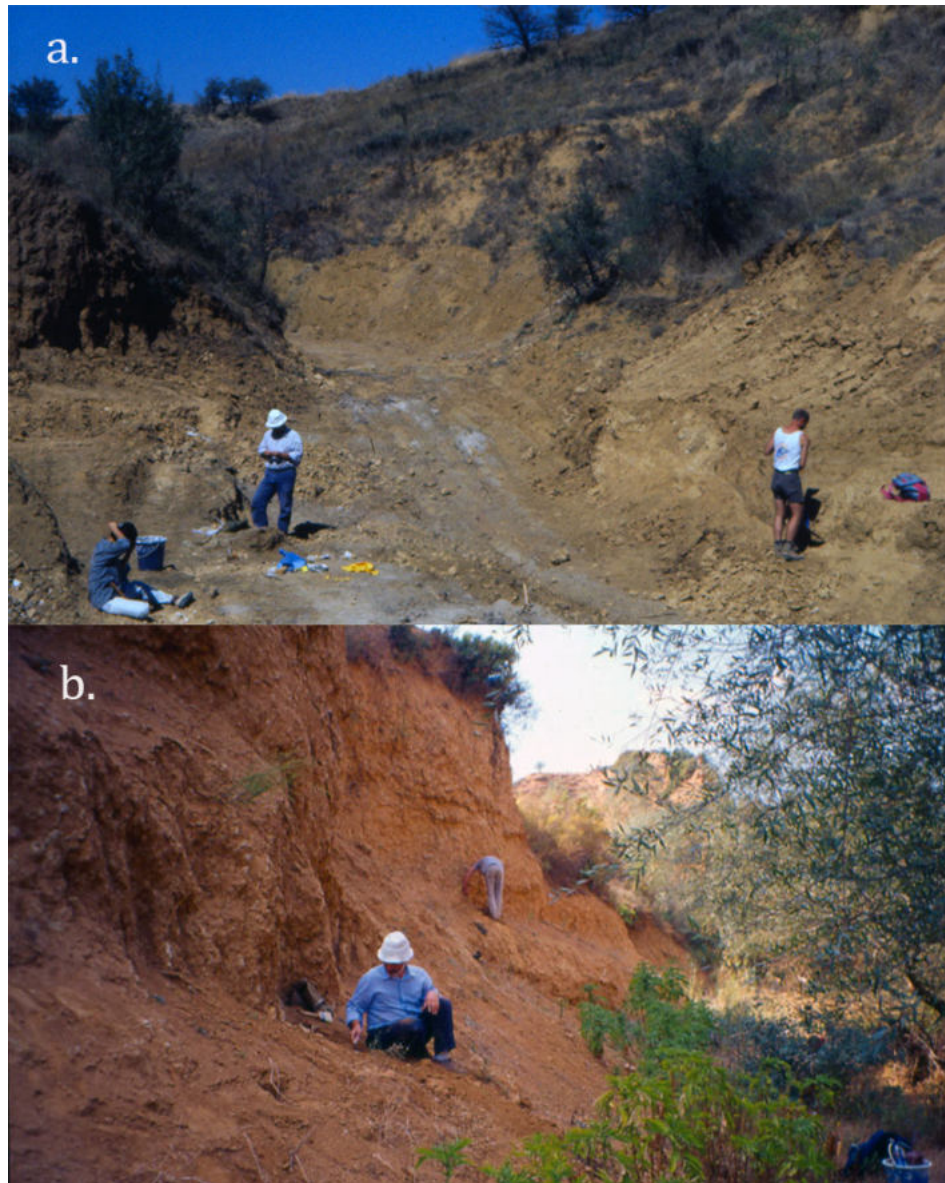


Fig. 4: Excavations in the PPI (a.) and XIR (b.) localities. Photographs by G.D. Koufos.

1.2.4 Paleoenvironment and paleodiet

O. macedoniensis is thought to have lived in a warm, open, savannah-like environment, with thick-grass floor, shrubs, and small trees as well as riparian forests along rivers (de Bonis et al., 1992; Koufos, 2006; Merceron et al., 2005; 2007, Mirzaie, 2010). More specifically, based on the mammalian faunal remains in RPl locality, the paleoenvironment was reconstructed as open, but probably less arid than other typical open Turolian environments (de Bonis et al., 1992). Dental microwear analyses suggested that *O. macedoniensis* was fed on roots and nuts (Ungar, 1996; King, 2001; Merceron et al., 2005), indicating a lifestyle in open landscapes. It is suggested that *O. macedoniensis* was consuming hard food items during dry periods, but presumably also fruits, fresh branches, and leaves during rainy periods. Additionally, various studies using different methods have indicated that the Vallesian paleoenvironment in the Eastern Mediterranean was open, arid, and different from the close forest-like environments of Western and Central Europe at this time (e.g., Fortelius et al., 1996; Koufos, 2006; Merceron et al., 2007; Ataabadi, 2010).

1.2.5 Characteristics of *O. macedoniensis*

Sexual dimorphism

O. macedoniensis shows strong dental sexual dimorphism, expressed by male-female differences in the size of the canine and post-canine dentition, which also suggest body size dimorphism (de Bonis and Melentis, 1978; de Bonis and Koufos, 1994). Traits likely related to sexual dimorphism can be observed in the mandible of *O. macedoniensis*, with male mandibles being larger and more robust than those of the females (de Bonis and Melentis, 1977; Koufos, 1993; for detailed information about the presence of sexual dimorphism in the mandible refer to Chapter 4). Dental features are more often used in determining the degree of sexual dimorphism in hominoids, particularly the morphology and size of the canine and post-canine lower teeth. Male canines in *O. macedoniensis*, for example, are longer and more robust than female ones; however, this feature is not as marked as in extant great apes (Koufos, 1993). The dental sexual dimorphism presented in this species is greater than that of the larger great apes, *Gorilla* and *Pongo* (Schrein, 2006; Scott et al., 2009; Koufos et al., 2016a). This condition has led some researchers to propose a multi-species hypothesis (Kay,

1982; Kay and Simons; 1983), although later studies found that the canine and post-canine dentition of *O. macedoniensis* specimens are morphologically homogeneous in their features, irrespective of size (de Bonis and Melentis, 1978; Koufos, 1995; Schrein, 2006; Scott, 2009). Moreover, a high degree of variation in the dentition is also present within other Miocene species, such as *Lufengipithecus lufengensis* (Kelley and Plavcan, 1998).

Craniodental characteristics

Cranial morphological characteristics of *O. macedoniensis* derive from the nearly complete face of the specimen XIR-1 (de Bonis et al., 1990; de Bonis and Koufos, 1993) and from the upper maxilla RPI-128 (de Bonis and Melentis, 1978), which will be described in detail in Chapter 3. In general, the face of *O. macedoniensis* is characterized by large interorbital distance, small and low orbits with a rather quadrangular shape, and a well-developed supraorbital torus and glabella (de Bonis et al., 1990; de Bonis and Koufos, 1993). In RPI several mandibles and mandibular remains have been found, which provide essential information about the morphology of the mandible and lower dentition of *O. macedoniensis* (Fig. 5). The mandible retains a symphysis with well-marked superior and inferior tori; it also shows powerful chewing capacity, based on the morphology of the gonial area and the well-marked crest (de Bonis and Melentis, 1977; Koufos 1993; de Bonis and Koufos, 1993; 1994). Moreover, it also retains an anteroposteriorly narrow mandibular condyle, a trait that differentiates it from the extant great apes, which have a more robust one (de Bonis and Melentis, 1977; Koufos 1993; de Bonis and Koufos, 1993; 1994). As for the upper dentition, I² is larger than I¹, while there is a gap between I² and the canine; the latter is relatively low compared with other extant great apes (de Bonis and Koufos, 1993). As mentioned before, male canines are larger than female ones, but in general, their size is relatively smaller than those of other hominoids (de Bonis and Koufos, 1994). The most important trait about the post-canine teeth of *O. macedoniensis* is that they have very thick enamel (de Bonis and Koufos, 1993). As for the lower dentition, the I₁ and I₂ are not so different in size as the upper incisors, but they are smaller than the incisors of extant great apes (de Bonis and Koufos, 2001). Lastly, the M₂ and M₃ of the male individuals are significantly larger compared to those of female specimens (de Bonis and Koufos, 1993).



Fig. 5: Maxillary fragments (RPI-128, RPI-775, RPI-80) and partial mandibles (RPI-88, RPI-89, RPI-79) of *O. macedoniensis* from the RPI locality. Photographs by G. D. Koufos.

1.2.6 The place of *O. macedoniensis*

Despite 40 years of research, the phylogenetic position of *O. macedoniensis* is still under discussion, and diverse hypotheses have been proposed. *O. macedoniensis* has been hypothesized to represent a member of the *Pan-Homo* clade (de Bonis, 1974; Begun, 2003; de Bonis and Koufos, 2004; Kunimatsu et al., 2007), the pongine clade (Köhler et al., 2001), or the gorilline clade (Dean and Delson, 1992). These hypotheses have been based on examining and comparing cranial and external dental anatomical features, using mostly cladistic analyses or traditional morphometric techniques.

De Bonis and Koufos (1994; 2001; 2004) suggested that *O. macedoniensis* can be placed within the sister group of the Mio-Pliocene hominins, meaning *Australopithecus* and *Homo*,

since it shares several characteristics with them: large interorbital distance, the shape of the mandibular symphysis, symmetric P³, canine reduction and masticatory robusticity. Although some of these features are primitive retentions (interorbital distance, shape of the mandibular symphysis), others have been proposed to be synapomorphies for the hominin lineage (symmetric P³, canine reduction, masticatory robusticity). Begun (1992; 2009) has argued that some of these features, such as thick-enameled teeth, are homoplasies and *O. macedoniensis* does not have characters that are shared between chimpanzees and *Australopithecus* (e.g., the structure of the premaxilla, frontal bone, and molar proportions). In addition to that, Begun (1994; 2000) and Begun and Kordos (1997) suggested the grouping of *O. macedoniensis* and dryopithecines, which form the sister group of African apes and humans. However, Dean and Delson (1992), commenting on the results of an early study by Begun (1992), suggested that *O. macedoniensis* (referred to as *Graecopithecus* by some researchers at that time) shows a more remarkable similarity to *Gorilla* (as well as to *Pan* and *Australopithecus*) than to *Dryopithecus* specimens. The proposed similarities of *Ouranopithecus* and *Gorilla* refer to their facial anatomy, such as the orbital margin shape and the supraorbital torus. They presented alternative cladograms, including *Dryopithecus* and *Ouranopithecus* within the hominine (African apes and humans), and suggested that *Ouranopithecus* may be a sister-taxon of *Gorilla*. Finally, a study by Köhler et al. (2001) indicated that *Ouranopithecus* and the Asian Upper Miocene hominoid *Lufengpithecus* should be attributed to the genus *Ankarapithecus*, and together to be one of the four suggested groups of fossil hominoids present the Miocene in Eurasia. Based on cranial and postcranial comparisons, Köhler et al. (2001) further suggested that several dryopithecines from Eurasia, including *O. macedoniensis*, share affinities with *Pongo* and can be considered ancestral to the pongine.

1.2.7 Beyond *O. macedoniensis*

Apart from *O. macedoniensis*, other Miocene hominoids were present in the eastern part of the Mediterranean. Cranial, dental, and postcrania of a late Miocene hominoid were found in Turkey, belonging to *Ankarapithecus meteai*, ~ 10 Ma (Alpagut et al., 1996), which as mentioned earlier is thought to share affinities with *Pongo*. Furthermore, in 2007, Gülec et al. described a new species attributed to the genus *Ouranopithecus*, *O. turkae* from Anatolia

(Turkey). Material belonging to *O. turkae* is limited to one adult male maxilla and subadult mandibular fragments (Gülec et al., 2007). The age of this species is younger than *O. macedoniensis*, dated to 8.7-7.4 Ma. The same study suggested that the two species share a significant amount of dentognathic characteristics, concluding that *O. turkae* is a sister taxon of *O. macedoniensis*. Unfortunately, no later work has been conducted on the original material from this species; thus, no more information is available. Lastly, the much-debated *Graecopithecus freybergi*, with an age of ~ 8 Ma, was found in Greece and Bulgaria (von Freyberg, 1951; von Koenigswald, 1972). Only a mandible and single lower premolar have been found from this specimen to date. As mentioned above, *O. macedoniensis* was first attributed to the genus *Graecopithecus*; however, later work by Koufos and de Bonis (2005) and more recently by Fuss et al. (2017) highlight their taxonomic differences. The same study by Fuss et al. (2017) suggests that *Graecopithecus freybergi* is an early hominin, although this view is not widely accepted (e.g., Benoit and Thackeray, 2017; cf. Chapter 5).

1.3 Objectives and research questions

Although abundant, material from the important fossil ape *O. macedoniensis* has been poorly studied using advanced techniques, such as VA and GM. The overall aims of this dissertation are:

- i. To reconstruct and analyze fragmentary fossil specimens belonging to *O. macedoniensis* and explore craniodental similarities (or dissimilarities) between this Miocene ape and primarily extant great apes. The studied similarities refer to facial, mandibular, and dental morphology.
- ii. To apply virtual techniques in an attempt to re-examine key material belonging to *O. macedoniensis*. The here used advanced methods contribute significantly to reconstructing morphological and phylogenetic affinities, as well as the paleobiology of our distant relatives.

Further, all three studies included in this dissertation cover specific aspects in reaching these overall aims. Study 1 (Chapter 3) presents the reconstruction of the facial anatomy of *O. macedoniensis* applying techniques from virtual anthropology. This study focuses on the XIR-1 cranium and RPI-128 maxilla; the only cranial fossils found heretofore belonging to

O. macedoniensis. The virtual reconstruction of the XIR-1 cranium aims to restore symmetry to its incomplete face using mirror imaging, while for the RPI-128 maxilla, virtual segmentation was used to reconfigure its initial anatomical position. Here, the main objective is to quantify, using advanced geometric morphometrics, shape variation between the virtual reconstruction of *O. macedoniensis* and a comparative sample of other fossil hominoids, extant great apes (*Gorilla*, *Pan*, and *Pongo*), and *Homo*.

Study 2 (Chapter 4) presents the 3D analysis of mandibular fragments belonging to *O. macedoniensis*. Five fossil specimens from the RPI locality were used in this study, including four partial mandibles (RPI-54; 56; 75; 79) and a ramus (RPI-391). This project explores mandibular shape similarities between *O. macedoniensis* and a comparative sample of extant great apes (*Gorilla*, *Pan*, and *Pongo*) and assesses mandibular shape variation and homogeneity within *O. macedoniensis*. In addition, the degree of mandibular sexual dimorphism is explored in *O. macedoniensis* and compared to that of extant great apes.

Study 3 (Chapter 5) presents a 3D analysis of the mandibular dentition of *O. macedoniensis*. It is a case study in which two original mandibular fragments (RPI-54 and 75) and an isolated lower molar (RPI-237) from *O. macedoniensis* are studied and compared with the literature. This study aims to observe and characterize the root morphology and length in the lower post-canine dentition of *O. macedoniensis* and compare it to extant and extinct taxa. In addition, the possibility of using root and pulp canal morphology to clarify the debatable phylogenetic position of *O. macedoniensis* was explored. Recent work has shown that root and pulp canal morphology can be used as indicators of taxonomy and can be applied to the fossil record (e.g., Moore et al., 2016; Fuss et al., 2017).

Study 1: What are the morphological affinities of the reconstructed facial area of *O. macedoniensis* in relation to the extant great apes?

This study is the first attempt to reconstruct the cranial fragments of *O. macedoniensis* using virtual anthropology techniques. Morphology is widely used to categorize living organisms. Since Miocene fossils are very fragmentary, understanding their morphological affinities with extant and extinct organisms is important. Phylogenetic affiliations of *O. macedoniensis* are based mostly on cladistic analyses. This study, of course, cannot itself resolve the

problem of this taxon's phylogenetic position, as morphology alone cannot necessarily reflect phylogeny. Nevertheless, the phenetic affinities of *O. macedoniensis* with the extant great apes can help evaluate existing hypotheses.

Study 2: Does male-female mandibular shape vary within *O. macedoniensis*? How do mandibular shape, size, and sexual dimorphism in *O. macedoniensis* compare to the extant great apes?

Mandibles (or fragments of mandibles) are commonly found in the fossil record; thus, their study has been valuable. In this study, the mandible of *O. macedoniensis* is studied, especially the corpus, symphysis, and ramus, as no complete mandible has been found. As mentioned above, using morphology solely to interpret phylogeny is problematic, especially for species with debatable phylogenetic relationships, as in *O. macedoniensis*. Therefore, the research questions of this study focus on mandibular variation and homogeneity within *O. macedoniensis*, especially as they relate to sexual dimorphism. *O. macedoniensis* shows a high level of sexual dimorphism in dental size, which has been studied extensively in the past (Schrein, 2006; Scott et al., 2009; Koufos et al., 2016a). In contrast, the expression of sexual dimorphism in mandibular size and shape of *O. macedoniensis* has not been studied extensively. Therefore, this study addresses this imbalance by examining the expression of sexual dimorphism in the mandibles of *O. macedoniensis* in more detail than in former studies.

Study 3: Is the study of the internal root morphology the key to resolving the debatable phylogenetic position of *O. macedoniensis*?

Like mandibles, teeth (either associated or isolated) are abundant in the fossil record. Without the emergence of new technologies (e.g., VA, CT scans, and specialized software), it would not have been possible to access the inner structures of the teeth. Recent studies support the use of internal dental structures, such as root pulp canals, in studying diversity in extant species (e.g., Moore et al., 2013; Moore et al., 2015). As for extinct species, assuming low degrees of homoplasy (Tobias, 1995; Kupczik et al., 2005), post-canine dental roots have been recently used as possible indicators of hominoid evolution and taxonomy (e.g., Emonet et al., 2014; Fuss et al., 2017). *Ouranopithecus*'s internal tooth morphology has been poorly

investigated, and although the sample of this study is limited, it provides new valuable insights about the possible phylogenetic relationships of this species. This study, therefore, focuses on characterizing the internal tooth structure of the *O. macedoniensis*, revealing characteristics of its root and pulp canal morphology.

CHAPTER 2

2 Materials and Methods

2.1 Comparative Sample

More than 180 scans of adult individuals belonging to extant species (great apes and humans), a few fossil specimens, and additional data from the literature were used in this dissertation. Permits for the external comparative sample were obtained before data collection (see Appendix II). Scans of the *O. macedoniensis* specimens used in the presented studies were performed at the Paleoanthropology High-Resolution CT Laboratory, University of Tübingen. Descriptions of the different fossil specimens of *O. macedoniensis* can be found in Chapters 3-5.

The extant comparative sample comprised of adult crania and mandibles belonging to great apes (*Gorilla*, *Pan*, and *Pongo*) and humans. The adult status was determined based on the dental status, more precisely, the full eruption of the third molar. The extinct comparative sample was limited, for that reason, data was either requested from the respective researchers and institutions (i.e., Study 1, see Chapter 3) or was obtained from the literature (i.e., Study 3, see Chapter 5). For detailed sample composition, please refer to the tables provided in Chapters 3-5.

2.2 Methodology

Studies 1-2: The methodology in these studies is based on geometric morphometric analyses of 3D landmarks on the cranium (Chapter 3) and mandible (Chapter 4). Chapter 3 also includes the virtual reconstructions (for detailed descriptions for each virtual reconstruction, please refer to page 39/ Chapter 3) of the XIR-1 face and RPI-128 maxilla in the software Avizo (©FEI Visualization Sciences Group, version 9.1). The use of landmarks (2 or 3D) is the core element in GM. Landmarks are defined as points within cartesian coordinates that are registered on a homologous structure (Bookstein, 1991). They can be categorized in the following types (e.g., Bookstein, 1997; Zelditch, 2012): Type I, which correspond to standard ("fixed") points easily identified on the skeletal material; Type II, which correspond to points of maximum curvature; and Type III, which refer to the most extreme points (e.g., most posterior/ anterior point).

In both studies, the 3D landmarks were registered on 3D models (surfaces) and in some instances, using a 3D digitizer (Microscribe). The surfaces originated either from the use of computed tomography (CT) or 3D surface scanners. Using x-ray technology, like the CT, is costly, but the resulting 3D matrix comprising small information units (Weber 2001; Scherf, 2013), reveals details about both the inner and outer morphology of the specimen. However, as a part of the comparative sample used in this dissertation is hosted in several museums and collections, its use was not always feasible. Instead, a portable 3D surface scanner was preferred. The Artec Space Spider scanner (property of the Paleoanthropology High-Resolution CT Laboratory, University of Tübingen) was utilized. This surface scanner is based on blue light technology and creates accurate high-resolution surface scans (max resolution of 50 microns). Lastly, when none of the options above was available, a mechanical digitizer was used (Microscribe 3D; property of the Paleoanthropology High-Resolution CT Laboratory, University of Tübingen). Contrary to the other options, this method does not produce any surface scan/representation. Instead, the 3D landmarks are collected from a stylus and a pedal, which are connected to a host computer. After the registration of the landmarks, only the visualization of the 3D measurements is possible.

Before the statistical analysis of shape, it is crucial to remove all other parameters from the dataset. One of the most established procedures is the Generalized Procrustes Analysis (or GPA; Gower, 1975; Rohlf and Slice, 1990; Rohlf and Markus, 1993), which transfers the raw landmarks' coordinates of all specimens in a common coordinate system, and in that process removes overall size, position, and orientation from the dataset (Rohlf and Slice, 1990; Rohlf and Markus, 1993). The new coordinates produced are called Procrustes shape coordinates (or just shape coordinates) and are used in all later steps of the statistical analyses unless indicated otherwise.

Calculation of inter- and intra-observer landmark error is an essential step to evaluate the reproducibility of any statistical analysis. An inter-observer error is needed when landmarks are registered by multiple observers on the same material, while an intra-observer error when they are registered only by a single observer. An intra-observer error was conducted in both studies, as the landmarks were registered by the same person. For a detailed description of the error tests refer to pages 38 (Chapter 3) and 80 (Chapter 4).

In Study 1, Principal Component Analyses (PCA) were conducted of two datasets (facial and maxillary) to examine all specimens' overall cranial shape variation in shape space. PCA is an ordination analysis, which shows how the total shape variance is partitioned among and within the sample in morpho-space (Bookstein, 1997; Rohlf, 1999). To investigate whether size-related effects influenced the position of *O. macedoniensis* in the PCA, a correlation analysis was conducted between the first two principal components and (log) centroid size. Moreover, full Procrustes shape distances were used to examine shape similarities of *Ouranopithecus* and the extant taxa. Procrustes distances refer to the sum of squared differences of the coordinates between the superimposed configurations and reveal the amount of shape variation within a sample (Rohlf and Slice, 1990; Adams et al., 2004; Bookstein et al., 2004). Permutation tests were performed to test the statistical significance of shape variation within the extant great apes (excluding all fossils in both datasets). To test whether there are great differences to separate the groups, a discriminant function analysis (DFA) was conducted, using the principal components as variables. As groups in this analysis are defined a priori, the fossils used (whose phylogenetic position is in question or were represented by only one specimen) were treated as unknown.

In Study 2, PCA was conducted on three datasets (bilateral, hemimandible, and ramus) in shape space. Permutation tests between sexes were performed for each extant species to test if there are sex-specific differences within each species. A correlation analysis between the first two principal components and (log) centroid size was conducted for all datasets to investigate whether the distribution of the specimens in the PCAs is influenced by size. Procrustes distances were used to explore shape differences within the *O. macedoniensis* sample and that present in each of the extant species. All pairwise Procrustes distances in *O. macedoniensis* were compared to those of each extant great apes via boxplots. In addition, the 95 % probability intervals from all pairwise Procrustes distances for each great ape were calculated and compared to the pairwise distances within *O. macedoniensis*. These analyses aimed to investigate whether there is greater variation in the small *O. macedoniensis* sample than in the extant great apes. To examine the size-related degree of sexual dimorphism expressed by the *O. macedoniensis* mandibles and compare it to levels observed in the extant

great apes, the pairwise *O. macedoniensis* male-female centroid size differences were plotted against distribution of all male-female pairwise differences for each extant great ape, using boxplots. The differences between the male and female centroid means were calculated, and for great apes also tested for significance.

Study 3: For this study (Chapter 5), the use of micro (μ)CT scans for the *O. macedoniensis* specimens was necessary as a virtual extraction of the post-canine teeth and the internal structure of the root canals was required. All necessary steps were conducted with the environment of the Avizo software (©FEI Visualization Sciences Group, version 9.1).

Due to the nature of the comparative sample, which originated from the literature, the therein protocols were used: Moore et al. (2013, 2015); Emonet (2009); Emonet et al. (2014); and Fuss et al. (2017). The study focused on the lower right post-canine dentition, as this was complete in both *O. macedoniensis* mandibles. The teeth were virtually segmented from the mandible in the Avizo software. Due to high-level fossilization, a manual or semi-automatic virtual segmentation of the teeth had to be carried out. After the segmentation, root length was measured, and root morphology was explored. For root length measurements, the protocol from Moore et al. (2013) was used, where the root length is measured linearly from the root apex to the surface of the cervical plane. The comparative data include root length measurements from extant great apes (*Gorilla gorilla*, *Pan troglodytes*, *Pongo pygmaeus*), humans, and extinct taxa, including *Sahelanthropus tchadensis* and *Graecopithecus freybergi*. For root and pulp canal evaluation, the protocol from Emonet (2009) was followed, where the number of roots (fused and unfused) is counted, while the dental root and pulp canal configuration is calculated using the following formula for multi-rooted teeth: $X_a M + Y_\beta D$. The variables X/Y are the mesial/distal number of roots; a/β are the mesial/distal number of pulp canals; and M/D stands for mesial/distal surface of the tooth.

Chapters 3 to 5 are presented in an article format as these chapters are already or will be published in peer-reviewed journals. Chapter 3 is published, Chapter 4 is currently submitted and under review, and Chapter 5 is ready for submission. At the beginning of each chapter, the manuscript status and the individual author's contributions are provided.

CHAPTER 3

Study 1

Text and analyses incorporated in this chapter are a manuscript that is published in the American Journal of Physical Anthropology.

Ioannidou, M., Koufos, G. D., de Bonis, L., & Harvati, K. (2019). A new three-dimensional geometric morphometrics analysis of the *Ouranopithecus macedoniensis* cranium (Late Miocene, Central Macedonia, Greece). *American Journal of Physical Anthropology*, 170(2), 295-307. <https://doi.org/10.1002/ajpa.239001>²

The original idea for this study was developed in collaboration with Prof. Dr. Harvati, Prof. Koufos and Prof. de Bonis. Regarding the data presented in this chapter, I was the main conductor and collected all data.

Author	Author position	Scientific ideas %	Data generation %	Analysis & interpretation %	Paper writing %
Ioannidou, M.	1	40	100	80	60
Koufos, G.	2	10	-	-	10
de Bonis, L.	3	10	-	-	-
Harvati, K.	4	40	-	20	30
Title of the paper		A new three-dimensional geometric morphometrics analysis of the <i>Ouranopithecus macedoniensis</i> cranium (Late Miocene, Central Macedonia, Greece)			
Status in Publication Process		Published in <i>American Journal of Physical Anthropology</i>			

² This article is licensed (license number: 5076940821902) under an agreement between the corresponding author ("Melania Ioannidou") and John Wiley and Sons ("John Wiley and Sons"), which permits reproduction of this article for purposes of this Dissertation. The terms and conditions are provided by John Wiley and Sons and Copyright Clearance Center.

A new three-dimensional geometric morphometrics analysis of the *Ouranopithecus macedoniensis* cranium (Late Miocene, Central Macedonia, Greece)

Abstract

Objectives: This study aims to virtually reconstruct the deformed face (XIR-1) and maxilla (RPI-128) of the late Miocene hominoid *Ouranopithecus macedoniensis* from Greece, through the application of mirror-imaging and segmentation. Additionally, analysis was conducted through 3D geometric morphometrics, utilizing a comparative sample of fossil hominoids, extant great apes (*Gorilla*, *Pan*, and *Pongo*) and humans, so as to explore shape variation and phenetic similarities between them.

Materials and methods: High-resolution computed tomography was used to create digital representations of the XIR-1 and RPI-128 specimens. The virtual reconstruction of the XIR1 cranium was achieved by mirror-imaging, while the RPI-128 maxilla was virtually segmented and reattached in a correct anatomical position. Anatomical landmarks were registered in three dimensions on a comparative sample of adult crania of extant great apes, humans and fossil hominoids. The data were processed with Procrustes superimposition and analyzed using multivariate statistics methods.

Results: Results show that *Ouranopithecus macedoniensis* falls within or close to the *Gorilla* convex hull in the principal component analyses, and it is closer to the mean Procrustes shape distance of primarily *Gorilla*. Both specimens, XIR-1 and RPI-128, are classified as *Gorilla* based on discriminant function analyses.

Discussion: The results of our geometric morphometrics analyses indicate that *Ouranopithecus macedoniensis* is morphologically more similar to *Gorilla* than to *Homo*, *Pan*, or *Pongo*, results that can contribute to the evaluation of existing hypotheses about its phylogenetic position.

Keywords: Geometric morphometrics, Hominoidea, Late Miocene, *Ouranopithecus*, Virtual anthropology

3.1 Introduction

The genus *Ouranopithecus* has been documented since 1974 in the late Miocene deposits of Northern Greece in the form of several mandibles, a number of isolated teeth, a maxilla (RPI-128; Fig. 1b) and an almost complete face (XIR-1; Fig. 1a; de Bonis, 1974; de Bonis & Melentis, 1977, 1978; de Bonis et al., 1990; Koufos, 1993, 1995; Koufos et al., 2016). *Ouranopithecus macedoniensis* is currently known from three localities in Macedonia (Northern Greece): Ravin de la Pluie (RPI) and Xirochori (XIR) in the Axios Valley; and Nikiti-1 (NKT) in the Chalkidiki Peninsula. Continuing excavations have yielded several maxillary and mandibular remains of this hominoid, especially from RPI; whereas postcranial remains are limited to two phalanges, also from RPI (de Bonis & Koufos, 2014; de Bonis et al., 1998; de Bonis & Melentis, 1977, 1978; Koufos & de Bonis, 2006). The chronostratigraphic range of *O. macedoniensis* is hypothesized to lie between 9.6 and 8.7 Ma on the basis of faunal correlation and magnetostratigraphic evidence (Koufos et al., 2016; Sen et al., 2000). *O. macedoniensis* has been hypothesized to represent either an early hominin (de Bonis & Koufos, 1994, 2001), a dryopithecine and a sister group to the extant African apes and humans (Begun, 1994; Begun & Kordos, 1997), or a close relative of *Gorilla* (Dean & Delson, 1992) or *Pongo* (Köhler et al., 2001).

3.2 Materials and Methods

The aim of our study is, first, to virtually reconstruct two different cranial remains of *O. macedoniensis*, the XIR-1 cranium and RPI-128 maxilla; and, second, to conduct a comparative 3D geometric morphometric analysis of the reconstructed *Ouranopithecus* facial morphology, in an attempt to understand its morphological affinities with extant great apes, humans and fossil hominoids. This is the first virtual reconstruction of *Ouranopithecus macedoniensis*, and itself cannot resolve the problem of this taxon's phylogenetic position, however its phenetic affinities mainly with the extant great apes can help evaluate existing hypotheses. The virtual reconstruction of the XIR-1 cranium aims to restore symmetry to its deformed face using mirror-imaging. Additionally, the virtual reconstruction of the RPI-128 maxilla uses virtual segmentation of the specimen to reconfigure it in its initial anatomical position. The most important advantage of such methods, relative to traditional

reconstruction techniques, is that they allow digital manipulation of the objects under study and therefore are not destructive or damaging to the precious fossil specimens. Our second goal is to analyze the virtual reconstructions with three-dimensional (3D) geometric morphometrics, in order to explore shape variation and phenetic similarities between *O. macedoniensis* and a comparative sample of other fossil hominoids, extant great apes (*Gorilla*, *Pan*, and *Pongo*) and humans.

The XIR-1 cranium

The specimen XIR-1, found in 1989, consists of a nearly complete face of an adult male (de Bonis et al., 1990, Fig. 1a). It is well preserved, but slightly distorted as a result of taphonomic processes during fossilization. The right side of the face is complete, including the right orbit, maxilla, nasal bone (which is slightly distorted) and nasal aperture, while the anatomical area from the frontal bone to the alveolar process is also preserved. The left part of the face includes the nasal bone, which seems intact, and the left maxilla. Additionally, the dentition of the individual is almost complete, with only the right third molar missing (de Bonis et al., 1990). The face of *Ouranopithecus* is characterized by a large interorbital distance, small and low orbits with a rather quadrangular shape, and a well-developed supraorbital torus, which has a small depression at its central part behind the brow ridge (de Bonis et al., 1990; de Bonis & Koufos, 1993). Moreover, it shows a well-defined glabella, while the lateral margins of the upper face are relatively vertical (de Bonis et al., 1990; de Bonis & Koufos, 1993).

The RPI-128 maxilla

RPI-128 was found in 1978, and like XIR-1, it belongs to an adult male (de Bonis & Melentis, 1978). The upper jaw is well preserved, while the permanent dentition is almost complete, only the left lateral incisor and canine are missing. Moreover, part of the zygomatic bone and a large part of the nasal cavity are also preserved. The canine roots have a strong posteromedial inclination, which gives a false impression of a receding anterior portion of the maxilla (de Bonis & Melentis, 1978; Fig. 1b).

Virtual reconstruction

XIR-1 and RPI-128 were micro CT scanned at the Paleoanthropology High Resolution Computed Tomography Laboratory, University of Tübingen (Phoenix X-Ray, v/tomex/s GE, tube voltage 220 kV, tube current 180 mA and beam collimation 1 mm). Both reconstructions were carried out using AVIZO software (©FEI Visualization Sciences Group, Version 9.1).

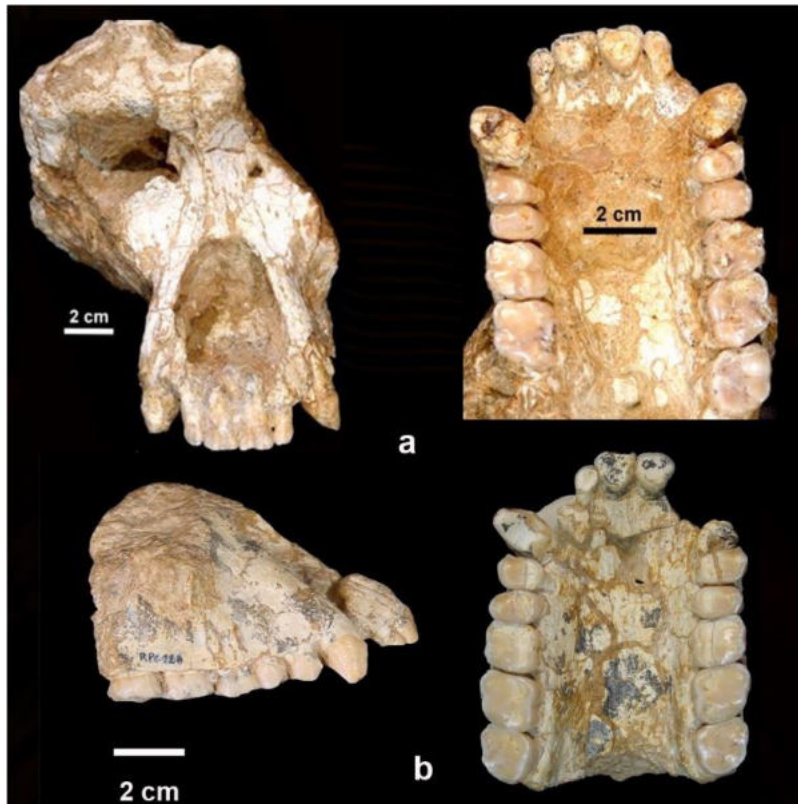


Fig. 1: (a) *O. macedoniensis* (XIR-1): face and maxilla with an almost complete dentition and (b) *O. macedoniensis* (RPI-128): maxilla with an almost complete dentition. Photographs by G. D. Koufos.

Before starting to virtually reconstruct any specimen, some basic requirements were met. Following Gunz et al., (2009), the degree of deformation, which corresponds to the deviation from the symmetry, has to be defined from the beginning. XIR-1 exhibits a well-preserved right side, with only some degree of deformation in the nasal aperture. We initially tried to segment out the different facial areas preserved in the XIR-1 cranium and repositioning them, but unfortunately this was not possible, as it was very hard to distinguish the matrix from the sediment. Hence, our reconstruction was based on restoring bilateral symmetry

with mirror-imaging, as one side of the specimen showed no deformation and the midline was undisturbed (Gunz et al., 2009). The virtual reconstruction of the XIR-1 cranium was conducted in two steps. The first step included the mirror-imaging of the right anatomical side to the left, to complete the face of the XIR-1 cranium, while the second aimed to correct the deformation of the nasal bones, by mirroring part of the intact left side to the deformed right one. As for the RPI-128, while this specimen is well preserved (Fig. 1b), it is glued at the area beneath the anterior nasal aperture (area A) and the premaxillary alveolar process of the front teeth (area B). However, when these two pieces (area A and B) were glued, the latter was shifted to a more superior position and there is most likely bone missing between them. The aim of our reconstruction was to virtually separate the two areas, so as to remove the glue and see if there is any direct contact between them.

Comparative analysis

Sample

Our comparative sample comprised of 106 adult specimens, including both fossil and extant taxa. Apart from the XIR-1 cranium and RPI- 128 maxilla, other fossils (Table 1) included a cast of a reconstruction (Begun 1994, 2009; surface scan) of *Hispanopithecus laietanus* (IPS 18000) from the Late Miocene deposits of Can Llobateres 2, Spain (Alba, 2012; Köhler et al., 2001; Moyà-Solà & Köhler, 1993, 1995), *Sahelanthropus tchadensis* (TM 266-01-60-1; Brunet et al., 2002, 2005; Zollikofer et al., 2005), and *Australopithecus africanus* from Sterkfontein, South Africa (Sts 71; Broom et al., 1946; virtual reconstruction, University of Vienna). The extant sample (Table 2) includes *Homo sapiens* (n = 20), *Pan troglodytes* (n = 22), *Gorilla gorilla* (n = 22), *Gorilla beringei* (n = 10), *Pongo pygmaeus* (n = 19), and *Pongo abelii* (n = 10). All extant taxa were represented by both adult female and male individuals, with ≥ 5 individuals per sex. Adult status was established using the criterion of full eruption of the third permanent molar.

Measurement protocol

Fifty-six landmarks (complete dataset), representing standard osteometric points on the cranium (Table 3; White, Black, & Folkens, 2011), were registered in three dimensions (3D)

following Singh et al. (2012), Guy et al. (2003), Bayome et al. (2013), and McNulty (2005). The landmarks used in our analysis were chosen so as to capture the maximum overall shape of the maxillofacial area, which is the area that the XIR-1 cranium preserves. Landmarks were either digitized directly from crania with a 3D digitizer (Microscribe 3DX, © Immersion Corporation) or collected from scans with the specialized software AVIZO.

Table 1: List of fossils used for the comparative analysis. ^a

Species	Sample	N. of individual	MA	Type of material	Collection
<i>Hispanopithecus laietanus</i>	IPS 18000	1	10	Surface scan of virtual reconstruction	1
<i>Ouranopithecus macedoniensis</i>	XIR-1 and RPI-128	2	9.6-8.7	CT scan	1
<i>Sahelanthropus tchadensis</i>	TM 266-01-60-1	1	7.2-6.8	3D Landmarks	2
<i>Australopithecus africanus</i>	Sts 71	1	2.8-2.5	Surface scan of virtual reconstruction	3

^a Collection codes: 1. University of Thessaloniki; 2. University of Poitiers; 3. University of Vienna.

Table 2: Extant great apes and humans used in the analysis. ^a

Species	Adults		Collection
	male	female	
<i>Homo sapiens</i>	10	10	1,2
<i>Gorilla gorilla</i>	11	11	3,4
<i>Gorilla beringei</i>	5	5	4
<i>Pan troglodytes</i>	12	10	1,3,4,5
<i>Pongo abelii</i>	5	5	4
<i>Pongo pygmaeus</i>	9	10	3,4

^a Collection codes: 1. University of Tübingen, 2. Copenhagen University, 3. Natural History Museum, Stuttgart, 4. Smithsonian National Museum of Natural History, 5. Senckenberg Museum of Natural History, Frankfurt.

The analysis was repeated using two datasets: the first includes the full complement of 56 landmarks (Fig. 2); while the second one includes only 27 landmarks (maxillary dataset),

those preserved in the RPl-128 reconstruction and TM 266-01-60-1. As mentioned in the virtual reconstruction section, the nasal aperture has a small deformation, and thus an additional analysis was performed excluding the landmarks around this area (landmarks 3, 18, 19, and 20). This landmark dataset was superimposed separately and a principal component analysis (PCA) was conducted on the fitted coordinates (Fig. S3). All landmarks were registered by MI, with the exception of those of *S. tchadensis*, which were collected by colleagues at the University of Poitiers following our detailed definitions. These landmarks were only used in the analyses of the maxillary landmark dataset.

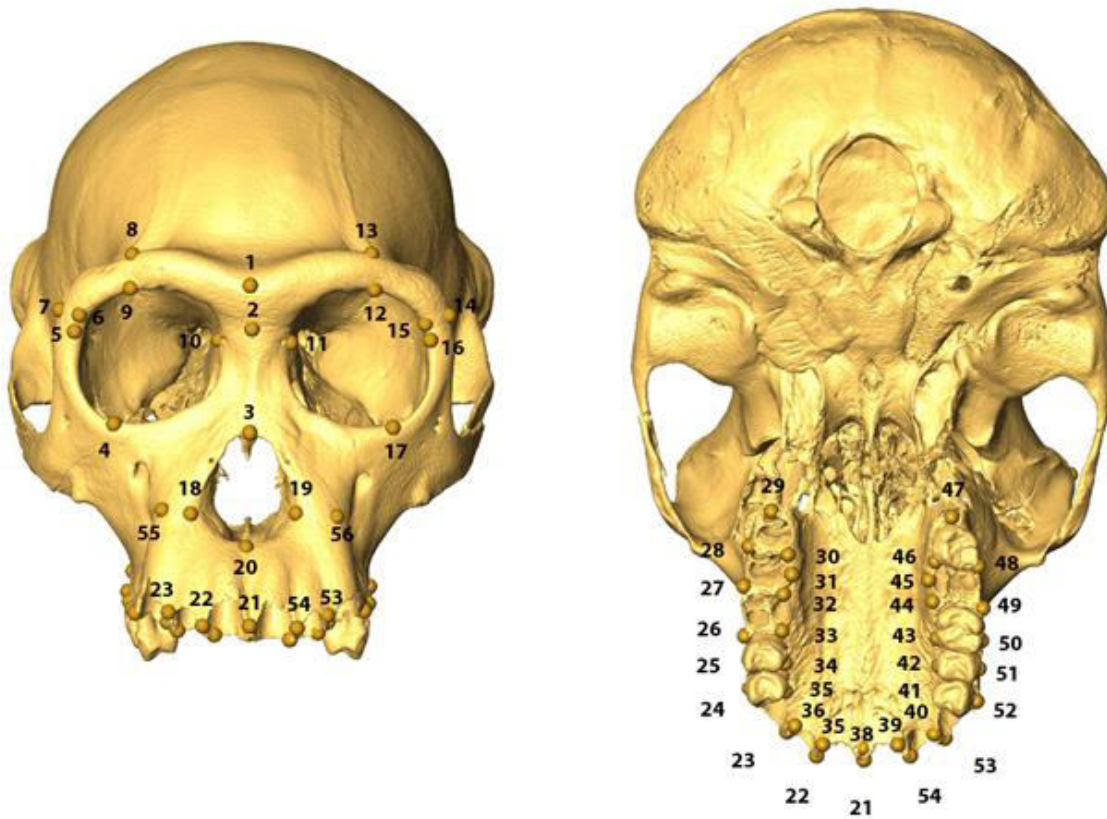


Fig. 2: The 56 registered three-dimensional landmarks used in the analysis on a surface scan of a female *Pan troglodytes* cranium.

Intra-observer error test

To calculate the intra-observer measurement error, one specimen was selected and the landmarks were registered by one of the authors (MI), five times using a Microscribe and five times using AVIZO, over a period of 1 month. For this purpose, a specimen of a *Pan*

trogodytes from the Osteological Collection of the University of Tübingen was scanned. The observed error ranged from 0.3 to 3.35 %, well within acceptable levels (Singleton, 2002).

Table 3: List of landmarks used for the comparative analysis. ^a

No. Landmarks
1. Glabella (g)
2. Nasion (n)
3. Rhinion (rhi)
4. Orbitale (or) right
5. Ectoconchion (ec) right
6. Frontomalare orbitale (fmo) right
7. Frontomalare temporale (fmt)
8. Mid-torus superior right
9. Mid-torus inferior right
10. Across (ec) point right
11. Across (ec) point left
12. Mid-torus inferior left
13. Mid-torus superior left
14. Frontomalare temporale (fmt) left
15. Frontomalare orbitale (fmo) left
16. Ectoconchion (ec) left
17. Orbitale (or) left
18. Alare (al) right
19. Alare (al) left
20. Subnasal (sn)
21. Alveolare (ids)
22. 1 st – 2 nd incisor alveolar septum right
23. 2 nd incisor – canine alveolar septum right
24. Canine – 1 st premolar alveolar septum right
25. 1 st – 2 nd premolar alveolar septum right
26. 2 nd premolar – 1 st molar alveolar septum right
27. 1 st – 2 nd molar alveolar septum right
28. 2 nd – 3 rd molar alveolar septum right
29. Midpoint distal 3 rd molar alveolar margin right
30. Inner 3 rd – 2 nd molar alveolar septum right
31. Endomorale (enm) right

32. Inner 2nd – 1st molar alveolar septum right
33. Inner 1st molar – 2nd premolar alveolar septum right
34. Inner 2nd – 1st premolar alveolar septum right
35. Inner 1st premolar – canine alveolar septum right
36. Inner canine – 2nd incisor alveolar septum right
37. Inner 2nd – 1st incisor alveolar septum right
38. Inner central incisors alveolar septum
39. Inner 1st – 2nd incisor alveolar septum left
40. Inner 2nd incisor – canine alveolar septum left
41. Inner canine – 1st premolar alveolar septum left
42. Inner 1st – 2nd premolar alveolar septum left
43. Inner 2nd premolar – 1st molar alveolar septum left
44. Inner 1st – 2nd molar alveolar septum left
45. Endomorale (enm) left
46. Inner 2nd – 3rd molar alveolar septum left
47. Midpoint distal 3rd molar alveolar margin left
48. 3rd – 2nd molar alveolar septum left
49. 2nd – 1st molar alveolar septum left
50. 1st molar – 2nd premolar alveolar septum left
51. 2nd – 1st premolar alveolar septum left
52. 1st premolar – canine alveolar septum left
53. Canine – 2nd incisor alveolar septum left
54. 2nd – 1st incisor alveolar septum left
55. Canine eminence (ce) right
56. Canine eminence (ce) left

^a See Fig. 2

Data processing

A generalized Procrustes analysis, which superimposes all the landmark configurations, was conducted in the EVAN Toolbox software (Version 1.6; EVAN-Society, e.V.). The aim of this procedure is to remove the non-shape variation (i.e., position and scale) and create new shape variables. Reflected relabeling was performed for the reconstruction of missing data (Gunz et al., 2009) using Morpheus (Slice, 1999). This procedure was applied to the *A. africanus* Sts 71 specimen, which was lacking landmarks on one anatomical side (landmarks 13–17, 22, 44–49, and 56).

Statistical analyses

Statistical analyses were performed using the EVAN Toolbox (Version 1.6; EVAN-Society, e.V.), PAST (Version 3.10; Hammer et al., 2001), R statistical environment (Geomorph package, Adams & Otárola-Castillo, 2013) and SPSS (IBM® SPSS® Statistics 21). A principal component analysis was conducted on both datasets to examine the overall cranial shape variation of all specimens in shape space. PCA is a way to explore shape variability, as it examines how the total variance is partitioned not only among but within the sample in morphospace (Bookstein, 1997; Rohlf, 1999). To further examine the shape similarities of *Ouranopithecus* and the represented extant taxa, we performed a shape analysis in Geomorph package (Adams & Otárola-Castillo, 2013), which uses the full Procrustes shape distances among specimens to quantify explained and unexplained components of shape variation (Adams & Otárola-Castillo, 2013).

Table 4: Classification and cross-validation results of the discriminant function analysis (full landmark dataset).^a

		Species	Predicted Group Membership				Total
			<i>Pongo</i>	<i>Gorilla</i>	<i>Pan</i>	<i>Homo</i>	
Cross-validated	Count	<i>Pongo</i>	28	0	1	.0	29
		<i>Gorilla</i>	0	32	0	.0	32
		<i>Pan</i>	0	0	22	0	22
		<i>Homo</i>	0	1	0	19	20
	%	<i>Pongo</i>	96.6	.0	3.4	.0	100.0
		<i>Gorilla</i>	0	100.0	.0	.0	100.0
		<i>Pan</i>	0	.0	100.0	.0	100.0
		<i>Homo</i>	.0	5.0	.0	95.0	100.0

^a 100 % of original grouped cases and 97.1 % of cross-validated grouped cases were correctly classified to genus.

The statistical significance of shape variation within the extant great apes (excluding all fossils in both full and maxillary datasets) was assessed via permutation tests (100 random permutations), using Goodall's F method (Goodall, 1991) and the results can be seen in

Tables 4 and 5. After performing this test, we calculated the mean Procrustes shape distance differences, to measure how similar are the *Ouranopithecus* specimens (XIR-1 and RPI-128) to the represented extant taxa used in the analysis. While Procrustes superimposition removes gross size, size-related (i.e., allometry) shape remains. Therefore, to investigate whether the position of *O. macedoniensis* in the PCA was influenced by such size-related effects, we conducted a correlation analysis between the first two principal components and log centroid size, using Pearson's correlation coefficient.

Finally, a discriminant function analysis (DFA) was also performed to maximize the among versus the within group variation, using principal components as variables. DFA uses a priori defined groups and therefore the fossils used in the analysis, whose phylogenetic position is in question or which were represented by only one specimen, were treated as unknown (see also Harvati et al., 2011). We used the Kaiser criterion and scree plot method (Jackson, 2005), to choose the number of (nonzero) PCs to include in the analysis.

Table 5: Classification and cross validation results of the discriminant function analysis (maxillary landmark dataset).^a

		Species	Predicted Group Membership				Total
			<i>Pongo</i>	<i>Gorilla</i>	<i>Pan</i>	<i>Homo</i>	
Cross-validated	Count	<i>Pongo</i>	22	0	7	0	29
		<i>Gorilla</i>	0	32	0	0	32
		<i>Pan</i>	7	0	14	1	22
		<i>Homo</i>	0	0	0	20	20
	%	<i>Pongo</i>	75.9	.0	24.1	.0	100.0
		<i>Gorilla</i>	.0	100.0	.0	.0	100.0
		<i>Pan</i>	31.8	.0	63.6	4.5	100.0
		<i>Homo</i>	.0	.0	.0	100.0	100.0

^a 89.3 % of original grouped cases and 85.4 % of cross-validated grouped cases were correctly classified to genus.

3.3 Results

Virtual reconstruction

XIR-1

An artificial mirror surface of the undistorted right side was created and placed over the original left side, using the transform editor tool in AVIZO, ensuring that the orbits were at the same height and had the same distance from glabella and nasion. This was achieved by measuring the distances virtually in AVIZO. This step was performed several times until a satisfactory fit was achieved and the facial elements were in the correct anatomical position. Unnecessary or redundant segments were edited out using the surface edit tool. From the original right side surface, only a small part of the supraorbital region was removed across the midplane. After editing out the original right side surface, the mirrored left side was virtually removed, except from the orbit, part of the supraorbital torus and part of the zygomatic bone (Fig. S1). Additionally, when both surfaces were processed, a last check of the distances between the orbits and the distance of each orbit from glabella was made and, if necessary, the surfaces were edited again. Moreover, to complete the dentition of the XIR-1 cranium, we decided to virtually segment the preserved left M3 and place it on the right side, in a correct anatomical position (Fig. S1). Finally, using the same mirror- imaging steps, the proximal part of the left nasal bone (the part that was crucial for placing landmarks) was virtually reconstructed from the intact right side.

RPI-128

The two original pieces of the maxilla were virtually segmented using both manual (brush tool) and semi-automatic (magic wand tool) segmentation methods in AVIZO. After segmentation we observed that no natural contact between the two pieces is preserved, thus it was not possible to achieve a perfect fit (Fig. S2). We therefore decided not to include any landmark at the problematic lower part of the maxilla in our geometric morphometrics analyses.

Principal component analysis

Complete landmark dataset

The first component summarizes 55.93 % of the total variance of the sample. PC 1 separates *Homo* on its negative side and the other extant great apes and fossils plot near the center or on the positive side (Fig. 3). The virtual reconstruction of XIR-1 shows a positive PC 1 score, overlapping with the great apes and away from modern humans, as expected. IPS 18000, the virtual reconstruction of *Hispanopithecus laietanus* (Begun, 1994, 2009), shows a similar score. On the other hand, Sts 71, the *A. africanus* specimen, shows a somewhat negative score and clusters within the *Pan* convex hull. PC 2 accounts for 11.21 % of the total variance and separates *Gorilla* on the positive side from *Pan* and *Pongo* on the negative side; *Homo* clusters around zero on this axis. XIR-1 falls within the range of *Gorilla* on PC 2. IPS 18000 also scores positively on PC 2, plotting close to the *Gorilla* convex hull, but also within the range of *Homo* species, while Sts 71 scores negatively, plotting within the *Pan* convex hull. As it can be seen in Fig. 3a–d, PC 1 is primarily associated with changes in the overall facial shape, including the orbits, supraorbital region, nasal aperture, and maxilla. Specifically, negative PC 1 scores, characterizing *Homo*, reflect wider and laterally extended orbits, a smaller but superoinferiorly elongated nasal aperture, and less prognathic midfaces, while as we move toward the positive end, where *Gorilla* and *Pongo* specimens fall, the orbits are shortened laterally, the nasal aperture is shorter but wider, and the midfaces are more prognathic. Along PC 2, individuals with positive PC 2 scores, characteristic of *Gorilla*, have wider nasal apertures and wider orbits, while as we move toward the negative end, where both *Pan* and *Pongo* fall, the orbits extend laterally, and the nasal aperture is narrower. As for the lower PCs, PC 3 (7.39 %) and PC 4 (3.76 %), they do not separate the taxa as well as the first two, as there was overlap between them. All specimens overlap mostly around zero, while the XIR-1 reconstruction is plotted within the *Gorilla* convex hull, but also close to the scores of the other great apes and humans, both in PC 3 and PC 4 (Fig. S3).

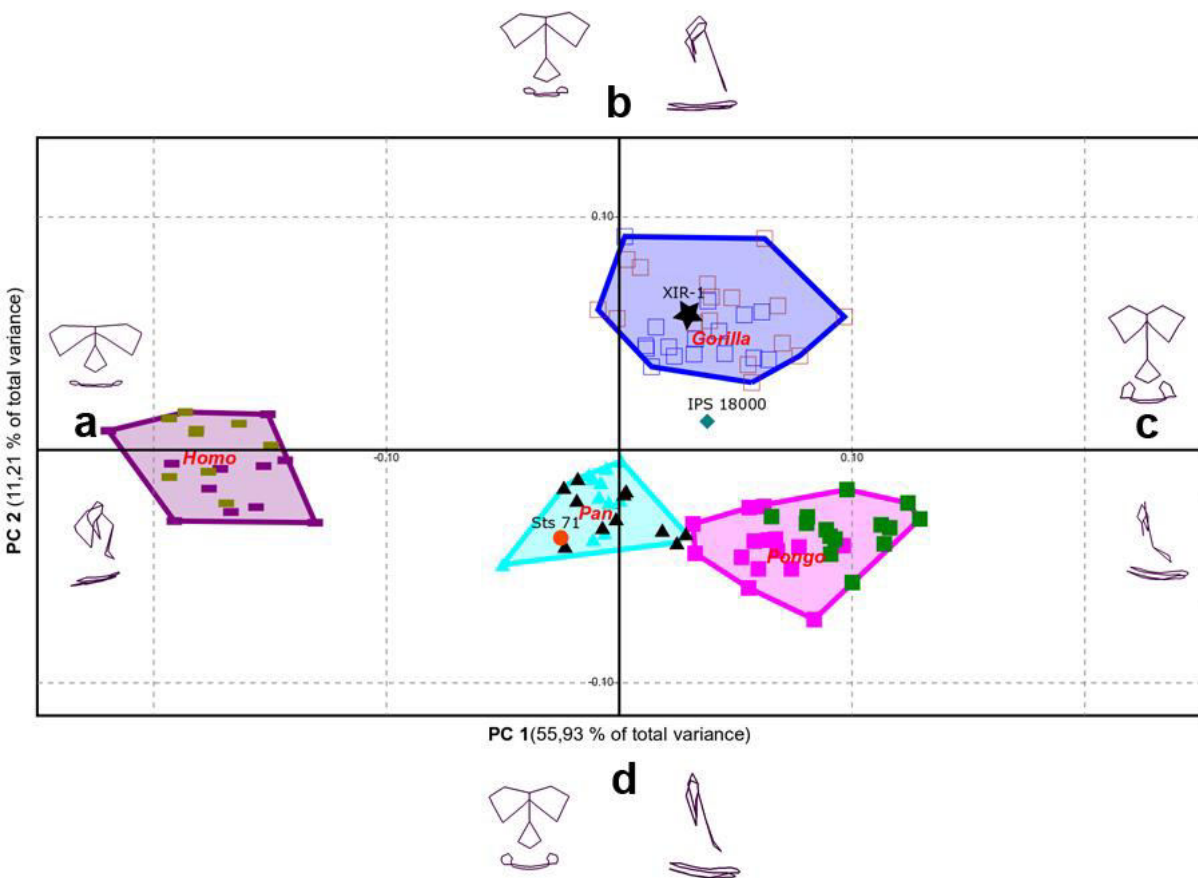


Fig. 3: PCA in shape space (full landmark dataset). PC 1 explains 55.93 % and PC 2 11.21 % of total variance. Convex hulls are drawn for *Homo* (purple for females and olive green for males), *Gorilla* (blue for females and brown for males), *Pan* (aqua blue for females and black for males) and *Pongo* (fuchsia for females and green for males). **a:** mean shape at the negative end of PC 1 in frontal and lateral view, **b:** mean shape at the positive end of PC 2 in frontal and lateral view, **c:** mean shape at the positive end of PC1 in frontal and lateral view, **d:** mean shape at the negative end of PC 2 in frontal and lateral view.

Maxillary landmark dataset

A second PCA was performed on a subset of the landmarks so as to include the second *Ouranopithecus* specimen, the RPI-128 maxilla (Fig. 4a–d). Here PC 1 (46.85 % of total variance) separates *Homo sapiens* on its positive side, while *Gorilla* plot on the negative side, with *Pan* and *Pongo* clustering around zero, overlapping with each other and also partially with *Gorilla*.

XIR-1 has a negative PC 1 score and plots with the *Gorilla* sample, while the RPI-128 specimen falls close to zero. The IPS 18000 reconstruction plots in the *Gorilla* sample, but within the values of *Pan* as well. TM 266-01-60-1 reconstruction has a negative score, overlapping with both *Gorilla* and *Pongo* along this axis, while Sts 71 has a positive score, and it is plotted between the *Pongo/Pan* and *Homo* samples. PC 2 (16.72 % of total variance) separates *Gorilla* and *Homo*, scoring negatively, from *Pan* and *Pongo*, scoring positively. On this PC both XIR-1 and RPI-128, as well as IPS 18000 overlap with *Gorilla* and *Homo*. *Sahelanthropus* has a positive PC 2 score and overlaps with both *Pongo* and *Pan* samples. Sts 71 shows a negative PC 2 score, overlapping with both *Gorilla* and *Homo*. As for the lower PCs, PC 3 (5.80 %) and PC 4 (4.10 %), again they do not visually separate any taxa, and most of them overlap with each other (Fig. S4). On PC 3, the XIR-1 reconstruction has a positive score and plotted outside of any convex hull, but closer to *Gorilla* and *Pongo*, while the RPI-128 reconstruction, also has a positive score but it is plotted away, at the extreme end of PC 3. In PC 4, the RPI-128 has a positive score, but clusters around to zero, while the XIR-1 has a negative score and overlaps with the other extant great apes and humans.

Additional PCA

The third PCA that was performed on the reduced dataset (excluding landmarks of the nasal region) showed virtually identical results with the full landmark dataset analysis (Fig. S5).

Mean Procrustes shape distances

Full landmark dataset

Based on the mean Procrustes shape distances (Table 6) the XIR-1 specimen has near equal Procrustes distance to primarily *Gorilla* (0.14) and *Pan* (0.15).

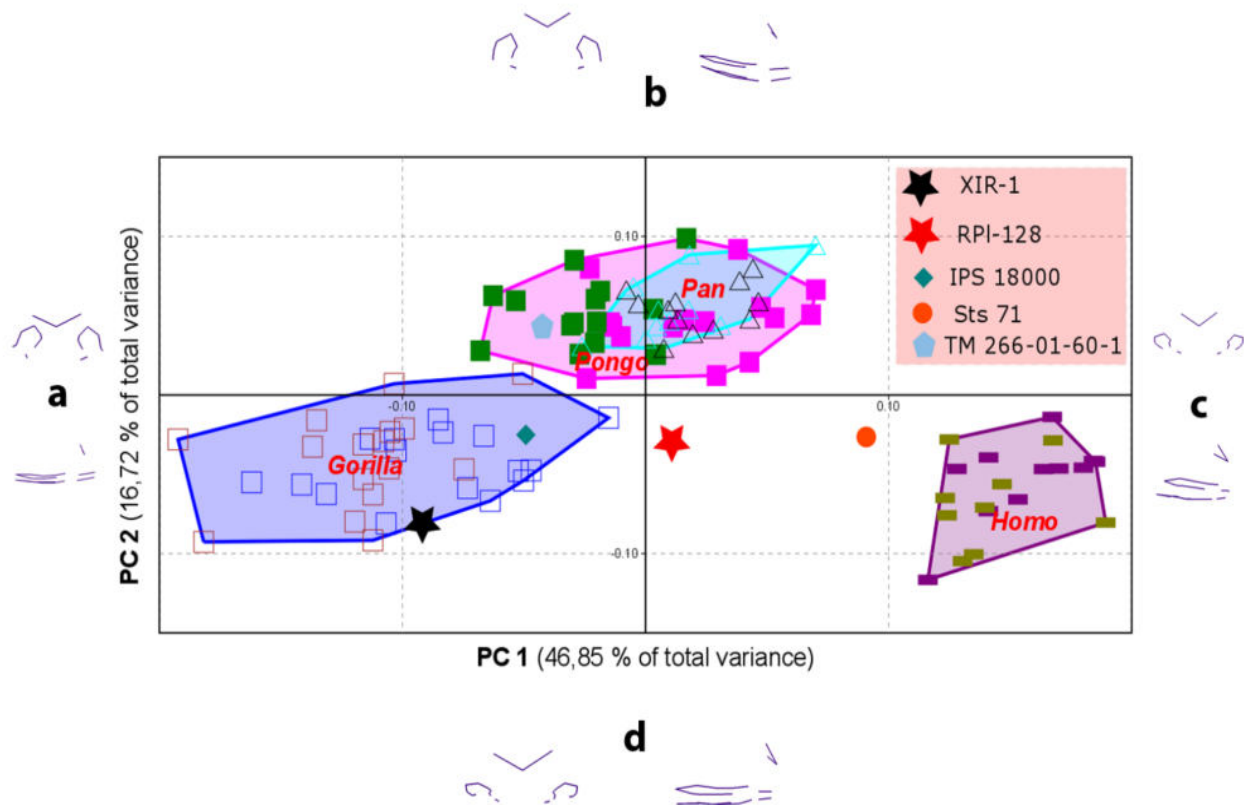


Fig. 4: PCA in shape space including the RPI-128 maxilla (maxillary landmark dataset). PC 1 explains 46.85 % and PC 2 16.72 % of total variance. Convex hulls are drawn for *Homo*, *Gorilla*, *Pan* and *Pongo*.

Maxillary landmark dataset

The XIR-1 is closer to the *Gorilla* Procrustes distance mean (Table 7), while the relationship of RPI-128 is not so clear, as its mean is similar to all the extant great apes, if we also take into account the standard deviation of each taxon (Table 8). However, the RPI-128 shows a nearer Procrustes distance to *Pongo* (0.15).

Exploration of allometry

In both analyses *Ouranopithecus* clusters with *Gorilla* mainly on PC 2. The question therefore arises whether its position on this axis might be influenced by size-related shape. We conducted a correlation analysis between PC 2 and log centroid size to address this question. While in the maxillary dataset PC 2 is not correlated with size ($r = .07$, $p = .49$; Fig. 5b), it is moderately correlated with size ($r = .49$, $p < .01$; Fig. 5a) in the full dataset analysis.

This suggests that size similarities may be in part responsible for the observed shape similarity between the two taxa, particularly in the upper face.

Table 6: Mean Procrustes shape distances among *Ouranopithecus* specimen (XIR-1) and the represented extant taxa (full landmark dataset).

Mean Procrustes shape distance	<i>Pongo</i>	<i>Gorilla</i>	<i>Pan</i>	<i>Homo</i>
<i>Ouranopithecus</i> (XIR-1)	0.17	0.14	0.15	0.25
St. deviation	±0.02	±0.01	±0.01	±0.02

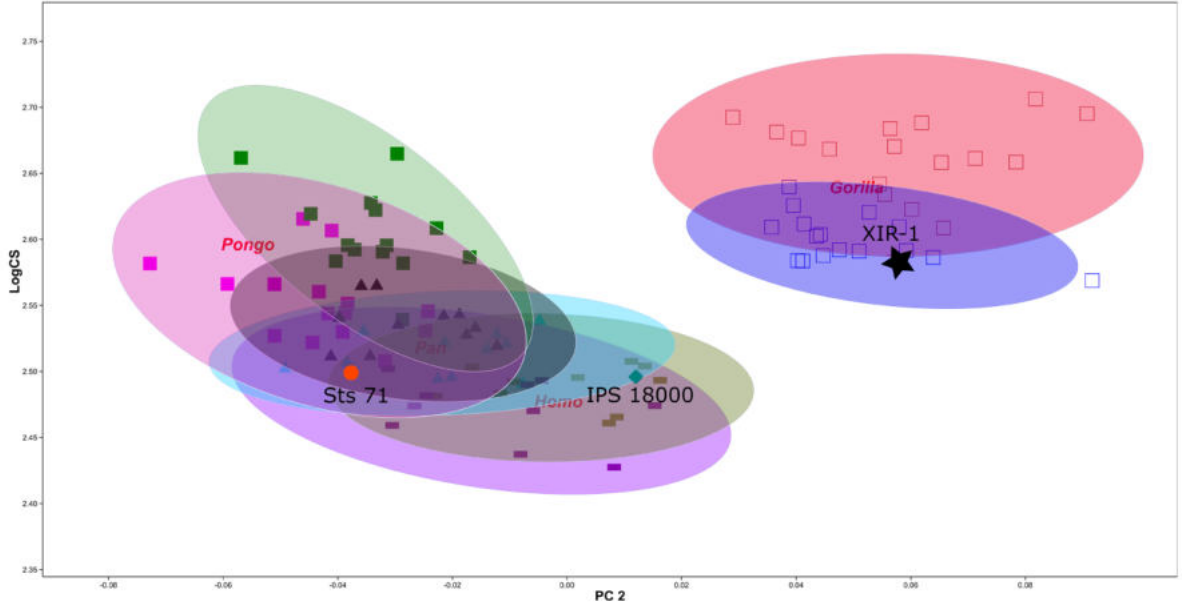
Table 7: Mean Procrustes shape distances among *Ouranopithecus* specimen (XIR-1) and the represented extant taxa (maxillary landmark dataset).

Mean Procrustes shape distance	<i>Pongo</i>	<i>Gorilla</i>	<i>Pan</i>	<i>Homo</i>
<i>Ouranopithecus</i> (XIR-1)	0.21	0.16	0.23	0.29
St. deviation	±0.02	±0.03	±0.02	±0.02

Table 8: Mean Procrustes shape distances among *Ouranopithecus* specimen (RPI-128) and the represented extant taxa (maxillary landmark dataset).

Mean Procrustes shape distance	<i>Pongo</i>	<i>Gorilla</i>	<i>Pan</i>	<i>Homo</i>
<i>Ouranopithecus</i> (RPI-128)	0.15	0.19	0.18	0.21
St. deviation	0.02	0.03	0.01	0.02

a.



b.

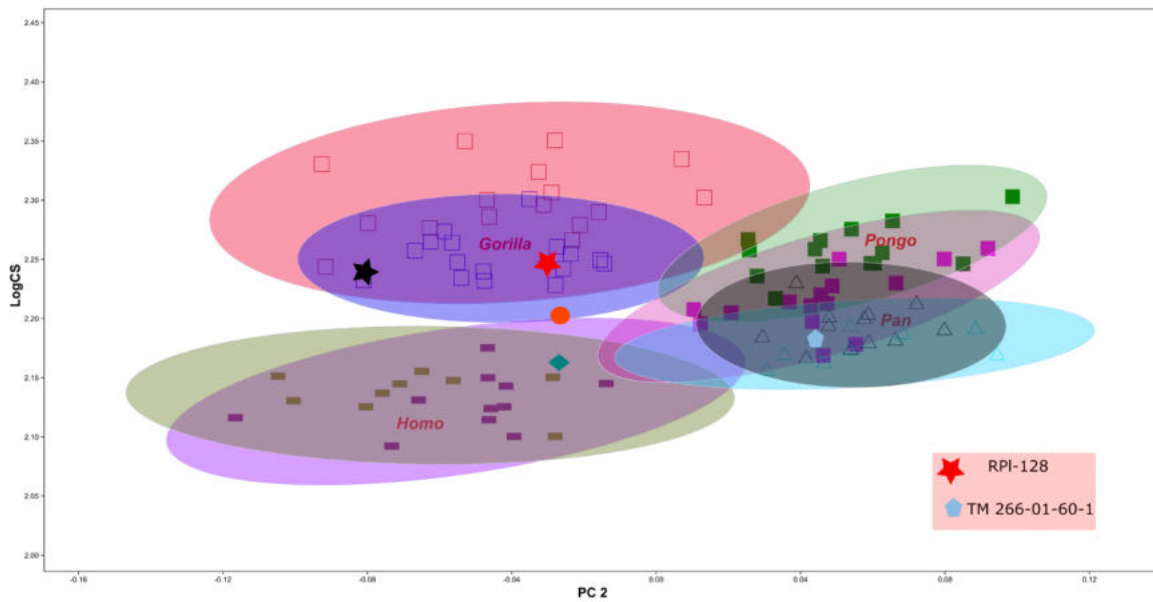


Fig. 5: Correlation between the second PC and centroid size **a.** in full landmark dataset and **b.** in maxillary landmark dataset. Density ellipses are drawn for *Homo* (purple for females and olive green for males), *Gorilla* (blue for females and brown for males), *Pan* (aqua blue for females and black for males) and *Pongo* (fuchsia for females and green for males).

Discriminant function analysis

Full landmark dataset

For this analysis the first six PCs were used, which account for more than 80 % of the variance. The first two discriminant axes account for 98.5 % of the variance and separate all taxa clearly, with *Pan* and *Pongo* plotting closest to each other and *Homo* and *Gorilla* most distinct along axes 1 and 2, respectively (Fig. 6). XIR-1 again plots within the *Gorilla* convex hull, whereas IPS 18000 falls outside any of the extant taxa convex hulls, between the *Gorilla*, *Pan*, and *Pongo* samples (Fig. 6). Sts 71 also falls outside any convex hull, but closer to *Pan*. XIR-1 and IPS 18000 are classified as *Gorilla*, with 99.9 % and 71.4 % posterior probability respectively, while Sts 71 is classified as *Pan* with a 71.4 % posterior probability. Overall cross-validation classification success of the analysis was 98.1 % (Table 9).

Maxillary landmark dataset

Here, the eight first PCs were used, accounting for more than 80 % of the variance. The first two discriminant axes account for 98.6 % of the variance and separate almost all taxa, with *Homo* separated from all extant great apes along axis 1, and *Gorilla* separated from *Pan* and *Pongo* along axis 2. XIR-1 and IPS 18000 plot within the *Gorilla* convex hull along axes 1 and 2, whereas RPI-128 falls outside any of the extant taxa convex hulls, but closer to *Gorilla* (Fig. 7). TM 266-01-60-1 plots within the *Pongo* and just outside the *Pan* convex hull, while Sts 71 falls close to *Homo*. Both *O. macedoniensis* specimens (XIR-1 and RPI-128) and IPS 18000 are classified as *Gorilla*, with 99.9 %, 89.7 %, and 95.8 % posterior probability, respectively. Sts 71 is classified as *Homo* (99.9 % posterior probability) and TM 266-01-60-1 as *Pongo* (98.5 % posterior probability). This analysis has a lower overall cross-validation classification success at 85.4 %, probably due to the reduced number of variables included (Table 10).

Table 9: Classification and cross validation results of the discriminant function analysis (full landmark dataset).^a

		Species	Predicted Group Membership				Total
			<i>Pongo</i>	<i>Gorilla</i>	<i>Pan</i>	<i>Homo</i>	
Cross-validated	Count	<i>Pongo</i>	28	0	1	.0	29
		<i>Gorilla</i>	0	32	0	.0	32
		<i>Pan</i>	0	0	22	0	22
		<i>Homo</i>	0	1	0	19	20
	%	<i>Pongo</i>	96.6	.0	3.4	.0	100.0
		<i>Gorilla</i>	0	100.0	.0	.0	100.0
		<i>Pan</i>	0	.0	100.0	.0	100.0
		<i>Homo</i>	.0	5.0	.0	95.0	100.0

^a 100 % of original grouped cases and 97.1 % of cross-validated grouped cases were correctly classified to genus.

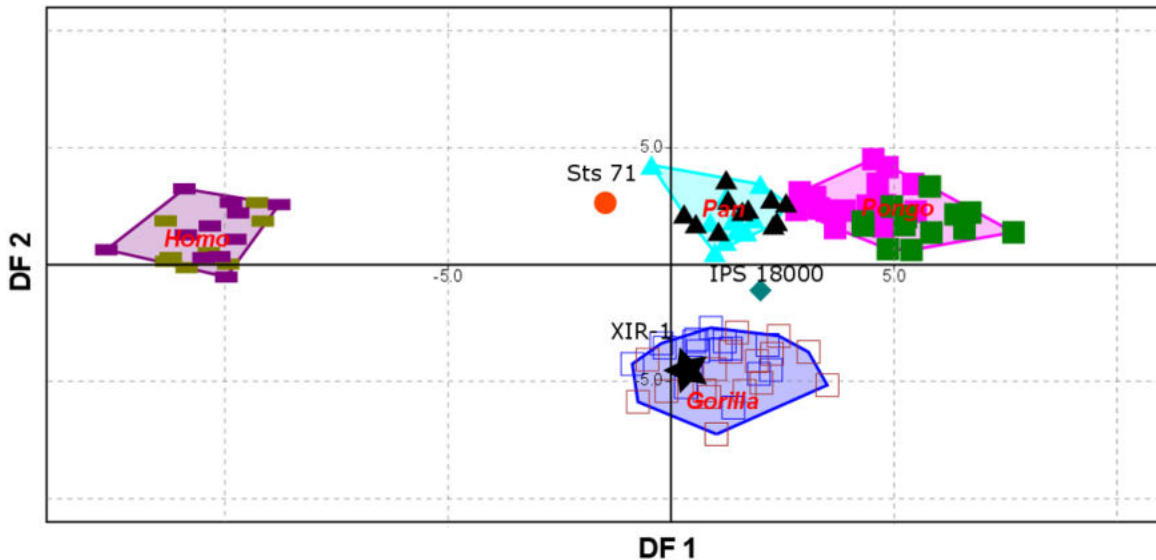


Fig. 6: Discriminant Function Analysis (DFA) using the first six components of shape space (full landmark dataset). Convex hulls are drawn for *Homo* (purple for females and olive green for males), *Gorilla* (blue for females and brown for males), *Pan* (aqua blue for females and black for males) and *Pongo* (fuchsia for females and green for males).

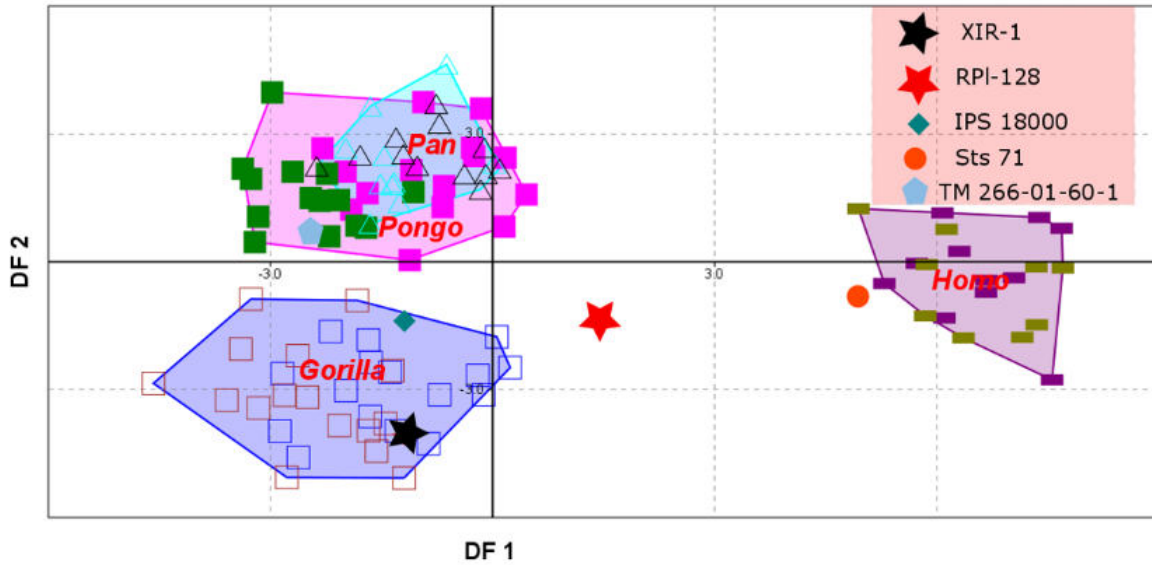


Fig. 7: Discriminant Function Analysis (DFA) using the first eight components of shape space (maxillary landmark dataset). Convex hulls are drawn for *Homo* (purple for females and olive green for males), *Gorilla* (blue for females and brown for males), *Pan* (aqua blue for females and black for males) and *Pongo* (fuchsia for females and green for males).

Table 10: Classification and cross validation results of the discriminant function analysis (maxillary landmark dataset).^a

		Species	Predicted Group Membership				Total
			<i>Pongo</i>	<i>Gorilla</i>	<i>Pan</i>	<i>Homo</i>	
Cross-validated	Count	<i>Pongo</i>	22	0	7	0	29
		<i>Gorilla</i>	0	32	0	0	32
		<i>Pan</i>	7	0	14	1	22
		<i>Homo</i>	0	0	0	20	20
	%	<i>Pongo</i>	75.9	.0	24.1	.0	100.0
		<i>Gorilla</i>	.0	100.0	.0	.0	100.0
		<i>Pan</i>	31.8	.0	63.6	4.5	100.0
		<i>Homo</i>	.0	.0	.0	100.0	100.0

^a 89.3 % of original grouped cases and 85.4 % of cross-validated grouped cases were correctly classified to genus.

3.4 Discussion

The fossil record of Miocene hominoids is scarce, and their phylogenetic relationships are still debated (e.g., Alba, 2012; Begun et al., 2012; Köhler et al., 2001; McNulty et al., 2015; Moyà-Solà et al., 2009). Several hypotheses have been proposed regarding the phylogenetic position of *Ouranopithecus macedoniensis*. One view suggests that *O. macedoniensis* is the sister group of the Mio–Pliocene hominins, *Australopithecus* and *Homo*, as it shares several characteristics with them (de Bonis & Koufos, 1994, 2001, 2004). Although some of these features are primitive retentions (e.g., large interorbital distance, shape of the mandibular symphysis), others have been proposed to be synapomorphies for the hominin lineage (e.g., symmetric P3, canine reduction, masticatory robusticity; de Bonis & Koufos, 2001). However, some authors argued instead that these features are actually homoplasies (Begun, 1992, 2009), and that *Ouranopithecus* lacks characters that are shared between chimpanzees and *Australopithecus* for instance (e.g., structure of the premaxilla, frontal bone, and molar proportions, Begun, 1992, 2002, 2009). The same authors suggested strong similarities between *O. macedoniensis* and dryopithecines, proposing that together they form the sister group of hominins and African apes (Begun, 1994, 2002; Begun & Kordos, 1997).

In this view, hominoids emerged in Africa in the early Miocene, but expanded to Eurasia and dispersed from there during the middle Miocene. This hypothesis also implies a Eurasian origin of hominins (Begun, 2002, 2015; Begun et al., 1997). Dean and Delson (1992), commenting on the results of a previous study (Begun, 1992), suggested that *Ouranopithecus* (referred as *Graecopithecus*) shows a greater similarity to *Gorilla* (as well as to *Pan* and *Australopithecus*), than to *Dryopithecus* specimens. They argued that specific areas in the *Ouranopithecus* facial anatomy, such as the orbital margin shape and the supraorbital torus, are similar to *Gorilla*. They presented alternative cladograms, including *Dryopithecus* and *Ouranopithecus* within Homininae and also suggested that *Ouranopithecus* may be a sister-taxon of *Gorilla*. The fossil record of *Gorilla* is practically unknown, and it was only recently suggested that *Chororapithecus* (dating to 8 Ma; Katoh et al., 2016) from Kenya could be related to the *Gorilla* lineage (Suwa et al., 2007). Finally, a study by Köhler et al. (2001) suggested that *Ouranopithecus* along with the Asian Upper Miocene hominoid *Lufengpithecus* should be attributed to the genus *Ankarapithecus*, and together to form one

of the four groups of fossil hominoids present the Miocene in Eurasia. Based on cranial and postcranial comparisons, Köhler et al. (2001) further suggested that several dryopithecines from Eurasia, including *O. macedoniensis*, share affinities with *Pongo* and can be considered ancestral to the pongines.

Only two previous studies have applied a geometric morphometrics approach to the analysis of *Ouranopithecus*. McNulty (2005) tried to assess the affinities of the Eurasian hominoids *Hispanopithecus* and *Rudapithecus* (referred as *Dryopithecus*), *Ouranopithecus* (referred as *Graecopithecus*) and *Sivapithecus* with 3D geometric morphometrics, focusing on the supraorbital region. He found that the morphology of the supraorbital torus of *Ouranopithecus* is linked to *Gorilla* and to the dryopithecines (*Hispanopithecus* and *Rudapithecus*), supporting the hypotheses of Dean and Delson (1992) and Begun (1992). Macchiarelli et al., (2009) used a reconstruction of a juvenile mandible of *O. macedoniensis* to assess its phylogenetic and taxonomic position through the dentine enamel junction morphology and the study of inner dental features. Their results did not clearly support any of the hypotheses outlined above. Although these authors suggest a phylogenetic relationships of *O. macedoniensis* with the African apes and humans, its dentition did not clearly support this view, as it showed no significant similarities with these taxa.

The results of our study show that the facial shape of *O. macedoniensis*, as captured by the landmarks used here, is most similar to *Gorilla*. Our PCA results show that *O. macedoniensis* falls either within (XIR-1) or closest to (RPI-128) the *Gorilla* convex hull (Fig. 5 and 6). An additional shape analysis using the full Procrustes shape distances shows that the XIR-1 is closer to the mean of primarily *Gorilla*, in both full and maxillary landmark dataset. The RPI-128 does not show a clear relationship, as the mean Procrustes shape distances of all great apes are similar to each other, however it shows a nearest Procrustes distance to *Pongo*. Moreover, both specimens are classified as a *Gorilla* in our DFA. The *H. laietanus* cast that is used in our analysis (although highly reconstructed) is plotted either with or close to the *Gorilla* sample as well. *Hispanopithecus* and *Ouranopithecus* are among the different hominoid taxa that were present in Eurasia during the middle to Late Miocene, and therefore this result supports a hypothesis in which the hominins could have evolved from a Eurasian taxon (Begun, 2002, 2015; Begun et al., 1997). Moreover, no special relationship between

Ouranopithecus and the hominins or the pongines included in our analysis is found. In our full landmark PCA, the *Australopithecus africanus* reconstruction (Sts 71) is grouped with the *Pan* sample, while when using the reduced maxillary dataset, it is plotted close to *Homo*. As for *Sahelanthropus tchadensis*, a proposed early hominin, it is placed within the *Pongo* convex hull in the PCA and is also classified as *Pongo*, a result that should be taken with caution. Nevertheless, no relationship with *O. macedoniensis* is observed. The large size of the *Ouranopithecus* face raises the question whether its similarities with *Gorilla* may be due to allometry. PC2, which in both analyses places the *Ouranopithecus* specimens with *Gorilla*, shows no relationship to size in the maxillary dataset, but is mildly correlated with size in the full dataset. This suggests that their similarity in size may partially affect the observed similarity of *Ouranopithecus* and *Gorilla*.

The results of this study are obtained only from similarity analyses, without taking into account cladistics which are based on evolutionary trends between primitive and derived characters, and thus phylogenetic implications only from the results of this analysis cannot be drawn. To link *Ouranopithecus* to the *Gorilla* clade, the former should share derived characters with the latter. In general, the characters used for phylogenetic analyses of the Miocene hominoids are dental (e.g., canine and postcanine tooth morphology, canine reduction and enamel thickness), cranial (e.g., cranial vault size and position of foramen magnum), and facial features (e.g., shape of orbits, supraorbital torus morphology, zygomatic bones), with the latter to be the focus of our shape analysis. Our results show that the similarity between *Ouranopithecus* (XIR-1) and *Gorilla* is driven by a similar shape of the nasoalveolar area, a feature considered ancestral (Begun, 1992; de Bonis & Koufos, 1997, 2001), but also by similarities in their orbital shape and their supraorbital torus morphology, traits that are proposed to be derived (de Bonis & Koufos, 1996, 1997, 2001). Unfortunately, the polarity of these features is not universally accepted. Furthermore, our shape analysis relies on landmarks which perhaps do not capture the totality of relevant information. For example, although the supraorbital torus is accepted as a derived character, different authors suggest that features on the *Ouranopithecus* supraorbital torus are similar to hominins (de Bonis & Koufos, 2001), African apes and humans (Begun, 1992), *Gorilla* (Dean & Delson, 1992), or *Pongo* (Köhler et al., 2001). Moreover, the relative value of these

characters for reconstructing phylogeny is unclear. Although facial morphology has been used to infer phylogeny (see e.g., Harvati, 2003; Lahr, 1996; Lockwood et al., 2004), previous work has shown the face to be influenced not only by phylogeny, but also by other factors including dietary and environmental adaptation in recent humans (see e.g., Harvati & Weaver, 2006; Noback & Harvati, 2015; Reyes-Centeno et al., 2017), and thus not to be the most reliable indicator of phylogenetic relationships. The present study is a first step in quantifying the facial morphology of *Ouranopithecus* and placing it in the context of hominoid morphological variation.

In summary, our results show that *Ouranopithecus macedoniensis* groups phenetically with *Gorilla*, relative to *Pan*, *Pongo*, or *Homo*. Moreover, *Ouranopithecus* and *Gorilla* share both primitive and derived facial characters, as captured from the landmarks used in our analysis. It is important to note that our study is based on observations of phenetic similarities between the XIR-1 and RPI-128 specimens and the comparative sample used, which was mainly comprised of extant taxa and very few fossil hominoids. Future work should aim to corroborate or reject these results by analyzing the different anatomical elements of *Ouranopithecus* by including a rigorous cladistic framework, and by expanding comparative samples to include additional Miocene hominoid specimens, so as to establish a clearer image of the relationships between the different taxa.

ACKNOWLEDGMENTS

This work was supported by the German Academic Exchange Service (DAAD), the Senckenberg Gesellschaft für Naturforschung, the Leventis Foundation and the Deutsche Forschungsgemeinschaft (DFG INST 37/706-1). We are grateful to Prof. D. Begun and K. Pitiri, University of Toronto, for the surface scan of the virtual reconstruction of *Hispanopithecus laietanus*. We are also very thankful to Prof. M. Brunet, Dr. F. Guy, and Dr. D. Neaux from the University of Poitiers, for the authorization and registration of the 3D landmarks on the *Sahelanthropus* cranium. We also thank Dr. C. Hemm and Dr. O. Kullmer, from the Senckenberg Museum of Natural History in Frankfurt, and Dr. S. Merker and C. Leidenroth, from the Natural History Museum in Stuttgart, for access to their collection of great apes. We also want to thank Dr. K. Helgen and Dr. M. Tocheri, from the Smithsonian National Museum of Natural History in Washington, D.C., for the USNM scans used (<http://>

humanorigins.si.edu/evidence/3d-collection/primate). These scans were acquired through the generous support of the Smithsonian 2.0 Fund and the Smithsonian's Collections Care and Preservation Fund. We are also grateful to Dr. M. Noback and Prof. N. Lynnerup, from the University of Copenhagen, for kindly giving us access to *Homo sapiens* scans. Finally, we thank the Transvaal Museum in Pretoria, South Africa and the Department of Anthropology, University of Vienna, for the copyrights regarding the CT images and data obtained from Sts 71, which are vested in the Northern Flagship Institution, Pretoria, South Africa. Lastly, the helpful comments of the associate editor and two anonymous reviewers helped improve this work.

REFERENCES

- Adams, D. C., & Otárola-Castillo, E. (2013). geomorph: An R package for the collection and analysis of geometric morphometric shape data. *Methods in Ecology and Evolution*, 4(4), 393–399.
- Alba, D. M. (2012). Fossil apes from the Vallès-Penedès basin. *Evolutionary Anthropology: Issues, News, and Reviews*, 21(6), 254–269.
- Bayome, M., Park, J. H., & Kook, Y. A. (2013). New three-dimensional cephalometric analyses among adults with a skeletal class I pattern and normal occlusion. *The Korean Journal of Orthodontics*, 43(2), 62–73.
- Begun, D. R. (1992). Miocene fossil hominids and the chimp-human clade. *Science*, 257(5078), 1929–1933.
- Begun, D. R. (1994). Relations among the great apes and humans: New interpretations based on the fossil great ape *Dryopithecus*. *American Journal of Physical Anthropology*, 37(S19), 11–63.
- Begun, D. R. (2002). European hominoids. In W. C. Hartwig (Ed.), *The primate fossil record* (pp. 339–368). Cambridge: Cambridge University Press.
- Begun, D. R. (2009). Dryopithecines, Darwin, de Bonis, and the European origin of the African apes and human clade. *Geodiversitas*, 31(4), 789–816.
- Begun, D. R. (2015). Fossil record of Miocene hominoids. In: W. Henke, & Tattersall (Eds.), *In Handbook of Paleoanthropology* (pp. 1261–1332). Berlin, Heidelberg: Springer.

- Begun, D. R., & Kordos, L. (1997). Phyletic affinities and functional convergence in *Dryopithecus* and other Miocene and living hominids. In: C.R. Begun, C. V. Ward, & M. D. Rose (Eds.), *In Function, phylogeny, and fossils* (pp. 291–316). Boston, MA: Springer.
- Begun, D. R., Nargolwalla, M. C., & Kordos, L. (2012). European Miocene hominids and the origin of the African ape and human clade. *Evolutionary Anthropology: Issues, News, and Reviews*, 21(1), 10–23.
- Begun, D. R., Ward, C. V., & Rose, M. D. (1997). Events in hominoid evolution. In: D. R. Begun, C. V. Ward, & M. D. Rose (Eds.), *In Function, phylogeny, and fossils* (pp. 389–415). Boston, MA: Springer.
- Bookstein, F. L. (1997). Landmark methods for forms without landmarks: Morphometrics of group differences in outline shape. *Medical Image Analysis*, 1(3), 225–243.
- Broom, R., Schepers, G. W. H., & Schepers, G. W. H. (1946). The South African fossil ape-men: The Australopithecinae (No. 2). Pretoria, South Africa: Transvaal Museum.
- Brunet, M., Guy, F., Pilbeam, D., Lieberman, D. E., Likius, A., Mackaye, H. T., ... Vignaud, P. (2005). New material of the earliest hominid from the Upper Miocene of Chad. *Nature*, 434(7034), 752–755.
- Brunet, M., Guy, F., Pilbeam, D., Mackaye, H. T., Likius, A., Ahounta, D., ... de Bonis, L. (2002). A new hominid from the Upper Miocene of Chad, Central Africa. *Nature*, 418(6894), 145–151.
- de Bonis, L. (1974). Première découverte d'un primates hominoïde dans le Miocène supérieur de Macédoine (Grèce). *Comptes rendus de l'Académie des Sciences, Paris, série D*, 278, 3063–3066.
- de Bonis, L., Bouvrain, G., Geraads, D., & Koufos, G. D. (1990). New hominid skull material from the late Miocene of Macedonia in Northern Greece. *Nature*, 345(6277), 712–714.
- de Bonis, L., & Koufos, G. D. (1993). The face and the mandible of *Ouranopithecus macedoniensis*: Description of new specimens and comparisons. *Journal of Human Evolution*, 24(6), 469–491.
- de Bonis, L., & Koufos, G. D. (1994). Our ancestors' ancestor: *Ouranopithecus* is a Greek link in human ancestry. *Evolutionary Anthropology: Issues, News, and Reviews*, 3(3), 75–83.

- de Bonis, L., & Koufos, G. D. (1996). Phyletic relationships and taxonomic assessment of *Ouranopithecus macedoniensis* (Primates, Mammalia). *Current Primatology Ecology and Evolution*, 13, 295–301.
- de Bonis, L., & Koufos, G. D. (1997). The phylogenetic and functional implications of *Ouranopithecus macedoniensis*. In D. R. Begun, C. V. Ward, & M. D. Rose (Eds.), *Function, phylogeny, and fossils: Miocene hominoid evolution and adaptations* (pp. 317–326). New York: Plenum.
- de Bonis, L., & Koufos, G. D. (2001). Phylogenetic relationships of *Ouranopithecus macedoniensis* (Mammalia, Primates, Hominoidea, Hominidae) of the late Miocene deposits of Central Macedonia (Greece). In L. Bonis, G. D. Koufos, & P. Andrews (Eds.), *Phylogeny of the neogene hominoid primates of Eurasia* (pp. 254–268). Cambridge, UK: Cambridge University Press.
- de Bonis, L., & Koufos, G. D. (2004). *Ouranopithecus* et la date de séparation des hominoïdes modernes. *Comptes Rendus Palevol*, 3(4), 257–264.
- de Bonis, L., & Koufos, G. D. (2014). First discovery of postcranial bones of *Ouranopithecus macedoniensis* (Primates, Hominoidea) from the late Miocene of Macedonia (Greece). *Journal of Human Evolution*, 74, 21–36.
- de Bonis, L., Koufos, G. D., Guy, F., Peigné, S., & Sylvestrou, I. (1998). Nouveaux restes du primate hominoïde *Ouranopithecus* dans les dépôts du Miocène supérieur de Macédoine (Grèce). *Comptes Rendus de l'Académie des Sciences-Series IIA-Earth and Planetary Science*, 327 (2), 141–146.
- de Bonis, L., & Melentis, J. (1977). Les Primates hominoïdes du Vallésien de Macédoine (Grèce). Étude de la mâchoire inférieure. *Geobios*, 10(6), 849–885.
- de Bonis, L., & Melentis, J. (1978). Les Primates hominoïdes du Miocène supérieur de Macédoine—Étude de la mâchoire supérieure. *Annales de Paléontologie (vertébrés)*, 64, 185–202.
- Dean, D., & Delson, E. (1992). Second gorilla or third chimp? *Nature*, 359 (6397), 676–677.
- Goodall, C. (1991). Procrustes methods in the statistical analysis of shape. *Journal of the Royal Statistical Society: Series B (Methodological)*, 53(2), 285–321.

- Gunz, P., Mitteroecker, P., Neubauer, S., Weber, G. W., & Bookstein, F. L. (2009). Principles for the virtual reconstruction of hominin crania. *Journal of Human Evolution*, 57(1), 48–62.
- Guy, F., Brunet, M., Schmittbuhl, M., & Viriot, L. (2003). New approaches in hominoid taxonomy: Morphometrics. *American Journal of Physical Anthropology: The Official Publication of the American Association of Physical Anthropologists*, 121(3), 198–218.
- Hammer, O., Harper, D. A., & Ryan, P. D. (2001). PAST: paleontological statistics software package for education and data analysis. *Palaeontologia electronica*, 4(1), 9.
- Harvati, K. (2003). Quantitative analysis of Neanderthal temporal bone morphology using three-dimensional geometric morphometrics. *American Journal of Physical Anthropology*, 120(4), 323–338.
- Harvati, K., Stringer, C., Grün, R., Aubert, M., Allsworth-Jones, P., & Folorunso, C. A. (2011). The later stone age calvaria from Iwo Eleru, Nigeria: Morphology and chronology. *PLoS One*, 6(9), e24024.
- Harvati, K., & Weaver, T. D. (2006). Human cranial anatomy and the differential preservation of population history and climate signatures. *The Anatomical Record Part A: Discoveries in Molecular, Cellular, and Evolutionary Biology: An Official Publication of the American Association of Anatomists*, 288(12), 1225–1233.
- Jackson, J. E. (2005). A user's guide to principal components (Vol. 587). New York, NY: John Wiley & Sons.
- Katoh, S., Beyene, Y., Itaya, T., Hyodo, H., Hyodo, M., Yagi, K., ... Nakaya, H. (2016). New geological and palaeontological age constraint for the gorilla–human lineage split. *Nature*, 530(7589), 215.
- Köhler, M., Solà, S. M., & Alba, D. M. (2001). Eurasian hominoid evolution in the light of recent *Dryopithecus* findings. In *Hominoid evolution and climatic change in Europe, Vol. 2: phylogeny of the Neogene hominoid primates of Eurasia* (pp. 193–212). Cambridge: Cambridge University Press.
- Koufos, G. D. (1993). Mandible of *Ouranopithecus macedoniensis* (Hominidae, Primates) from a new late Miocene locality of Macedonia (Greece). *American Journal of Physical Anthropology*, 91(2), 225–234.

- Koufos, G. D. (1995). The first female maxilla of the hominoid *Ouranopithecus macedoniensis* from the late Miocene of Macedonia, Greece. *Journal of Human Evolution*, 29(4), 385–399.
- Koufos, G. D., & de Bonis, L. (2006). New material of *Ouranopithecus macedoniensis* from late Miocene of Macedonia (Greece) and study of its dental attrition. *Geobios*, 39(2), 223–243.
- Koufos, G. D., Kostopoulos, D. S., & Vlachou, T. D. (2016). Revision of the Nikiti 1 (NKT) fauna with description of new material. *Geobios*, 49 (1–2), 11–22.
- Lahr, M. M. (1996). The evolution of modern human diversity: A study of cranial variation (Vol. 18). Cambridge: Cambridge University Press.
- Lockwood, C. A., Kimbel, W. H., & Lynch, J. M. (2004). Morphometrics and hominoid phylogeny: Support for a chimpanzee–human clade and differentiation among great ape subspecies. *Proceedings of the National Academy of Sciences of the United States of America*, 101(13), 4356–4360.
- Macchiarelli, R., Mazurier, A., Illerhaus, B., & Zanolli, C. (2009). *Ouranopithecus macedoniensis* (Mammalia, Primates, Hominoidea): Virtual reconstruction and 3D analysis of a juvenile mandibular dentition (RPI-82 and RPI-83). *Geodiversitas*, 31(4), 851–863.
- McNulty, K. P. (2005). A geometric morphometric assessment of the hominoid supraorbital region: Affinities of the Eurasian Miocene hominoids *Dryopithecus*, *Graecopithecus*, and *Sivapithecus*. In: D. E. Slice (Ed.), *In Modern morphometrics in physical anthropology* (pp. 349–373). Boston, MA: Springer.
- McNulty, K. P., Begun, D. R., Kelley, J., Manthi, F. K., & Mbua, E. N. (2015). A systematic revision of *Proconsul* with the description of a new genus of early Miocene hominoid. *Journal of Human Evolution*, 84, 42–61.
- Moyà-Solà, S., Köhler, M., Alba, D. M., Casanovas-Vilar, I., Galindo, J., Robles, J. M., ... Beamud, E. (2009). First partial face and upper dentition of the middle Miocene hominoid *Dryopithecus fontani* from Abocador de Can Mata (Vallès-Penedès Basin, Catalonia, NE Spain): Taxonomic and phylogenetic implications. *American Journal of Physical Anthropology: The Official Publication of the American Association of Physical Anthropologists*, 139(2), 126–145.

- Moyà-Solà, S. M., & Köhler, M. (1993). Recent discoveries of *Dryopithecus* shed new light on evolution of great apes. *Nature*, 365(6446), 543–545.
- Moyà-Solà, S. M., & Köhler, M. (1995). New partial cranium of *Dryopithecus* Lartet, 1863 (Hominoidea, Primates) from the upper Miocene of Can Llobateres, Barcelona, Spain. *Journal of Human Evolution*, 29(2), 101–139.
- Noback, M., & Harvati, K. (2015). The contribution of diet to global human cranial variation. *Journal of Human Evolution*, 80, 34–50.
- Reyes-Centeno, H., Ghirotto, S., & Harvati, K. (2017). Genomic validation of the differential preservation of population history in the human cranium. *American Journal of Physical Anthropology*, 162, 170–179.
- Rohlf, F. J. (1999). Shape statistics: Procrustes superimpositions and tangent spaces. *Journal of Classification*, 16(2), 197–223.
- Sen, S., Koufos, G. D., Kondopoulou, D., & de Bonis, L. (2000). Magnetostratigraphy of the Late Miocene continental deposits of the lower Axios valley, Macedonia, Greece. *Geological Society Greece Special Publications*, 9, 197–206.
- Singh, N., Harvati, K., Hublin, J. J., & Klingenberg, C. P. (2012). Morphological evolution through integration: A quantitative study of cranial integration in *Homo*, *Pan*, *Gorilla* and *Pongo*. *Journal of Human Evolution*, 62 (1), 155–164.
- Singleton, M. (2002). Patterns of cranial shape variation in the Papionini (Primates: Cercopithecinae). *Journal of Human Evolution*, 42(5), 547–578.
- Slice, D. E. (1999). Morpheus et al.: Software for morphometric research. Dept. Ecology and Evolution, State Univ., New York, at Stony Brook.
- Suwa, G., Kono, R. T., Katoh, S., Asfaw, B., & Beyene, Y. (2007). A new species of great ape from the late Miocene epoch in Ethiopia. *Nature*, 448 (7156), 921–924.
- White, T. D., Black, M. T., & Folkens, P. A. (2011). *Human Osteology*. San Diego: Academic Press.
- Zollikofer, C. P., de León, M. S. P., Lieberman, D. E., Guy, F., Pilbeam, D., Likius, A., ... Brunet, M. (2005). Virtual cranial reconstruction of *Sahelanthropus tchadensis*. *Nature*, 434(7034), 755–759.

Supplementary Material

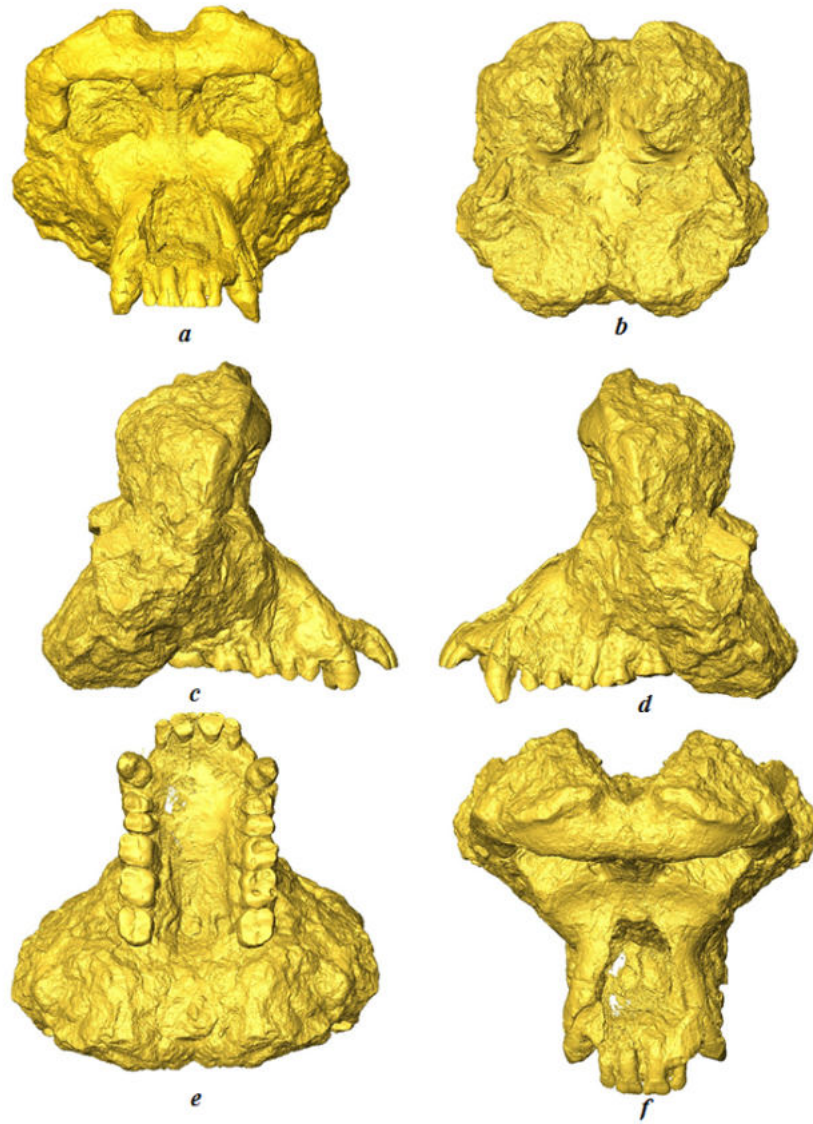


Fig. S1: The final result of the XIR-1 cranium reconstruction after merge in (a) frontal, (b) occipital, (c) right lateral, (d) left lateral, (e) basal view, and (f) superior view.

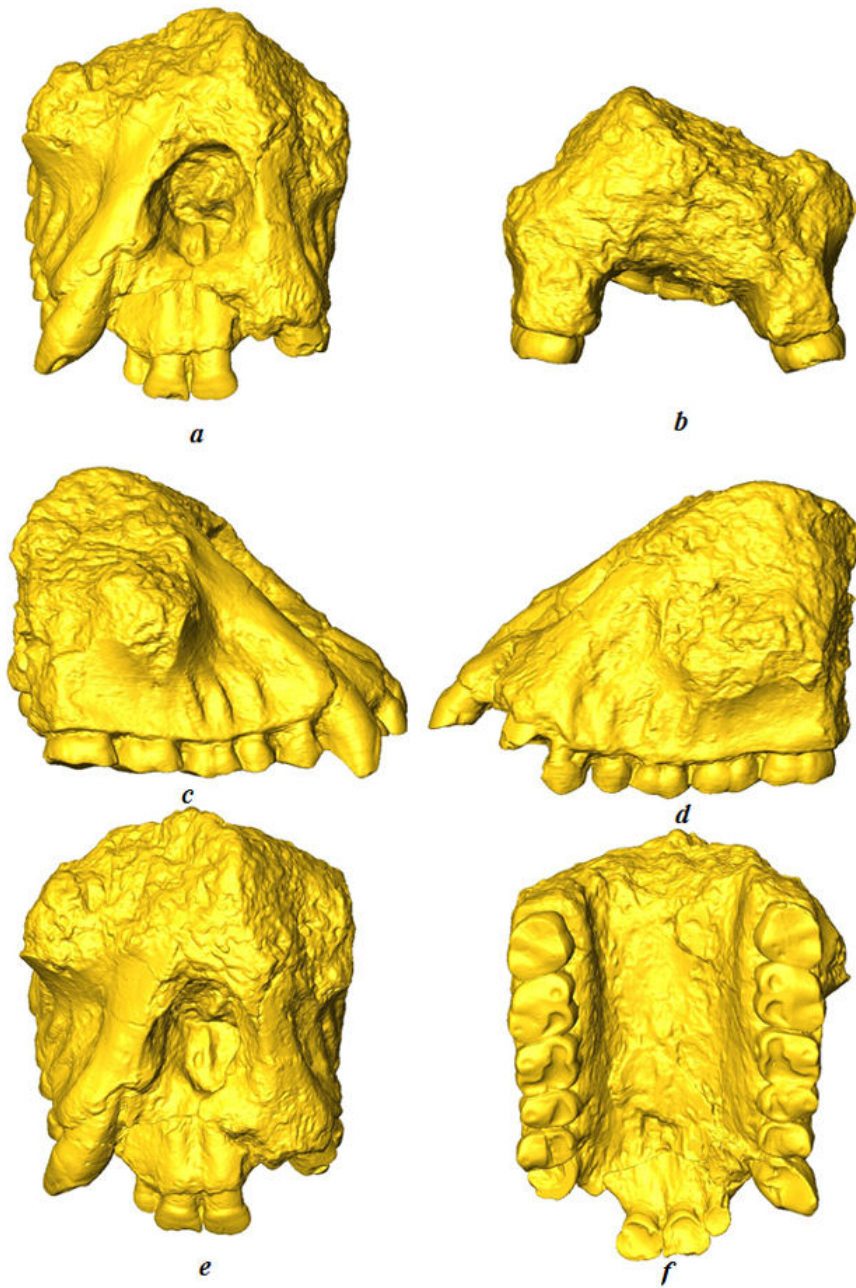


Fig. S2: The final result of the RPI-128 maxilla reconstruction after merge in (a) frontal, (b) occipital, (c) right lateral, (d) left lateral, (e) basal view, and (f) superior view.

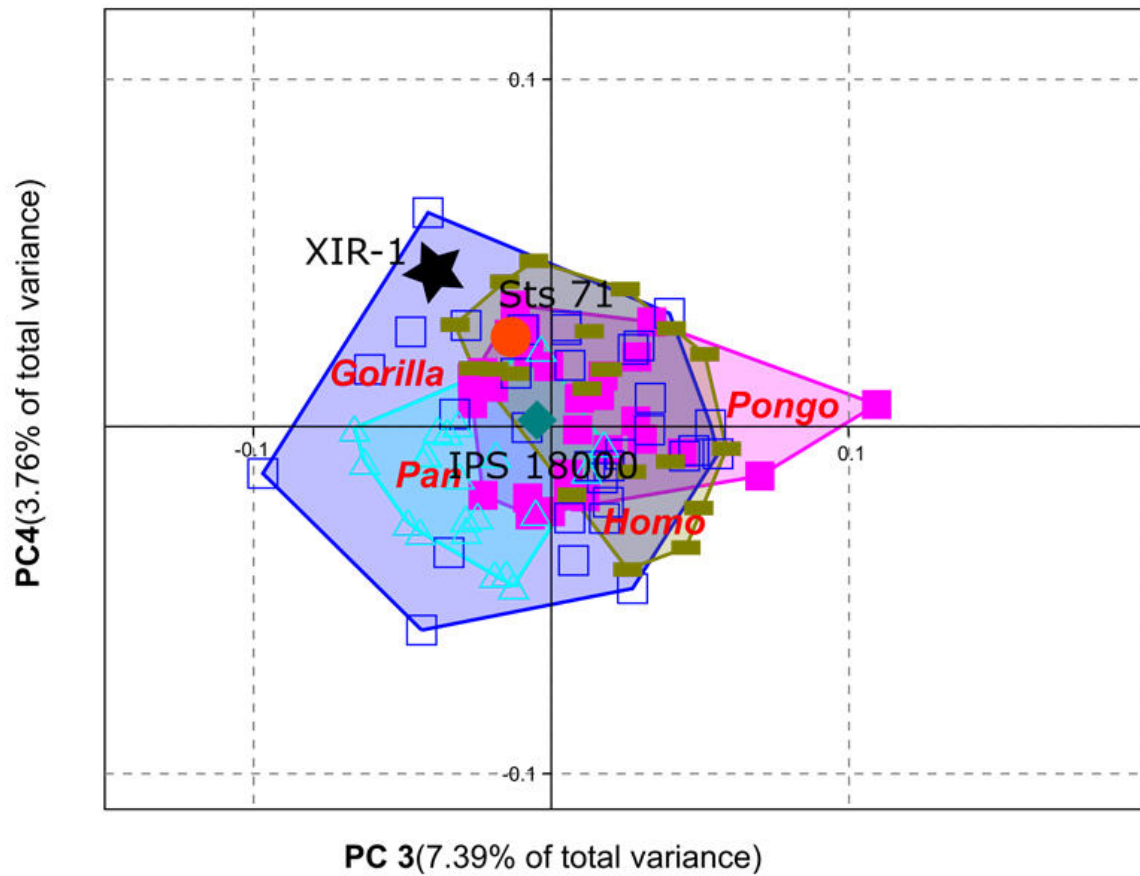


Fig. S3: PCA in shape space (full landmark dataset). PC 3 explains 7.39 % of total shape variation, while PC 4 explains 3.76 % of total shape variation. Convex hulls are drawn for *Homo*, *Gorilla*, *Pan* and *Pongo*.

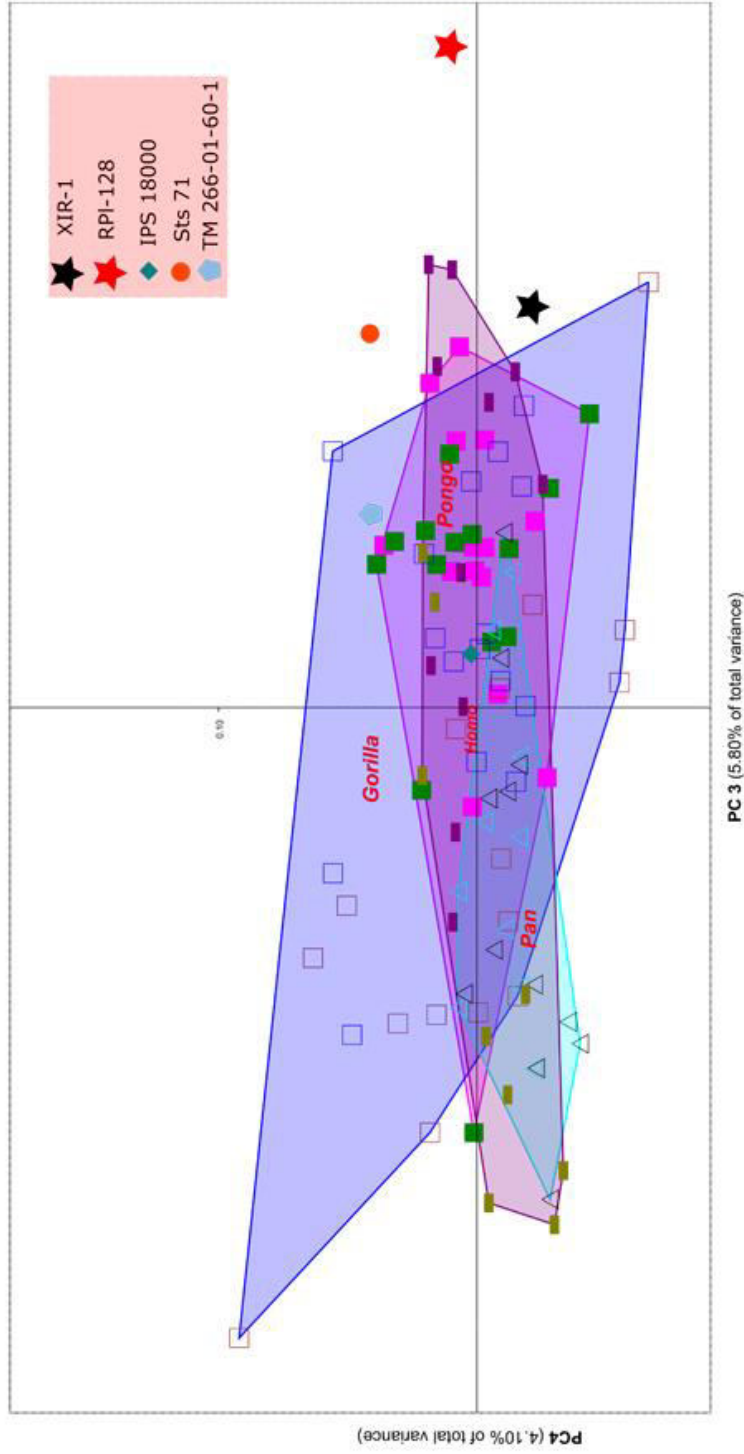


Fig. S4: PCA in shape space including the RPI-128 maxilla (maxillary landmark dataset). PC 3 explains 5.80 % of total shape variation, while PC 4 explains 4.10 % of total shape variation. Convex hulls are drawn for *Homo*, *Gorilla*, *Pan* and *Pongo*.

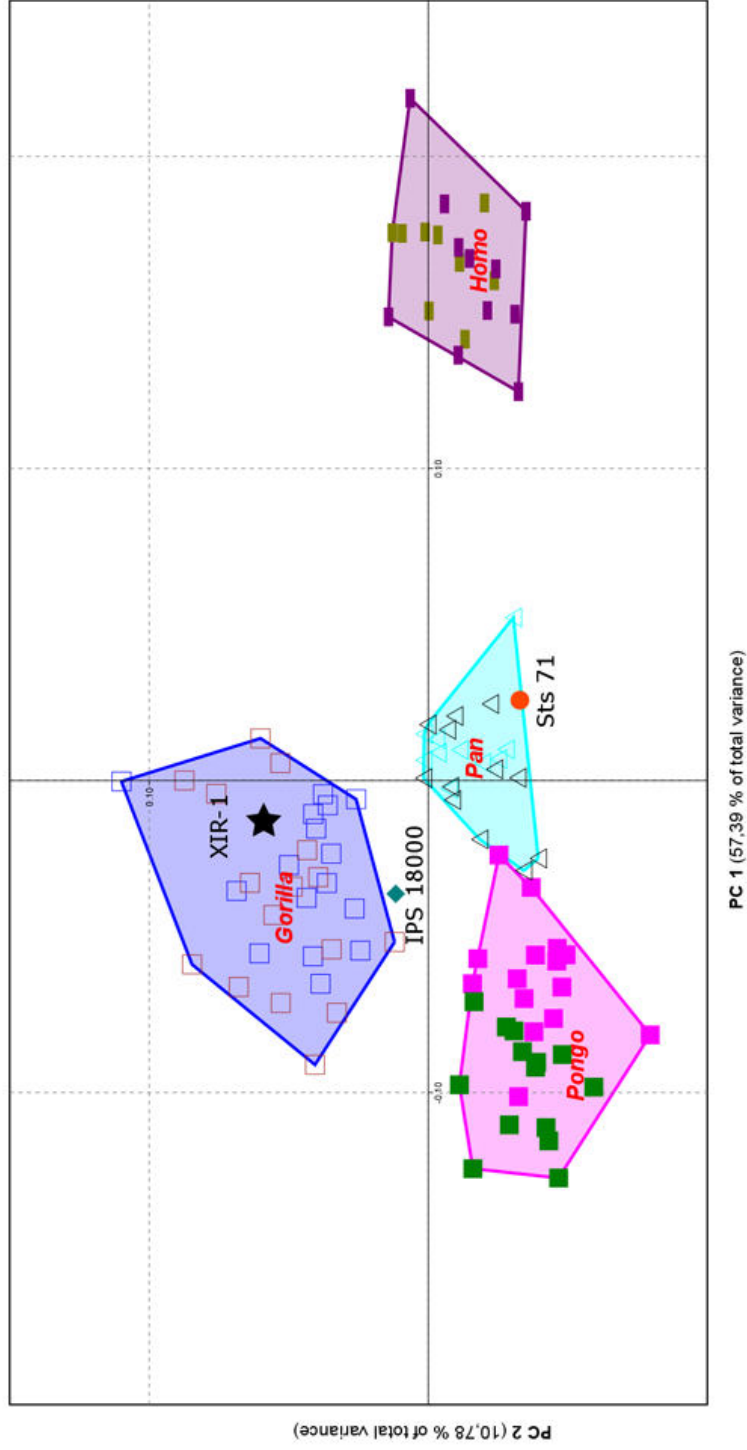


Fig. S5: PCA in shape space, excluding the landmarks around the nasal area. PC 1 explains 57.39 % of total shape variation, while PC 2 explains 10.78 % of total shape variation. Convex hulls are drawn for *Homo*, *Gorilla*, *Pan* and *Pongo*.

CHAPTER 4

Study 2

Text and analyses incorporated in this chapter are part of a manuscript that is accepted (currently in press) in the *American Journal of Physical Anthropology*.

Ioannidou M., Koufos G. D., de Bonis L. & Harvati K. 3D geometric morphometrics analysis of mandibular fragments of *Ouranopithecus macedoniensis* from the late Miocene deposits of Central Macedonia, Greece. (in press, *American Journal of Physical Anthropology*)

The original idea for this study was developed in collaboration with Prof. Dr. Harvati, Prof. Koufos and Prof. de Bonis. Regarding the data presented in this chapter, I was the main conductor and collected all data.

Author	Author position	Scientific ideas %	Data generation %	Analysis & interpretation %	Paper writing %
Ioannidou, M.	1	40	100	80	70
Koufos, G.	2	10	-	-	-
de Bonis, L.	3	10	-	-	-
Harvati, K.	4	40	-	20	30
Title of the paper	3D geometric morphometrics analysis of mandibular fragments of <i>Ouranopithecus macedoniensis</i> from the late Miocene deposits of Central Macedonia, Greece				
Status in Publication Process	Accepted (in press) in <i>American Journal of Physical Anthropology</i>				

3D geometric morphometrics analysis of mandibular fragments of *Ouranopithecus macedoniensis* from the late Miocene deposits of Central Macedonia, Greece

Abstract

Objectives: To explore mandibular shape differences between *Ouranopithecus macedoniensis* and a comparative sample of extant great apes using three-dimensional (3D) geometric morphometrics. Other objectives are to assess mandibular shape variation and homogeneity within *Ouranopithecus*, explore the effects of size on mandibular shape, and explore the degree of mandibular sexual size dimorphism *Ouranopithecus*.

Materials and methods: The comparative sample comprises digitized mandibles from adult extant great apes. The 3D analysis includes three datasets: one with landmarks registered on the mandibular corpus and symphysis of mandibles preserving both sides; one on hemimandibles only; and one focused on the ramus and gonial area. Multivariate statistical analyses were conducted, such as ordination analyses (PCA), intra-specific Procrustes distances pairs, pairwise male-female centroid size differences, and correlation analyses.

Results: The male and female specimens of *Ouranopithecus* have mandibular shapes that are quite similar, although differences exist. The Procrustes distances results suggest more shape variation in *Ouranopithecus* than in the extant great apes. *Ouranopithecus* shows some similarities in mandibular shape to the larger great apes, *Gorilla* and *Pongo*. Moreover, the degree of sexual dimorphism in the small *Ouranopithecus* sample is greater than any of the great apes. Based on our correlation analyses of principal components (PC) with size, some PCs are significantly correlated with size, with correlation varying from moderate to substantial.

Discussion: This study attempted to understand better the variation within *O. macedoniensis* and the expression of sexual dimorphism in this taxon in more detail than has been done previously. The overall mandibular morphology of *Ouranopithecus* shows some similarities to those of the larger great apes, which likely reflects similarities in size. Compared to *Gorilla* and *Pongo*, *O. macedoniensis* shows an elevated degree of morphological variation, although limitations relating to sample size apply. Sexual dimorphism in the

mandibles of *O. macedoniensis* appears to be relatively high, seemingly greater than in *Gorilla* and high even in comparison to *Pongo*, but this again is possibly in part an artifact of a small sample size.

Keywords: Hominoid evolution, Miocene hominoids, mandibular variation, sexual dimorphism, virtual anthropology

4.1 Introduction

Ravin de la Pluie (RPI) in the Axios valley is one of the three localities where the material of *Ouranopithecus macedoniensis* has been found to date. The rich material from RPI includes maxillary and mandibular remains, numerous isolated teeth, and a few postcranial specimens (de Bonis, 1974; de Bonis and Melentis, 1977, 1978; Koufos and de Bonis 2006; de Bonis et al. 1990; 1998; de Bonis and Koufos, 2014; Koufos et al., 2016a). De Bonis and Koufos (1994) interpreted the material from RPI as consisting of individuals that most probably died at the same time during a single river flood event, based on the geology of this locality. Additionally, ongoing excavations in the other two *O. macedoniensis* localities, Xirochori 1 (XIR), in the Axios valley, and Nikiti 1 (NKT), in the Chalkidiki Peninsula, have produced other very important specimens, including an almost complete face (XIR-1; de Bonis et al., 1990; Koufos, 1993, 1995). Based on faunal correlation and magnetostratigraphic evidence at these three localities, the chronostratigraphic range of *O. macedoniensis* is between 9.6 and 8.7 Ma (Koufos et al., 2016b; Sen et al., 2000).

While there are several well-preserved *O. macedoniensis* mandibles, only a few studies have been conducted on these (de Bonis and Melentis, 1977; de Bonis and Koufos, 1993, 1994; Koufos 1993). None of this previous work assessed the mandibular shape of *O. macedoniensis* using more advanced techniques, such as geometric morphometrics (GM). GM is a quantitative means of analyzing shape (Corti, 1993; Slice, 2007), and allows for more informative documentation of shape differences than traditional morphometric techniques (Adams et al., 2004; Slice, 2007).

Here we investigate the mandibular specimens from RPI, including four partial mandibles preserving both corpora and the symphysis (RPI-54, RPI-56, RPI-75, and RPI-79) and RPI-391, a right mandibular ramus (Fig. 1). Most of the specimens have well-preserved dentitions, and apart from one specimen their overall shape appears undistorted, presenting only minor taphonomic damage. With this study, we aim to explore mandibular shape variation between *Ouranopithecus* and a comparative sample of extant great apes (*Gorilla*, *Pan*, and *Pongo*), using three-dimensional (3D) geometric morphometrics. We also assess patterns of variation within *Ouranopithecus*, especially as they relate to sexual dimorphism, and compared to those of the extant great apes. Lastly, we address the effects of size-related

shape differences among taxa. Questions to be discussed in this study include, (1) Does mandibular shape vary between males and females of *Ouranopithecus macedoniensis*? (2) Is the mandibular shape of *Ouranopithecus macedoniensis* distinct from those of the extant great apes? (3) How do size and sexual dimorphism in *Ouranopithecus macedoniensis* compare to those of extant great apes?

Mandibular morphology and sexually dimorphic traits in *Ouranopithecus macedoniensis*

The mandibular shape of *Ouranopithecus* has been described previously (de Bonis and Melentis, 1977; Koufos 1993; de Bonis and Koufos, 1993, 1994) as having a primitive symphysis with well-marked superior and inferior tori, and having powerful chewing capacity, based on the morphology of the gonial area and the well-marked crest (masseteric tuberosity) (de Bonis and Koufos, 2001). It also retains an antero-posteriorly narrow mandibular condyle, a trait that differentiates it from the extant great apes, in which the condyle is more robust. Although *O. macedoniensis* is recognized as a single-species, it is characterized by strong dental sexual dimorphism in the post-canine dentition, which is greater than that of the larger great apes, *Gorilla* and *Pongo* (Schrein, 2006; Scott et al., 2009; Koufos et al., 2016a). Traits likely related to sexual dimorphism can also be observed in the mandible of *Ouranopithecus*, with male mandibles being larger and more robust than those of the females (de Bonis and Melentis, 1977; Koufos, 1993). However, dental dimorphism, particularly the morphology and size of the canines and the size of the post-canine lower teeth, is more commonly studied because of the abundance of teeth in fossil assemblages. Here, we address this imbalance by examining the expression of sexual dimorphism in the mandibles of *Ouranopithecus* in more detail than has been done previously.

4.2 Materials and Methods

Sample

***Ouranopithecus macedoniensis* specimens**

All the RPI material was micro-CT scanned at the Paleoanthropology High Resolution Computed Tomography Laboratory, University of Tübingen (Phoenix X-Ray, v/tomex/s GE, tube voltage 220 kV, tube current 210 mA, and 0.6 mm copper filter).

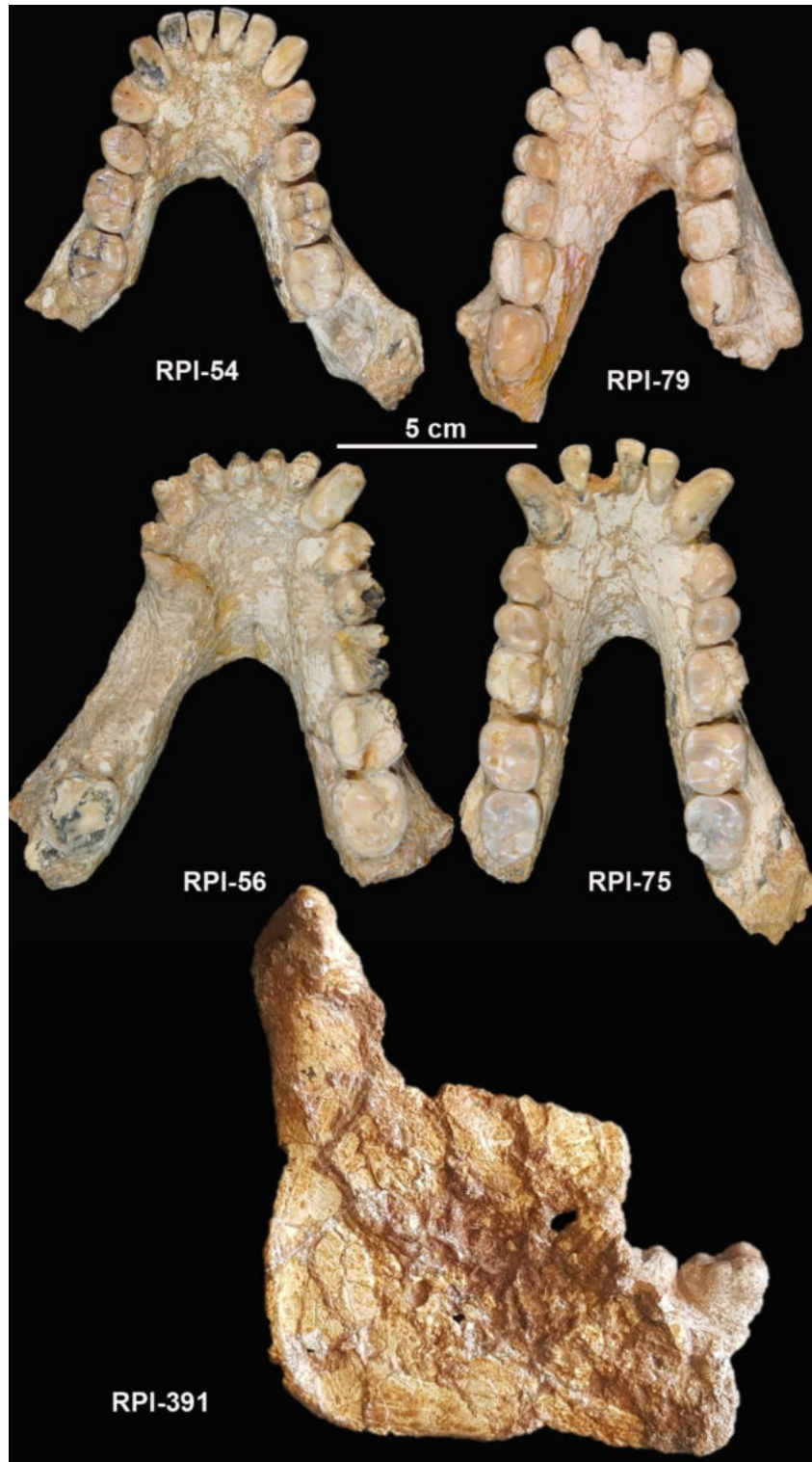


Fig. 1: The four *O. macedoniensis* partial mandibles (RPI-54, RPI-75, RPI-79 and RPI-56) and the RPI-391 ramus. Photographs by G. D. Koufos and M. Ioannidou.

RPI-54: This mandible, the type specimen of *O. macedoniensis* (first attributed to *Dryopithecus macedoniensis*; de Bonis, 1974), belongs to a late juvenile/young adult individual, and it is a female based on the size and shape of its canine (de Bonis, 1974; Kelley, 1995). It preserves the entire dentition, except the left M₃; the right M₃ is not yet erupted. The teeth are well preserved and hardly worn. Additionally, the mandible preserves both corpora and the symphysis, while both ascending rami are missing (de Bonis, 1974; de Bonis and Melentis, 1977; Fig. 1).

RPI-56: This specimen belongs to an old male individual, based on canine size and dental wear (de Bonis and Melentis, 1977). It does not preserve its entire dentition, but many teeth are present (I₁ to M₃ right; I₁ to P₃, and M₃ left). Both corpora and symphysis are well preserved, and both ascending rami are missing (de Bonis, 1974; de Bonis and Melentis, 1977; Fig. 1).

RPI-75: This specimen preserves the entire permanent dentition. Canine size and shape indicate that it belongs to a male individual (Kelley, 1995). Both corpora of the mandible are well preserved, although both are partly damaged on the lateral surface at the level of the P₄ due to post-mortem taphonomic processes. However, the overall shape is unaltered. Both ascending rami are missing (de Bonis and Melentis, 1977; Fig. 1).

RPI-79: This mandible belongs to a female individual, based on its canine size. It has an almost complete permanent dentition, as only the right M₃ is missing. The teeth are quite worn. Both corpora and symphysis of this mandible are present; however, the right corpus and symphysis exhibit displacement from the midplane due to post-mortem taphonomic processes. Both ascending rami are missing (Fig. 1).

RPI-391: This specimen probably belongs to a male individual, determined from the large size of the teeth preserved, while based on the dental wear, it is younger than RPI-75 (de Bonis and Koufos, 1993). The right ramus and part of the corpus are preserved, with M₂ and M₃ present (Fig. 1). The coronoid process is partly preserved, although its superior part is missing along with the sigmoid notch. While the overall shape appears largely undeformed, a slight flattening can be observed. Moreover, the condyle is fairly complete, preserving the

glenoid process and glenoid fossa, although the area below the condyle is broken and distorted, without altering its shape (de Bonis and Koufos, 1993, Fig. 1).

Comparative sample

53 mandibles from adult extant great apes were digitized, including *Gorilla gorilla gorilla* (n=17), *Pan troglodytes* (n=19), and *Pongo pygmaeus pygmaeus* (n=17) (Table 1). Variation in the *Pan troglodytes* sample may exist, as the subspecies composition is unknown (see Taylor and Groves, 2003; Robinson, 2012 for variation in *Pan* subspecies). All extant taxa are represented by both adult female and male individuals. Adult status was established using the criterion of full eruption of the permanent third molar. The landmarks were registered on 3D models of mandibles obtained from either medical CT scans or surface scans using the EVA Artec (Artec Group, Luxembourg, Luxembourg) handheld high precision scanner, property of the Paleoanthropology High Resolution Computed Tomography Laboratory, University of Tübingen.

Table 1: Number of extant great apes and *Ouranopithecus macedoniensis* fossils used in this study

Species	Sex		Collection*
	Male	Female	
<i>Gorilla gorilla</i>	8	9	1,2
<i>Pan troglodytes</i>	10	9	1,3,4
<i>Pongo pygmaeus</i>	9	8	2,3,4
<i>Ouranopithecus macedoniensis</i>	2	2	5

*1: Natural History Museum, Stuttgart; 2: Smithsonian National Museum of Natural History; 3: Natural History Museum, Berlin; 4: Senckenberg Museum of Natural History, Frankfurt; 5: Aristotle University, Thessaloniki

Landmarks and error test

The analysis included three datasets: one with bilateral landmarks on both mandibular corpora and symphysis (20 landmarks; Fig. 2a; Table 2); one with landmarks registered on the hemimandible (left side including corpus and symphysis; 12 landmarks); and one on the ramus and gonial area (right side; 9 landmarks in total; Fig. 2b; Table 2).

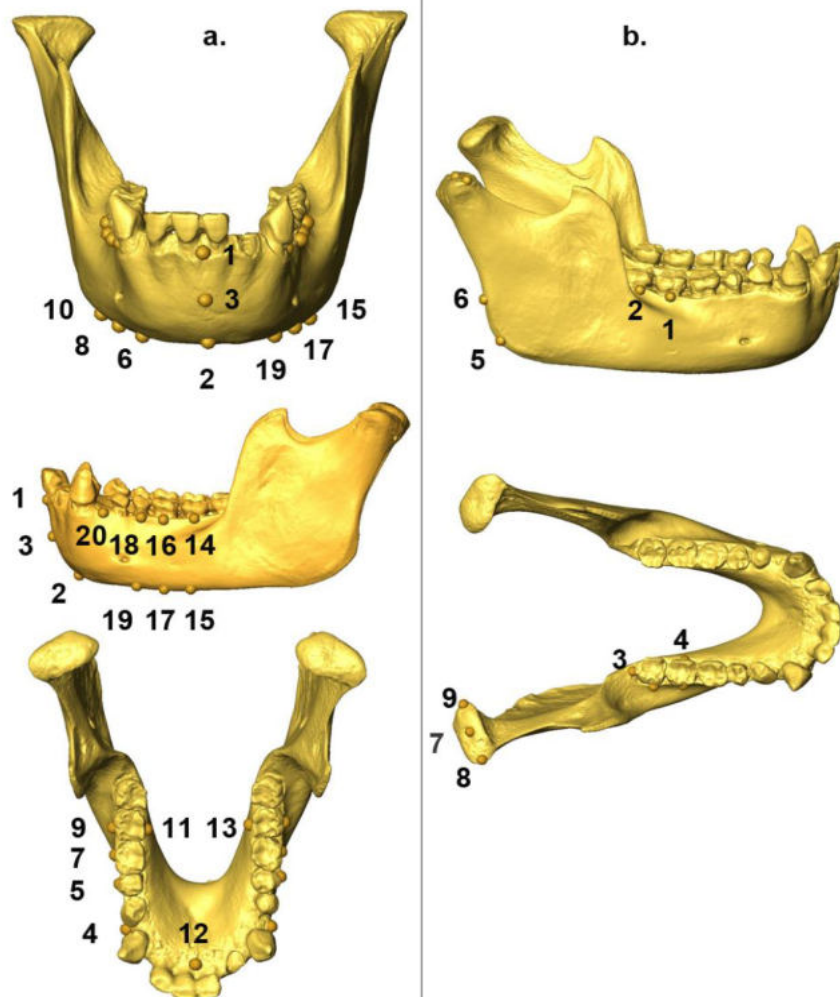


Fig. 2: Three-dimensional (3D) landmarks used in the analysis, registered on a surface scan of a female *Pan troglodytes* mandible. a. corpus and symphysis (for the hemimandible analysis landmarks 1-3 and 12-20 were used); b. ramus.

The registration of the landmarks was carried out in Avizo software (©FEI Visualization Sciences Group, version 9.1). The landmarks were collected along both corpora (bilateral analysis), symphysis, and ramus of the mandible to analyze variation in height, length, and width in the anatomical areas selected. In the first dataset, the missing landmarks of the mandible RPI-56 (landmarks 13, 14, 16, and 18) were reconstructed using reflected relabeling of the existing landmarks of the right side (Gunz et al., 2009). The second dataset

was used to include RPI-79, which was excluded from the bilateral analyses because the right side shows displacement from the mid-sagittal plane (landmarks 1-3 and 12-20 were used; Table 2). The landmarks selected for this study are a combination of landmarks (Type I, II, and III) used in previous studies by Nicholson and Harvati (2006), Miller et al. (2008), Zollikofer et al. (2009), Robinson, (2012); and Singh (2014). Type I landmarks correspond to standard identifiable osteometric points, as opposed to type II and III which mostly characterize an anatomical region (Bookstein, 1991). Most of the landmarks used in this study are Type II and III, since Type I landmarks are not easily definable on the mandible. All landmarks were collected by MI. Intra-observer error was evaluated based on a standard deviation threshold of 5 % (Robinson and Terhune, 2017), and assessed by collecting the landmarks from the same specimen 5 times, over a period of two weeks. The precision of the landmark registration was considered acceptable, as the standard deviation of each landmark was significantly lower than the threshold, ranging from 0.38-1.05 % (see Table 2).

Statistical analyses

The landmark configurations from all three datasets were subjected to generalized Procrustes analysis (GPA) in EVAN Toolbox (Version 1.6; EVAN-Society, e.V.), which superimposes (scales, translates, and rotates) all the landmark configurations and produces the superimposed Procrustes shape coordinates (Bookstein, 1997; Rohlf, 1993; Slice, 2007). A principal component analysis (PCA) was conducted on all the datasets in shape space, using PAST (Version 4.05; Hammer et al., 2001). The PCA in shape space was performed on the Procrustes shape coordinates in order to examine the overall mandibular shape variation of all specimens. We also conducted permutation tests between sexes of each extant species (separately) to test if there are sex differences in each species, using R (Geomorph package; Adams and Otárola-Castillo, 2013; 1000 permutations). While Procrustes superimposition eliminates size as a variable, it does not eliminate allometric size-related effects. We, therefore, conducted a correlation analysis between the first two principal components and log centroid size (on all datasets), using Pearson's correlation coefficient, to investigate whether the distribution of the specimens in the PCA is influenced by size. In addition, we used Procrustes distances to explore shape difference within the *Ouranopithecus* sample

compared to that present in each of the extant species. Using boxplots, we compared all pairwise distances in *Ouranopithecus* with those of each extant ape. The differences in the means of inter-individual distances among *Ouranopithecus* and the extant great apes were tested for significance (one-way ANOVA in SPSS; IBM® SPSS® Statistics 27).

We also calculated the 95 % probability intervals from all pairwise Procrustes distances for each great ape species and located the pairwise distances for *Ouranopithecus* with respect to these. These analyses were performed in order to investigate whether there is more variation in the small *Ouranopithecus* sample than in the extant great apes. To investigate the degree of sexual dimorphism expressed by the *Ouranopithecus* mandibles, and to compare it to levels of sexual dimorphism in the extant great apes, we plotted the pairwise *Ouranopithecus* male-female centroid size differences within a distribution of all male-female pairwise differences for each extant great ape, using boxplots. We also calculated the differences between the male and female centroid means, which were also tested for significance (only great apes; independent-samples t-test were run in SPSS). As the sample size of *Ouranopithecus* is so small (and there is only 1 female specimen in the bilateral analysis), the significance test could not be performed.

Table 2: List of landmarks, definitions, and intra-observer error: bilateral and ramus analyses. For the hemimandible analysis the landmarks used are: 1-3 and 12-20.

Count	Landmarks	Definition (Type)	Error (%)
<i>Bilateral analysis</i>			
1	Infradentale (id)	Midline point at the superior tip of the alveolar border between the mandibular central incisors* (Type I/II)	0.38
2	Gnathion (gn)	Most anterior midline point on the chin of the mandible* (Type I/II)	0.65
3	Mid-point between landmarks 1 (id) and 2 (gn)	Point in-between landmarks 1 (id) and 2 (gn) (Type III)	0.96
4, 20	C - P ₃ alveolar R/L	Point on alveolar border between C and P ₃ (Type II)	0.72/0.80
5, 18	P ₄ superior R/L	Midline point of the P ₄ alveolus (Type II)	0.62/0.65
6, 19	P ₄ inferior R/L	Point on the bottom of the mandibular corpus below P ₄ (Type II)	1.05/0.77
7, 16	M ₁ superior R/L	Midline point of the M ₁ alveolus (Type II)	0.52/0.70
8, 17	M ₁ inferior R/L	Point on the bottom of the mandibular corpus below M ₁ (Type II)	0.88/0.90

9, 14	M ₂ superior R/L	Midline point the middle of the M ₂ alveolus (Type II)	0.59/0.61
10, 15	M ₂ inferior R/L	Point on the bottom of the mandibular corpus below M ₂ (Type II)	0.98/1.02
11, 13	Endomolare R/L	Most medial point on the inner surface of the alveolar margin opposite the center of the M ₂ crown*(Type III)	1.04/0.90
12	Mandibular orale	Most superior tip at the lingual side of the alveolar border between central incisors (Type II)	0.70
Ramus			
1	Right M ₂ superior	Point at the middle of the M ₂ alveolus (Type II)	0.74
2	Right M ₃ superior	Point at the middle of the M ₃ alveolus (Type II)	0.70
3	Right midpoint distal M ₃ alveolar border	Midpoint on the distal surface of the alveolar margin of the M ₃ (Type III)	0.48
4	Right endomolare	Most medial point on the inner surface of the alveolar margin opposite the center of the M ₂ crown*(Type III)	0.88
5	Right gonion (g)	Most lateral, posterior, and inferior point at the vertex of the curve of the mandibular angle (Type III)	0.79
6	Right posterior ramus	Point at the posterior margin of ramus at level of M ₃ (Type II)	0.93
7	Right condyle superior	Most superior point on the mandibular condyle (Type III)	0.50
8	Right condyle lateral	Most lateral point on the mandibular condyle (Type III)	0.74
9	Right condyle medial	Most medial point on the mandibular condyle (Type III)	0.62

*as defined in White et al., 2011

4.3 Results

Principal component analysis

Bilateral analysis: Fig. 3a displays the first two principal components (PCs), which together account for 57.75 % of total shape variation. PC 1 is associated with changes in the length of the mandible and width of the dental arcade, and PC 2 with symphysis height. The scores along these first two PCs show a clear separation among all three extant taxa, although there is some overlap between the convex hulls of *Gorilla* and *Pongo*. The permutation tests show significant male-female differences along the PC axes in *Pongo* (Goodall's F statistics = 2.94, $p < 0.01$), but not in *Gorilla* and *Pan* (Goodall's F statistics = 1.19, $p = 0.29$; Goodall's F statistics =

1.83, $p = 0.06$; respectively). The male *Ouranopithecus* specimens (RPI-75 and RPI-56) plot close together, outside of any convex hull and on the negative end of PC 1, while the single female (PRI-54) plots within the *Gorilla* convex full.

Low PC 1 scores (37.89 % of total shape variation) indicate a relatively antero-posteriorly elongate mandible and medio-laterally narrow dental arcade relative to mandibular length, while high scores indicate a relatively antero-posteriorly shorter mandible and medio-laterally wider dental arcade (Fig. 3a i. and ii. respectively). Low PC 2 scores (19.86 % of total shape variation) indicate a relatively supero-inferiorly shallow corpus and symphysis, while high scores reflect a relatively supero-inferiorly deeper corpus and symphysis (Fig. 3a iii. and iv. respectively). When the first two PCs were tested for correlation against long centroid size, PC 1 was significantly correlated with centroid size ($r = -0.67$, $p < 0.01$), while PC 2 was not ($r = -0.08$, $p = 0.51$).

The male mandibles of *Ouranopithecus* are antero-posteriorly elongate with a relatively medio-laterally narrow dental arcade, while female mandibular shape is antero-posteriorly shorter and has a relatively medio-laterally wider dental arcade. The mandibles of *Ouranopithecus* also have a relatively supero-inferiorly deep corpus and symphysis, deeper than many individuals of *Gorilla*, but relatively shallower than many *Pan* and *Pongo* individuals. However, overall the shape is more similar to the mandibular shape of the larger great apes, *Pongo* and *Gorilla*, than *Pan*.

Hemimandible: The first two PCs account for 50.67 % of total shape variance (Fig.3b). Although there is partial overlap among the convex hulls of the extant taxa, the three great ape genera are relatively distinct along these axes. The permutation tests show no significant male-female difference in *Gorilla* (Goodall's F statistics= 1.56, $p = 0.12$), while this difference is significant in *Pan* and *Pongo* (Goodall's F statistics= 2.48, $p < 0.01$; Goodall's F statistics= 2.23, $p < 0.01$; respectively). Three of *Ouranopithecus* specimens cluster on the positive end of PC1, with RPI-54 being slightly negative, outside the convex hulls of the extant taxa, but closer to those of *Gorilla* and *Pongo*. RPI-75 plots relatively distant from the other male (RPI-56), and two female specimens. As for size-PC correlations, PC1 is moderately but significantly correlated with centroid size ($r = -0.43$, $p < 0.01$), while PC2 is not ($r = -0.15$, $p = 0.26$). High PC1 scores (32.61 % of total shape variation) indicate a relatively antero-

posteriorly elongate hemimandible, while low scores indicate a relatively antero-posteriorly shorter hemimandible. Low PC2 scores (18.06 % of total shape variation) indicate a relatively supero-inferiorly shallow corpus, while high scores reflect a relatively supero-inferiorly deeper corpus.

Ramus: Fig. 4 displays the first two PCs, which together account for 69.24 % of total shape variation. The convex hulls of the three extant taxa all overlap somewhat along these two axes. The permutation tests show no significant difference between females and males along the PC axes in *Gorilla* and *Pan* (Goodall's F statistics = 2.01, $p=0.08$; Goodall's F statistics= 1.95, $p= 0.09$; respectively); while differences are significant in *Pongo* (Goodall's F statistics= 4.46, $p<0.01$). RPI-391 plots within the *Pongo* convex hull. High PC 1 scores (51.42 % of total variance) indicate a relatively more inferiorly and laterally positioned gonion with respect to the corpus, whereas low scores indicate a relatively more superiorly and medially positioned gonion.

High PC 2 scores (17.82 % of total variance) indicate a relatively wider gonial angle, while low PC 2 scores indicate a relatively narrow angle. In this dataset, PC 1 was significantly but mildly correlated with centroid size ($r=0.39$, $p<0.01$), while PC 2 was not ($r=-0.24$, $p=0.08$). The ramus shape of *Ouranopithecus*, as it is represented by RPI-391, exhibits a relatively narrow gonial angle, similar to that of *Pongo* specimens.

Procrustes Distances

Bilateral analysis: The distances between the three *Ouranopithecus* specimens were either at the upper end or just outside the maximum range of the intra-specific distances of the extant species (Fig. 5a, Table 3). The distances between the three *Ouranopithecus* mandibles fell within the 95 % probability interval of the observed distribution of intra-specific pairwise distances of *Gorilla*, while they fell outside in the respective 95 % probability intervals of *Pan* and *Pongo* (Fig. 6; Table S1). Moreover, there are significant differences in the means of the inter-individual distances between *Ouranopithecus* and *Pan* and *Pongo*, while they are not significant between *Ouranopithecus* and *Gorilla* (Table 4).

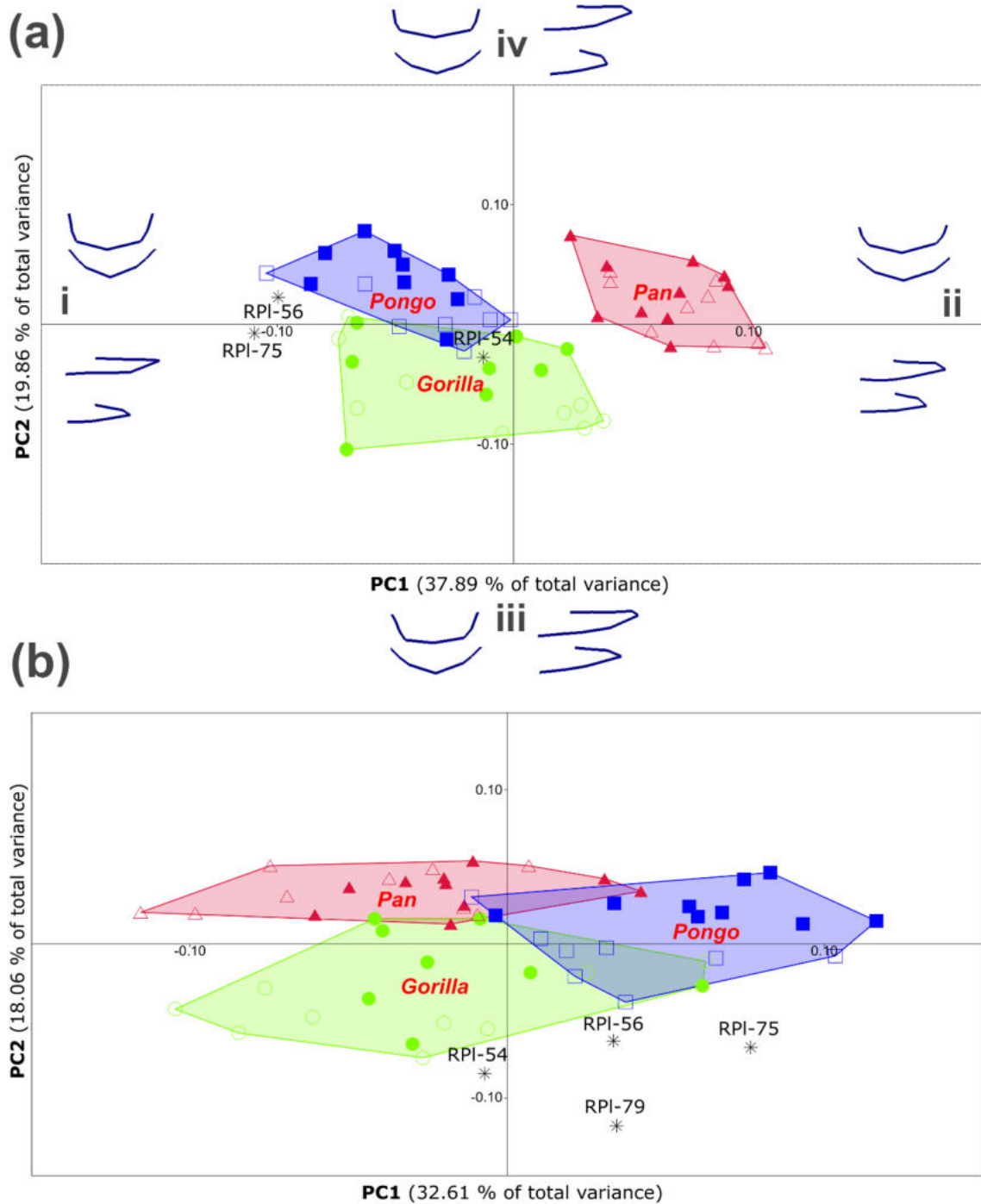


Fig. 3: PCA results of the bilateral (a.) and hemimandible (b.) analyses in shape space: a. PC 1 (37.89 %) vs PC 2 (19.86 %). **i-iv:** Shape changes, in frontal and lateral view, for negative and positive extreme values associated with PC 1 (i. and ii.) and PC 2 (iii. and iv.); and b. PC 1 (32.61 %) vs PC 2 (18.06 %). Convex hulls for *Gorilla* - green circle; male (filled symbol), female (open symbol), *Pan* - red triangle; male (filled symbol), female (open symbol) and *Pongo* - blue square; male (filled symbol), female (open symbol).

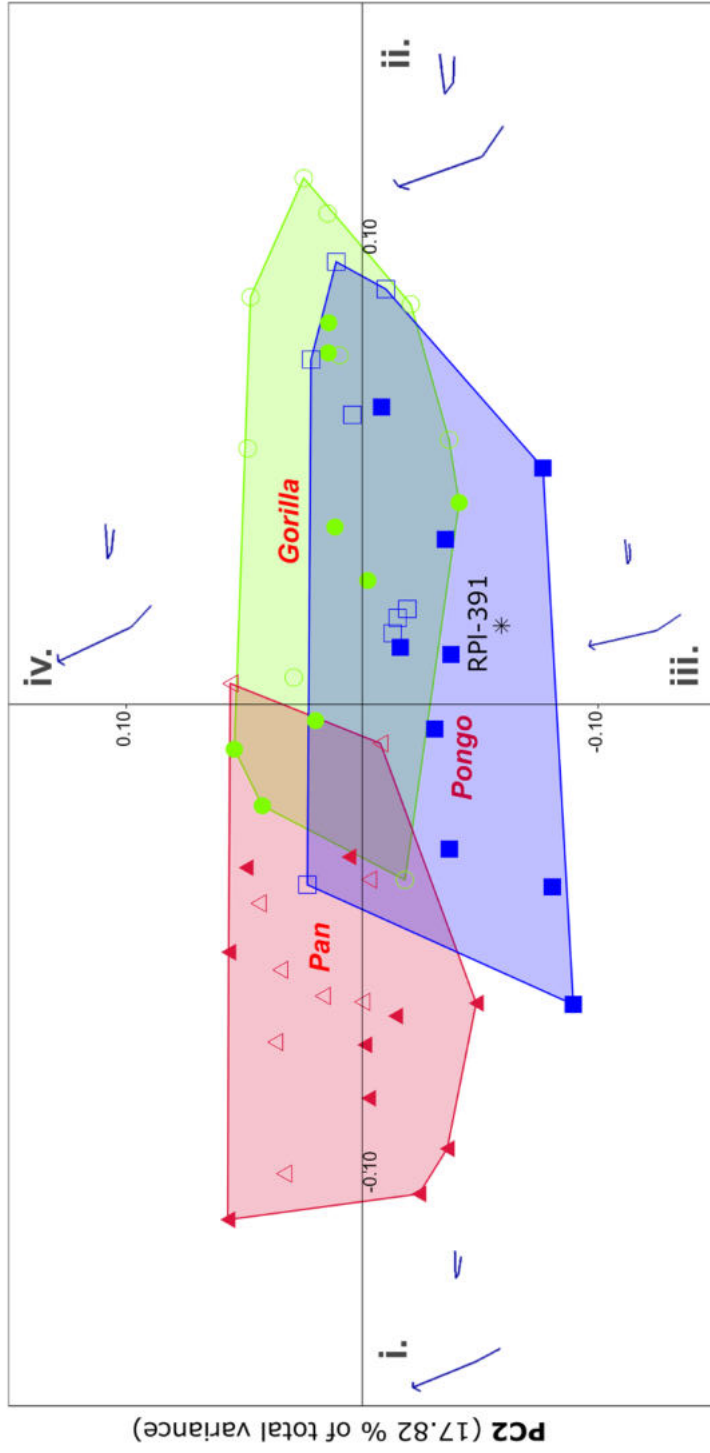


Fig. 4: PCA results of the ramus dataset in shape space: PC 1 (51.42 %) vs PC 2 (17.82 %). **i-iv:** Shape changes, in lateral view, for negative and positive extreme values associated with PC 1 (i. and ii.) and PC 2 (iii. and iv.)

Table 3: Intra-specific distance statistics of *Ouranopithecus* and the extant great apes.

	Mean	SD
Bilateral analysis		
<i>O. macedoniensis</i>	0.16	0.01
<i>G. gorilla</i>	0.12	0.03
<i>P. troglodytes</i>	0.09	0.02
<i>P. pygmaeus</i>	0.10	0.02
Hemimandible		
<i>O. macedoniensis</i>	0.15	0.01
<i>G. gorilla</i>	0.12	0.03
<i>P. troglodytes</i>	0.10	0.02
<i>P. pygmaeus</i>	0.11	0.02

Table 4 Inter-individual variability among *Ouranopithecus* and the extant great apes (one-way ANOVA).

Species	<i>O. macedoniensis</i>	<i>G. gorilla</i>	<i>P. troglodytes</i>	<i>P. pygmaeus</i>
Bilateral analysis				
<i>O. macedoniensis</i>	-	ns	p< 0.01	p< 0.01
<i>G. gorilla</i>		-	p< 0.01	p< 0.01
<i>P. troglodytes</i>		p< 0.01	-	ns
<i>P. pygmaeus</i>		p< 0.01		-
Hemimandible				
<i>O. macedoniensis</i>	-	ns	p< 0.01	p< 0.01
<i>G. gorilla</i>		-	p< 0.01	p< 0.01
<i>P. troglodytes</i>		p< 0.01	-	ns
<i>P. pygmaeus</i>		p< 0.01		-

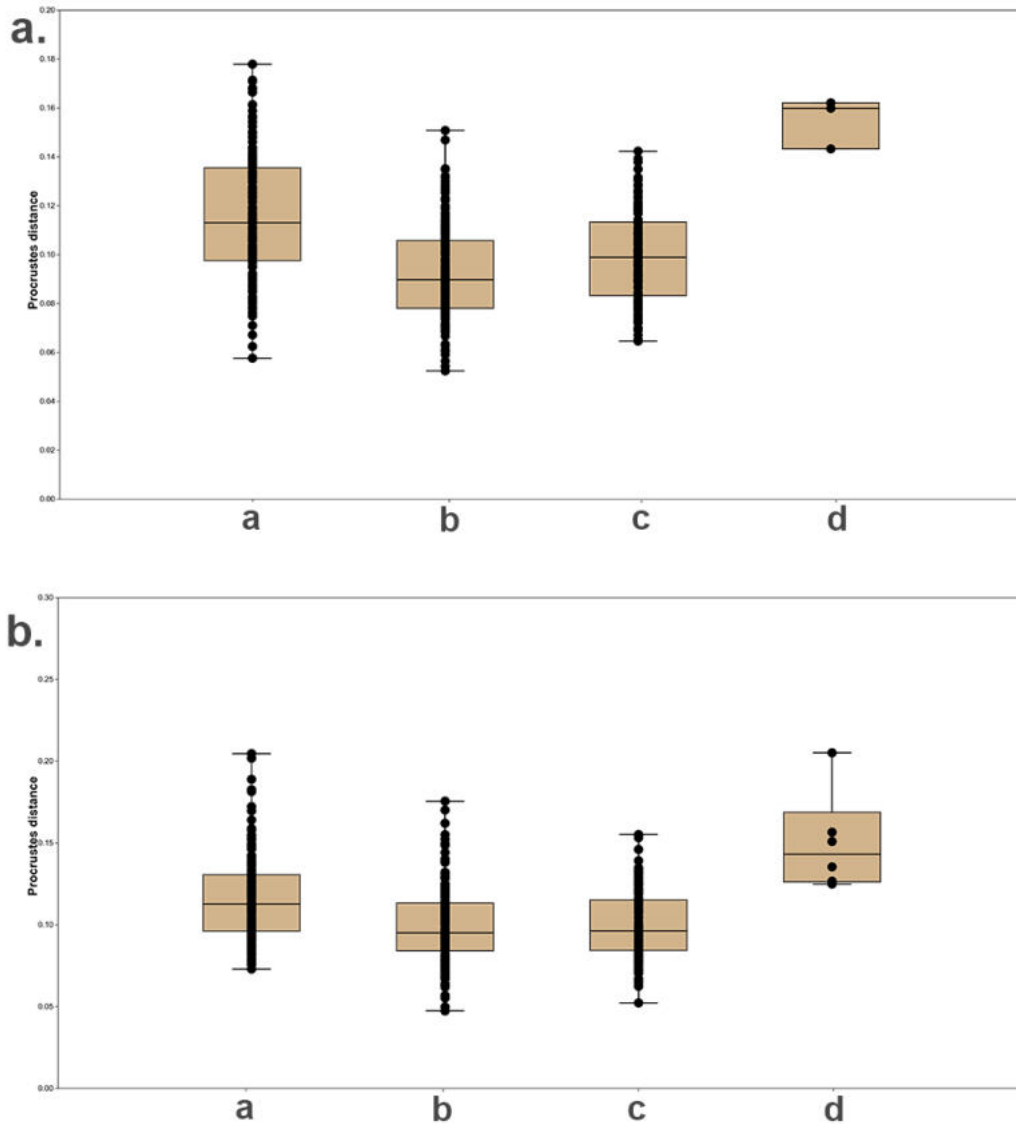


Fig. 5: Boxplots of the intra-specific Procrustes distances pairs of the great apes and *O. macedoniensis*, a. bilateral and b. hemimandible analyses. a: *Gorilla-Gorilla*, b: *Pongo-Pongo*, c: *Pan-Pan*, d: *Ouranopithecus-Ouranopithecus*.

Hemimandible: Similar to the bilateral analysis, the Procrustes distances between the four *Ouranopithecus* specimens were at the upper end of the intra-specific distances of the extant species (Fig. 5b, Table 3). The pairwise distances between the *Ouranopithecus* hemimandibles fell within the 95 % probability interval of *Gorilla* (Fig. 7a-c), except for the pairwise Procrustes distance between RPI-79 and RPI-56. Three of the *Ouranopithecus*

pairwise distances (RPI-79 and RPI-56; RPI-79 and RPI-75; RPI-56 and RPI-75) fell outside the 95 % probability interval in the observed distribution of the intra-specific ranges of *Pan* and *Pongo* (Fig. 7; Table S2). Differences in the means of the inter-individual distances between *Ouranopithecus* and *Pan* and *Pongo* are significant, while they are not significant between *Ouranopithecus* and *Gorilla* (Table 4).

Ramus: As there is only one specimen belonging to *Ouranopithecus macedoniensis*, we could only check to which individual the RPI-391 showed the closest Procrustes distance: it is most similar in its overall shape to a male *Pongo* individual (Table S3).

Sexual dimorphism

Bilateral analysis: Fig. 8a contains boxplots showing the pairwise male-female centroid size differences in the extant great apes and *Ouranopithecus*. The largest differences are in *Pongo*, while the smallest are in *Pan*.

The *Ouranopithecus* male-female differences fall in the range of *Pongo* male-female pairs, but also in the upper part of the *Gorilla* range. *Ouranopithecus* shows, on average, the greatest mean differences in male-female pairwise comparisons followed by *Pongo* and *Gorilla*, while *Pan* shows the smallest differences (Table 5; see also Table S4). Significance tests on male-female centroid means of each great ape species indicated that there is a significant difference between the means of the sexes in *Gorilla* and *Pongo*, but not in *Pan* (Table 5; see also Fig. S1). Fig. S1 illustrates the male-female centroid size differences in *Gorilla*, *Pongo*, *Pan*, and *Ouranopithecus*. The centroid size differences in *Ouranopithecus* show that there is a significant difference between the two males and one female, the same as *Gorilla* and *Pongo*.

Hemimandible: *Ouranopithecus* again exhibits, on average, the greatest pairwise differences between males and females in this dataset. Among the extant great apes, the greatest differences are in *Pongo* male-female pairs while the lowest in *Pan* (Fig. 8b). As in the

previous dataset, *Ouranopithecus* shows the greatest mean differences in male-female pairwise comparisons and *Pan* the smallest differences (Table 5; see also Table S4).

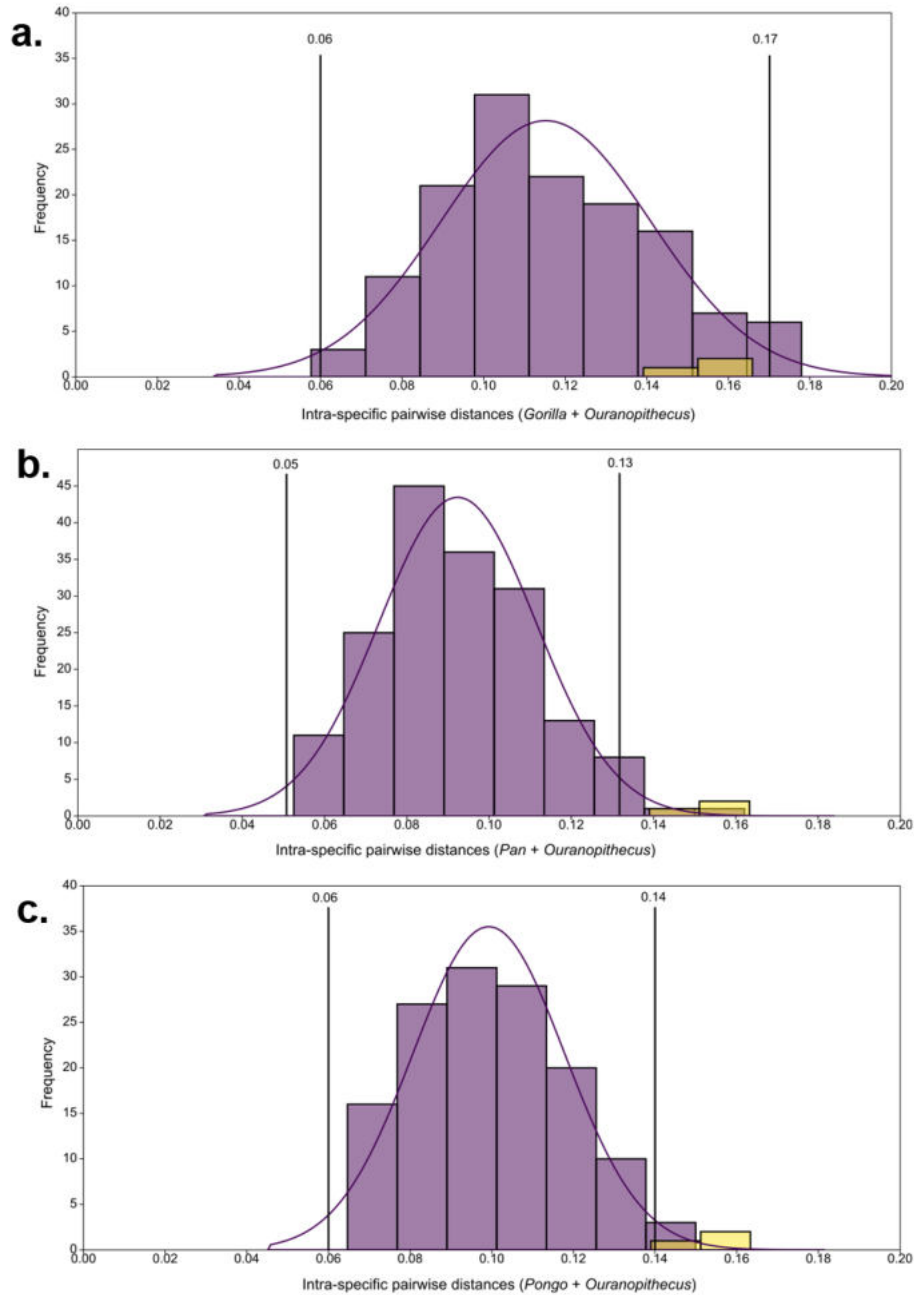


Fig. 6: Distribution and density curve of pairwise intra-specific distances within species in extant great apes and *Ouranopithecus* (bilateral analysis). a. *Gorilla* and *Ouranopithecus*, b. *Pan* and *Ouranopithecus*, and c. *Pongo* and *Ouranopithecus*.

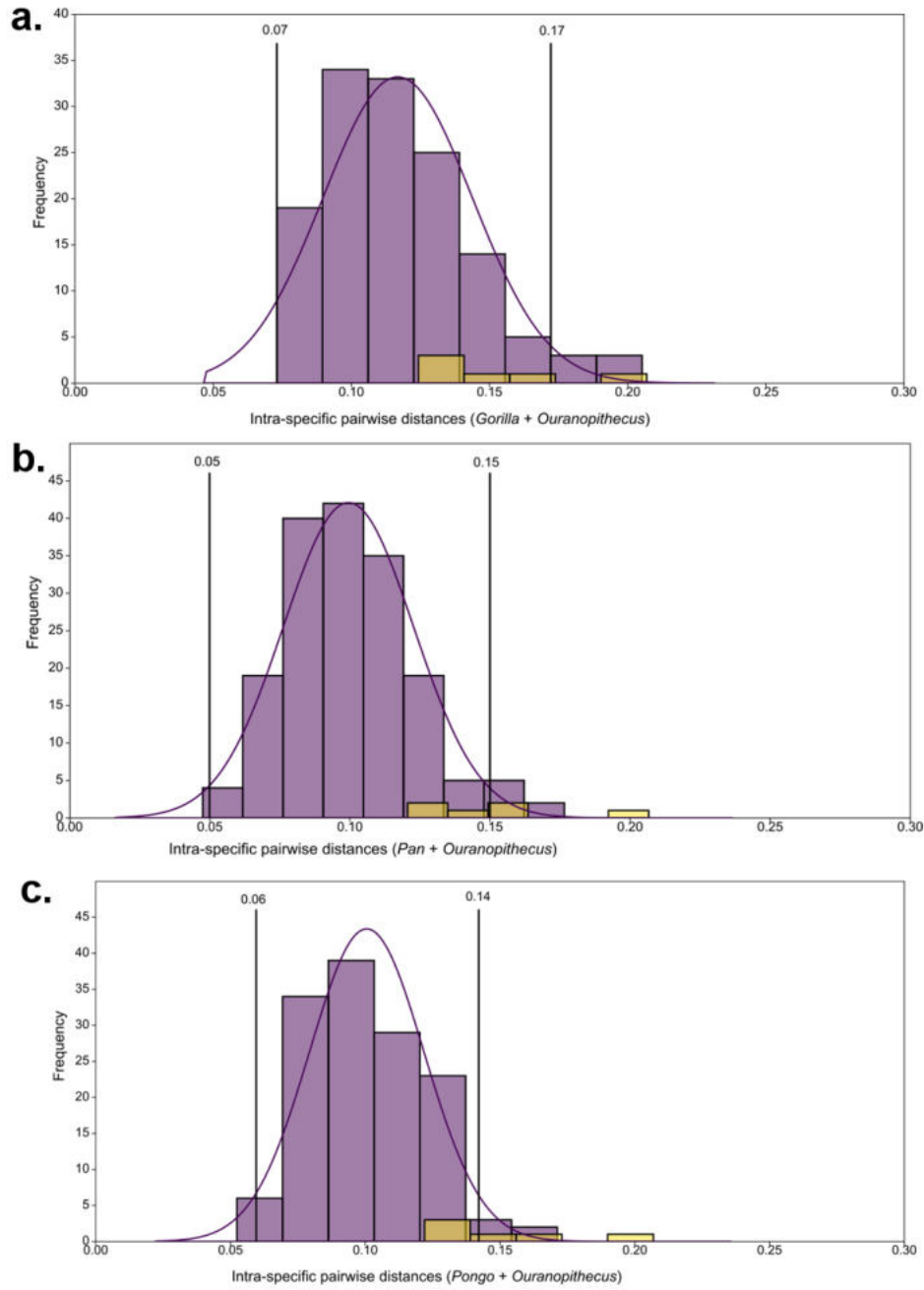


Fig. 7: Distribution and density curve of pairwise intra-specific distances within species in extant great apes and *Ouranopithecus* (hemimandible analysis). a. *Gorilla* and *Ouranopithecus*, b. *Pan* and *Ouranopithecus*, and c. *Pongo* and *Ouranopithecus*.

Significance tests on male-female centroid means of each great ape species indicated that there is a significant difference between the means of the sexes in *Gorilla* and *Pongo*, but not in *Pan* (Table 5; see also Fig. S2). Fig. S2 illustrates the centroid size differences in male-female *Gorilla*, *Pongo*, *Pan*, and *Ouranopithecus*. The centroid size differences in *Ouranopithecus* show that there is a significant difference between males and females, the same as in *Gorilla* and *Pongo*.

Table 5: Mean centroid sizes and results of independent-samples t-tests of males and females of the extant great apes and *O. macedoniensis*.

Bilateral analysis				
	<i>Male (mean)</i>	<i>Female (mean)</i>	<i>Male-female difference</i>	<i>T/p-value</i>
<i>O. macedoniensis</i>	158.90	131.52	27.38	-
<i>G. gorilla</i>	169.13	153.88	15.26	-4.55/<0.01
<i>P. troglodytes</i>	138.14	132.33	5.81	-1.71/ns
<i>P. pygmaeus</i>	169.69	146.01	23.68	-6.8/<0.01
Hemimandible				
<i>O. macedoniensis</i>	110.79	84.01	26.78	-
<i>G. gorilla</i>	114.35	103.97	10.38	-3.97/<0.01
<i>P. troglodytes</i>	90.22	86.64	3.58	-1.72/ns
<i>P. pygmaeus</i>	116.27	99.93	16.34	-6.46/<0.01

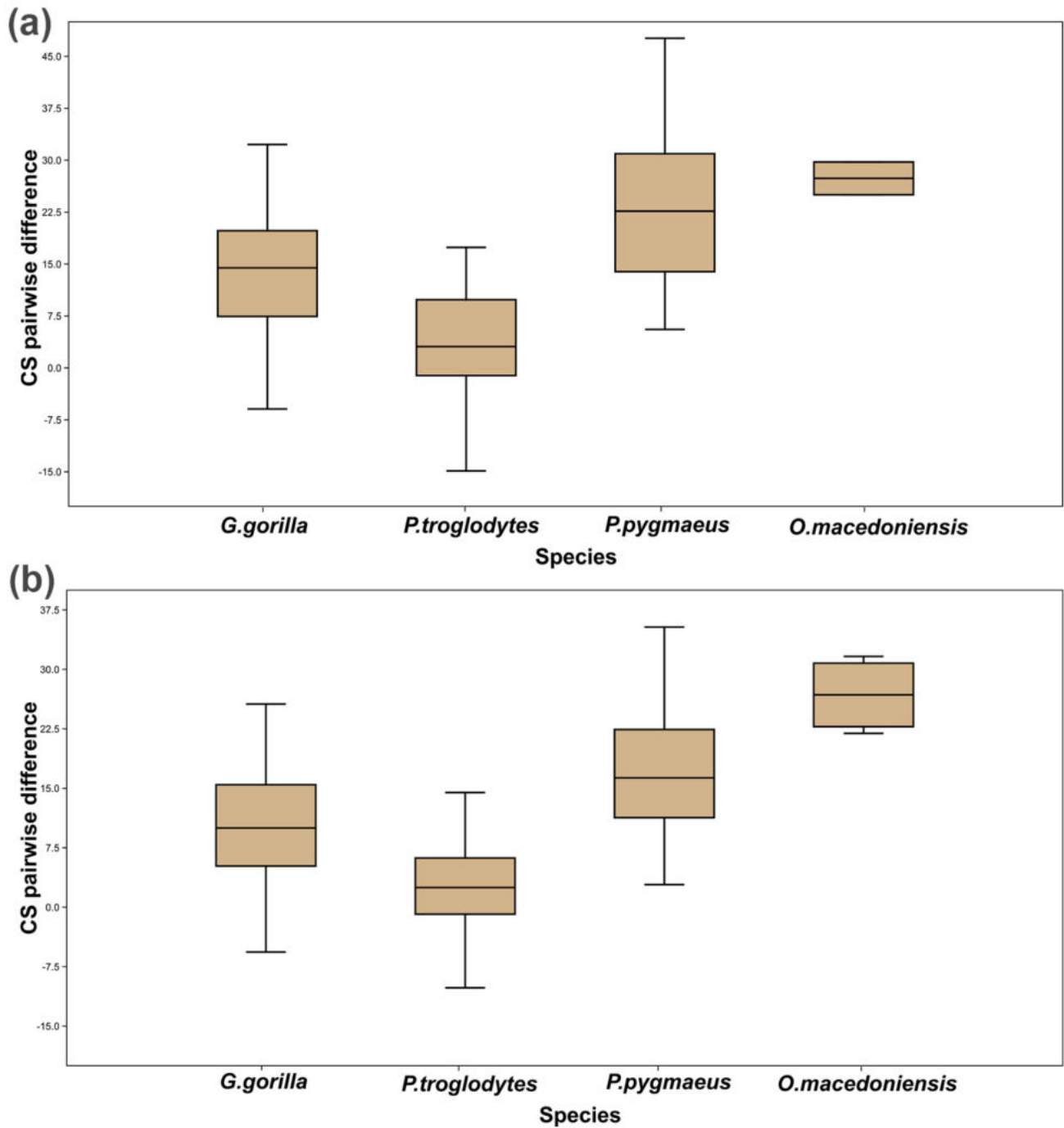


Fig. 8: Boxplots of the pairwise male-female centroid size differences of *Ouranopithecus macedoniensis* and each of the extant great apes, a. bilateral and b. hemimandible analyses.

4.4 Discussion

Variation in mandibular shape in primates reflects a combination of complex factors, such as adaptive response to biomechanical loads and feeding behavior (e.g., Beecher, 1977; Daegling and Jungers, 2000; Taylor, 2002; Terhune, 2013), sexual dimorphism (e.g., Humphrey et al., 1999; Collard and Wood, 2001; Robinson, 2003) or taxonomy (e.g., Kelley and Pilbeam, 1986; Daegling and Jungers, 2000). With respect to the great apes, differences in mandibular shape exist to some extent at the genus level across great apes, e.g., in the corpus and symphysis (e.g., Daegling and Jungers, 2000; Guy et al., 2008; Pitiri and Begun, 2019), and ramus (e.g., Aitchison, 1965; Humphrey et al., 1999; Terhune et al., 2014). In general, the mandibles of the larger great apes, *Gorilla* and *Pongo*, are more similar to each other than they are to *Pan* (Humphrey et al., 1999; Collard and Wood, 2001; Robinson, 2003). Based on this knowledge, researchers have previously used the extant great apes as models to interpret mandibular variation and potential impact on taxonomic interpretations in fossil samples (e.g., Rosas and Bastir, 2004; Scott and Lockwood, 2004; Lague et al., 2008; Scott et al., 2009; Ritzman et al., 2016). Here, we aimed to explore mandibular shape and size variation within *O. macedoniensis* in comparison to extant great apes in an attempt to understand better the variation within *O. macedoniensis* and the expression of sexual dimorphism in this taxon.

Mandibular shape and homogeneity in *Ouranopithecus macedoniensis*

Our PCA results indicate that mandibular morphology, as represented by our 3D landmarks, can distinguish among extant great apes (even though some overlap exists) and *Ouranopithecus macedoniensis*. The *O. macedoniensis* mandibles are more similar in shape to the larger great apes, *Gorilla* and *Pongo*, than they are to *Pan*. Mandibular shape varies between males and females, as does size. Mandibular shape of male *Ouranopithecus*, in particular, as captured by the landmarks used in our analysis, is relatively long with a deep corpus and a narrow dental arcade. The morphology of the female *Ouranopithecus* mandible (RPI-54) is characterized by smaller size but mainly exhibits broadly similar features as that of the male individuals, although shorter in length and height, and with a wider dental arcade in comparison to males. Overall, the *Ouranopithecus* mandibles resemble in some of these characteristics the larger great apes, *Gorilla* and *Pongo*, and therefore appear to follow the

pattern of similarity among the larger-bodied taxa observed previously (Humphrey et al., 1999; Collard and Wood, 2001; Robinson, 2003), with mandibles of *Gorilla* and *Pongo* be more similar to each other than they are to *Pan*.

The *O. macedoniensis* male mandibles cluster relatively close to each other in the PCA plots (bilateral and hemimandible analysis; Fig. 3a-b). The female specimen (RPI-79), the only adult female examined here, also plots close to the male *Ouranopithecus* specimens in the hemimandible analysis (the only analysis in which it could be included). In contrast, the female late juvenile/young adult RPI-54 plots away from the other *Ouranopithecus* specimens (both bilateral and hemimandible analysis; Fig. 3a-b). This might be partly due to its developmental stage in addition to sex differences in mandibular shape. In African apes, mandibular shape changes during growth, evident in different parts of the mandible (e.g., mandibular width, ramus). It has also been shown that corpus width changes with dental eruption (Daegling, 1996; Taylor, 2002; Taylor and Groves, 2003). The RPI-54 is at a late stage of ontogeny (full eruption of M2) with moderate occlusal wear, suggesting that its mandibular shape should not differ greatly from that of adults. However, a small degree of ontogenetic variation cannot be excluded.

Only one *Ouranopithecus* specimen, RPI-391, could be included in our analysis of the ramus, limiting this analysis. This specimen shows a narrow gonial angle and a gonion positioned superiorly, resembling the shape of *Pongo*. However, it also exhibits some taphonomic distortion (flattening), which could have influenced the results. Our PCA showed substantial overlap in ramal morphology of the great apes, in contrast to a previous study that found a distinct shape in *Gorilla*, and clustering of *Pan* and *Pongo* (Terhune et al., 2014). However, in that study, 2D landmarks and semilandmarks were registered on different anatomical regions on the ramus than in this study, such as the coronoid process and mandibular notch. Due to the state of preservation of the only ramus specimen, RPI-391, we could not use the same landmark set as Terhune et al. (2014). The differences in our results may therefore stem from the differences in our datasets.

In this study, we aimed to assess the degree of morphological variation in the mandibular shape of *Ouranopithecus*, compared to that observed in extant great apes. Based on the intra-specific Procrustes distances, *Ouranopithecus* shows somewhat greater inter-individual

distances than the extant great apes, as these mostly fall at the highest extreme of the ranges of the extant apes for both the bilateral and hemimandible analysis. However, only one female specimen of *O. macedoniensis*, a late juvenile/young adult, could be included in the bilateral analysis, which lowers the statistical reliability. Moreover, the pairwise distances between the *Ouranopithecus* mandibles fall within the 95 % probability interval of all pairwise distances of *Gorilla* in both the bilateral and hemimandible analysis, except for the Procrustes distance between specimens RPI-79 and RPI-56 (a female and a male, respectively) in the latter. The distances between the *Ouranopithecus* mandibles fall outside the respective pairwise distance ranges of *Pan* and *Pongo* in the bilateral analysis, while in the hemimandible analysis, three of the *Ouranopithecus* pairwise distances (RPI-79 and RPI-56; RPI-79 and RPI-75; RPI-56 and RPI-75) fall outside the 95 % probability interval of *Pan* and *Pongo*. Significance tests on the mean differences between *O. macedoniensis* and the great apes indicate that differences with *Pan* and *Pongo* are significant, while those with *Gorilla* are not. This suggests that there is more mandibular shape variation in the small *Ouranopithecus* sample than in two of the three great apes, although limitations relating to sample size apply.

Sexual dimorphism and size-related differences

Another aim of this study was to explore the degree of sexual dimorphism expressed in the shape and size of the mandible in *Ouranopithecus* and to compare this to sexual dimorphism present in the extant great apes. There were no significant male-female shape differences within *Gorilla* and *Pan* (except in hemimandible analysis), but there were significant differences between the sexes in mandibular corpus, symphysis, and ramus shape in *Pongo*. Our comparison of differences between male-female centroid means of both bilateral and hemimandible analyses further indicates that sexual dimorphism in size is more strongly expressed in the larger great apes, *Gorilla* and *Pongo*, but is largely absent in *Pan*, a finding also supported by the significance tests (Table 5). Our results are therefore consistent with other studies demonstrating that mandibular sexual size dimorphism is expressed only in the larger great apes, *Gorilla* and *Pongo*, including previous work using multivariate statistical analyses (Chamberlain and Wood, 1985; Taylor and Grooves, 2003; Taylor, 2006; Schmittbuhl et al., 2007; Robinson 2003; 2012; Singh, 2014). By comparison, *Ouranopithecus*

shows the greatest differences between male and female centroid size means, suggesting that it was more sexually dimorphic than the extant great apes. However, this result could be influenced by our small sample sizes. Based on the male-female centroid size pairwise differences in the mandibular and hemimandible analyses, *Ouranopithecus* is more similar to *Pongo* than to *Gorilla* or *Pan* in its level of mandibular size dimorphism, although the *Ouranopithecus* values fall in the upper part of the *Pongo* range. Overall, our results suggest that the degree of mandibular size sexual dimorphism in *Ouranopithecus* may exceed that of *Pongo*, an interpretation that is in line with results from previous studies on the dentition (Scott et al., 2009; Koufos et al., 2016a). Lastly, our correlation analyses between size and shape showed that PC 1 is significantly correlated with size in all three shape analyses, with the degree of correlation varying from moderate to substantial. This suggests that size partly determines the morphology of these taxa, including *Ouranopithecus*, and contributes to the greater similarity in mandibular shape between *Ouranopithecus* and the two larger apes relative to *Pan*.

As mentioned in the introduction, *O. macedoniensis* shows a high level of dental size variation, which led some researchers to propose a two-species hypothesis (Kay, 1982; Kay & Simons; 1983). However, an alternative interpretation is that this variation is instead related to a high degree of sexual dimorphism, given that *Ouranopithecus* is characterized by morphological homogeneity in the dentition (Koufos, 1995; Schrein, 2006; Scott et al., 2009; Koufos et al., 2016a). Moreover, a high degree of dental variation, exceeding the ranges expressed by the larger great apes, is also present within other Miocene species, such as *Proconsul major* and *Lufengpithecus lufengensis* (Kelley and Elter, 1989; Wood and Xu, 1991; Uchida, 1996; Kelley and Plavcan, 1998; Scott et al., 2009). Therefore, sexual dimorphism in the small *O. macedoniensis* may be elevated compared to the extant great apes but is comparable to that described for other well-represented Miocene hominoids. As has been previously suggested, the most dimorphic extant taxa do not necessarily set the upper limits of variation in fossil primates (e.g., Kelley and Xu, 1991; Kelley, 1993; Scott et al., 2009).

Similar to many fossil specimens (see, e.g., Gingerich, 1983; Kidwell and Holland, 2002; Forey et al., 2004, and references therein), and despite our efforts to avoid distorted anatomical regions (e.g., use only of the undistorted anatomical side of RPI-79), the *Ouranopithecus*

specimens might also be affected by taphonomic processes resulting in slight distortions and asymmetries, which may account for shape and (to a lesser extent) variation observed in our sample. Another issue is that the mandibular shape was analyzed in parts due to incomplete preservation, and our sample was very limited, which means that alternative variables may have produced different results. However, no complete mandible(s) of *O. macedoniensis* have been found to date. Finally, our sample includes a late juvenile/young adult fossil individual, which may have introduced a small level of ontogenetic variations. Despite these limitations, this study provides important new insights into the patterns of mandibular shape and size variation in *O. macedoniensis*.

Conclusions

Our results, based on 3D geometric morphometrics and multivariate statistical analyses, show that mandibular shape can differentiate *Ouranopithecus macedoniensis* from the extant great apes. *O. macedoniensis* shows some shape similarities to the larger great apes, *Gorilla* and *Pongo*, a similarity probably due, in part, to a similar size. Compared to *Gorilla* and *Pongo*, *O. macedoniensis* shows an elevated degree of morphological variation, notable given the small sample size but perhaps exaggerated somewhat by the inclusion in the small sample of a subadult individual. Sexual dimorphism in the mandibles of *O. macedoniensis* appears to be quite high, seemingly greater than in *Gorilla* and high even compared to *Pongo*, but this again is perhaps partly an artifact of small sample size.

ACKNOWLEDGMENTS

This work was supported by the Senckenberg Gesellschaft für Naturforschung, the Leventis Foundation, and the Deutsche Forschungsgemeinschaft (DFG INST 37/706-1). We would like to thank Dr. C. Hemm and Dr. O. Kullmer (Senckenberg Museum of Natural History, Frankfurt), Dr. S. Merker and C. Leidenroth (State Museum of Natural History, Stuttgart), and Dr. F. Mayer and C. Funk (Museum für Naturkunde - Leibniz Institute for Evolution and Biodiversity Science, Berlin) for access to their collection of great apes. We are grateful to Dr. K. Helgen and Dr. M. Tocheri (Smithsonian National Museum of Natural History, Washington, D.C.) for the scans of USNM specimens used here (<http://humanorigins.si.edu/evidence/3d-collection/primate>). These scans were acquired through the generous support of the

Smithsonian 2.0 Fund and the Smithsonian's Collections Care and Preservation Fund. Special thanks to Dr. A. Bosman, Dr. A. Karakostis, and C. Röding for their help in parts of the statistical analyses. Dr. K. McGrath, L. Limmer, and A. Lockey for proofreading and providing useful comments about the manuscript. We also thank the editor, associate editor, Dr. K. McNulty, and the two anonymous reviewers for their suggestions and comments, which helped to considerably improve this paper.

REFERENCES

- Adams, D. C., & Otárola-Castillo, E. (2013). geomorph: an R package for the collection and analysis of geometric morphometric shape data. *Methods in Ecology and Evolution*, 4(4), 393-399.
- Adams, D. C., Rohlf, F. J., & Slice, D. E. (2004). Geometric morphometrics: ten years of progress following the 'revolution'. *Italian Journal of Zoology*, 71(1), 5-16.
- Aitchison, J. (1965). Contrasts in the mandibles and mandibular teeth of the chimpanzee, orangutan and gorilla. *Dent Mag Oral Top*, 81, 105-108.
- Beecher, R. M. (1977). Function and fusion at the mandibular symphysis. *American Journal of Physical Anthropology*, 47(2), 325-335.
- Bookstein, F. L. (1991). *Morphometric Tools for Landmark Data: Geometry and Biology*. Cambridge University Press, Cambridge
- Bookstein, F. L. (1997). *Morphometric tools for landmark data: geometry and biology*. Cambridge University Press.
- Collard, M., & Wood, B. (2001). Homoplasy and the early hominid masticatory system: inferences from analyses of extant hominoids and papionins. *Journal of Human Evolution*, 41(3), 167-194.
- Corti, M. (1993). Geometric morphometrics: an extension of the revolution. *Trends in Ecology & Evolution*, 8(8), 302.
- Chamberlain, A. T., & Wood, B. A. (1985). A reappraisal of variation in hominid mandibular corpus dimensions. *American Journal of Physical Anthropology*, 66(4), 399-405.
- Daegling, D. J. (1996). Growth in the mandibles of African apes. *Journal of Human Evolution*, 30(4), 315-341.

- Daegling, D. J., & Jungers, W. L. (2000). Elliptical Fourier analysis of symphyseal shape in great ape mandibles. *Journal of Human Evolution*, 39(1), 107-122.
- de Bonis, L. (1974). Première découverte d'un primates hominoïde dans le Miocène supérieur de Macédoine (Grèce). *Comptes rendus de l'Académie des Sciences, Paris, série D*, 278, 3063-3066.
- de Bonis, L., & Koufos, G. D. (1993). The face and the mandible of *Ouranopithecus macedoniensis*: description of new specimens and comparisons. *Journal of Human Evolution*, 24(6), 469-491.
- de Bonis, L., & Koufos, G. D. (1994). Our ancestors' ancestor: *Ouranopithecus* is a Greek link in human ancestry. *Evolutionary Anthropology: Issues, News, and Reviews*, 3(3), 75-83.
- de Bonis, L., & Koufos, G. D. (2001). 11 Phylogenetic relationships of *Ouranopithecus macedoniensis* (Mammalia, Primates, Hominoidea, Hominidae) of the late Miocene deposits of Central Macedonia. *Hominoid Evolution and Climatic Change in Europe: Volume 2: Phylogeny of the Neogene Hominoid Primates of Eurasia*, (pp. 254-268). Cambridge University Press.
- de Bonis, L., & Koufos, G. D. (2014). First discovery of postcranial bones of *Ouranopithecus macedoniensis* (Primates, Hominoidea) from the late Miocene of Macedonia (Grèce). *Journal of Human Evolution*, 74, 21-36.
- de Bonis, L., & Melentis, J. (1977). Les Primates hominoïdes du Vallésien de Macédoine (Grèce). Étude de la mâchoire inférieure. *Geobios*, 10(6), 849-885.
- de Bonis, L., & Melentis, J. (1978). Les Primates hominoïdes du Miocène supérieur de Macédoine—Étude de la mâchoire supérieure. In *Annales de Paléontologie (vertébrés)*, 64, 185-202.
- de Bonis, L., Bouvrain, G., Geraads, D., & Koufos, G. (1990). New hominid skull material from the late Miocene of Macedonia in Northern Greece. *Nature*, 345(6277), 712.
- de Bonis, L., Koufos, G. D., Guy, F., Peigné, S., & Sylvestrou, I. (1998). Nouveaux restes du primate hominoïde *Ouranopithecus* dans les dépôts du Miocène supérieur de Macédoine (Grèce). *Comptes Rendus de l'Académie des Sciences-Series IIA-Earth and Planetary Science*, 327(2), 141-146.

- Forey, P. L., Fortey, R. A., Kenrick, P., & Smith, A. B. (2004). Taxonomy and fossils: a critical appraisal. *Philosophical Transactions of the Royal Society of London. Series B: Biological Sciences*, 359(1444), 639-653.
- Gingerich, P. (1983). Rates of evolution: effects of time and temporal scaling. *Science*, 222, 159-162.
- Gunz, P., Mitteroecker, P., Neubauer, S., Weber, G. W., & Bookstein, F. L. (2009). Principles for the virtual reconstruction of hominin crania. *Journal of human evolution*, 57(1), 48-62.
- Guy, F., Mackaye, H. T., Likius, A., Vignaud, P., Schmittbuhl, M., & Brunet, M. (2008). Symphyseal shape variation in extant and fossil hominoids, and the symphysis of *Australopithecus bahrelghazali*. *Journal of Human Evolution*, 55(1), 37-47.
- Hammer, Ø., Harper, D. A., & Ryan, P. D. (2001). PAST: paleontological statistics software package for education and data analysis. *Palaeontologia electronica*, 4(1), 9.
- Humphrey, L. T., Dean, M. C., & Stringer, C. B. (1999). Morphological variation in great ape and modern human mandibles. *The Journal of Anatomy*, 195(4), 491-513.
- Kay, R. F. (1982). *Sivapithecus simonsi*, a new species of Miocene hominoid, with comments on the phylogenetic status of the Ramapithecinae. *International Journal of Primatology*, 3(2), 113-173.
- Kelley, J. (1993). Taxonomic implications of sexual dimorphism in *Lufengpithecus*. In *Species, species concepts and primate evolution* (pp. 429-458). Springer, Boston, MA.
- Kelley, J. (1995). Sex determination in Miocene catarrhine primates. *American Journal of Physical Anthropology*, 96(4), 391-417.
- Kelley, J. & Pilbeam, D. (1986). The dryopithecines: taxonomy, comparative anatomy, and phylogeny of Miocene large hominoids. *Comparative Primate Biology*, 1, 361-411.
- Kelley, J., & Etlar, D. (1989). Hominoid dental variability and species number at the late Miocene site of Lufeng, China. *American Journal of Primatology*, 18(1), 15-34.
- Kelley, J., & Plavcan, J. M. (1998). A simulation test of hominoid species number at Lufeng, China: implications for the use of the coefficient of variation in paleotaxonomy. *Journal of Human Evolution*, 35(6), 577-596.
- Kelley, J., & Xu, Q. (1991). Extreme sexual dimorphism in a Miocene hominoid. *Nature*, 352(6331), 151-153.

- Kidwell, S. M., & Holland, S. M. (2002). The quality of the fossil record: implications for evolutionary analyses. *Annual Review of Ecology and Systematics*, 33(1), 561-588.
- Koufos, G. D. (1993). Mandible of *Ouranopithecus macedoniensis* (Hominidae, Primates) from a new late Miocene locality of Macedonia (Greece). *American Journal of Physical Anthropology*, 91(2), 225-234.
- Koufos, G. D. (1995). The first female maxilla of the hominoid *Ouranopithecus macedoniensis* from the late Miocene of Macedonia, Greece. *Journal of Human Evolution*, 29(4), 385-399.
- Koufos, G. D., & de Bonis, L. (2006). New material of *Ouranopithecus macedoniensis* from late Miocene of Macedonia (Greece) and study of its dental attrition. *Geobios*, 39(2), 223-243.
- Koufos, G. D., de Bonis, L., & Kugiumtzis, D. (2016a). New material of the hominoid *Ouranopithecus macedoniensis* from the Late Miocene of the Axios Valley (Macedonia, Greece) with some remarks on its sexual dimorphism. *Folia Primatologica*, 87(2), 94-122.
- Koufos, G. D., Kostopoulos, D. S., & Vlachou, T. D. (2016b). Revision of the Nikiti 1 (NKT) fauna with description of new material. *Geobios*, 49(1-2), 11-22.
- Lague, M. R., Collard, N. J., Richmond, B. G., & Wood, B. A. (2008). Hominid mandibular corpus shape variation and its utility for recognizing species diversity within fossil Homo. *Journal of Anatomy*, 213(6), 670-685.
- Miller, S. F., White, J. L., & Ciochon, R. L. (2008). Assessing mandibular shape variation within *Gigantopithecus* using a geometric morphometric approach. *American Journal of Physical Anthropology*, 137(2), 201-212.
- Nicholson, E., & Harvati, K. (2006). Quantitative analysis of human mandibular shape using three-dimensional geometric morphometrics. *American Journal of Physical Anthropology*, 131(3), 368-383.
- Pitirri, M. K., & Begun, D. (2019). A new method to quantify mandibular corpus shape in extant great apes and its potential application to the hominoid fossil record. *American Journal of Physical Anthropology*, 168(2), 318-328.

- Ritzman, T. B., Terhune, C. E., Gunz, P., & Robinson, C. A. (2016). Mandibular ramus shape of *Australopithecus sediba* suggests a single variable species. *Journal of Human Evolution*, *100*, 54-64.
- Robinson, C.A., 2003. Extant hominoid and Australopith mandibular morphology; assessing alpha taxonomy and phylogeny in hominoids using mandibular characters. Ph.D. Dissertation, New York University.
- Robinson, C. (2012). Geometric morphometric analysis of mandibular shape diversity in Pan. *Journal of Human Evolution*, *63*(1), 191-204.
- Robinson, C., & Terhune, C. E. (2017). Error in geometric morphometric data collection: Combining data from multiple sources. *American Journal of Physical Anthropology*, *164*(1), 62-75.
- Rohlf, F. J. (1993). Relative warp analysis and an example of its application to mosquito. *Contributions to Morphometrics*, *8*, 131.
- Rosas, A., & Bastir, M. (2004). Geometric morphometric analysis of allometric variation in the mandibular morphology of the hominids of Atapuerca, Sima de los Huesos site. *The Anatomical Record Part A: Discoveries in Molecular, Cellular, and Evolutionary Biology: An Official Publication of the American Association of Anatomists*, *278*(2), 551-560.
- Schmittbuhl, M., Rieger, J., Le Minor, J. M., Schaaf, A., & Guy, F. (2007). Variations of the mandibular shape in extant hominoids: generic, specific, and subspecific quantification using elliptical Fourier analysis in lateral view. *American Journal of Physical Anthropology*, *132*(1), 119-131.
- Schrein, C. M. (2006). Metric variation and sexual dimorphism in the dentition of *Ouranopithecus macedoniensis*. *Journal of Human Evolution*, *50*(4), 460-468.
- Scott, J. E., & Lockwood, C. A. (2004). Patterns of tooth crown size and shape variation in great apes and humans and species recognition in the hominid fossil record. *American Journal of Physical Anthropology*, *125*(4), 303-319.
- Scott, J. E., Schrein, C. M., & Kelley, J. (2009). Beyond Gorilla and Pongo: alternative models for evaluating variation and sexual dimorphism in fossil hominoid samples. *American Journal of Physical Anthropology*, *140*(2), 253-264.

- Sen, S., Koufos, G. D., Kondopoulou, D., & de Bonis, L. (2000). Magnetostratigraphy of the late Miocene continental deposits of the lower Axios valley, Macedonia, Greece. *Geological Society Greece Special Publications*, 9, 197-206.
- Singh, N. (2014). Ontogenetic study of allometric variation in Homo and Pan mandibles. *The Anatomical Record*, 297(2), 261-272.
- Slice, D. E. (2007). Geometric morphometrics. *Annual Review of Anthropology*, 36, 261-281.
- Taylor, A. B. (2002). Masticatory form and function in the African apes. *American Journal of Physical Anthropology*, 117(2), 133-156.
- Taylor, A. B. (2006). Size and shape dimorphism in great ape mandibles and implications for fossil species recognition. *American Journal of Physical Anthropology*, 129(1), 82-98.
- Taylor, A. B., & Groves, C. P. (2003). Patterns of mandibular variation in Pan and Gorilla and implications for African ape taxonomy. *Journal of Human Evolution*, 44(5), 529-561.
- Terhune, C. E. (2013). Dietary correlates of temporomandibular joint morphology in the great apes. *American Journal of Physical Anthropology*, 150(2), 260-272.
- Terhune, C. E., Robinson, C. A., & Ritzman, T. B. (2014). Ontogenetic variation in the mandibular ramus of great apes and humans. *Journal of Morphology*, 275(6), 661-677.
- Uchida, A. (1996). Dental variation of Proconsul from the Tinderet region, Kenya. *Journal of Human Evolution*, 31(6), 489-497.
- White, T. D., Black, M. T., & Folkens, P. A. (2011). *Human osteology*. Academic press.
- Wood, B. A., & Xu, Q. (1991). Variation in the Lufeng dental remains. *Journal of Human Evolution*, 20(4), 291-311.
- Zollikofer, C. P., De León, M. S. P., Chaimanee, Y., Lebrun, R., Tafforeau, P., Khansubhaand, S., & Jaeger, J. J. (2009). The face of Siamopithecus: new geometric-morphometric evidence for its anthropoid status. *The Anatomical Record: Advances in Integrative Anatomy and Evolutionary Biology*, 292(11), 1734-1744.

Supplementary Material

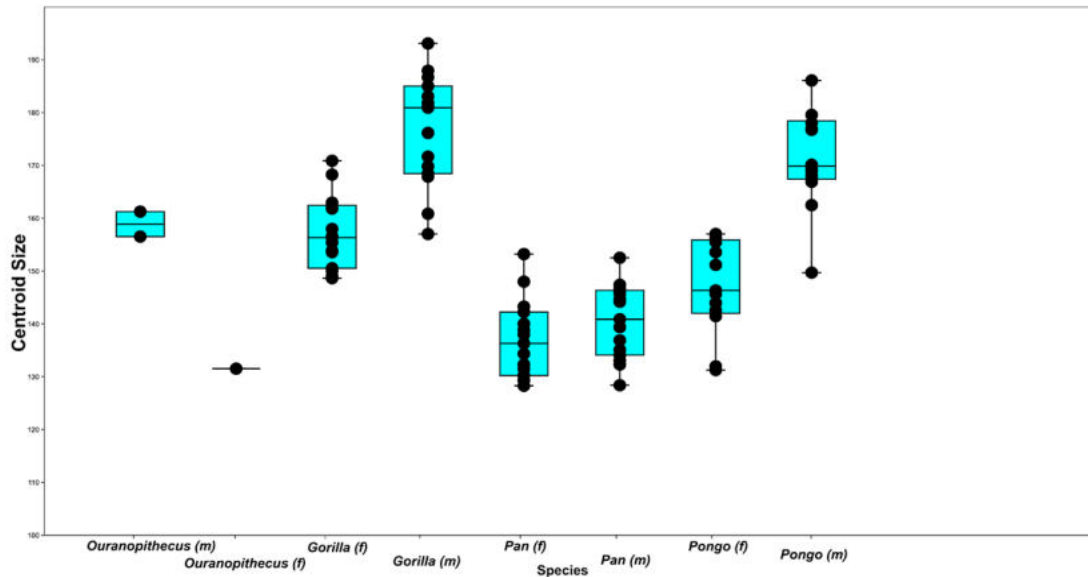


Fig. S1: Boxplots of the male-female centroid size differences in *Ouranopithecus*, *Gorilla*, *Pan*, and *Pongo* (bilateral analysis).

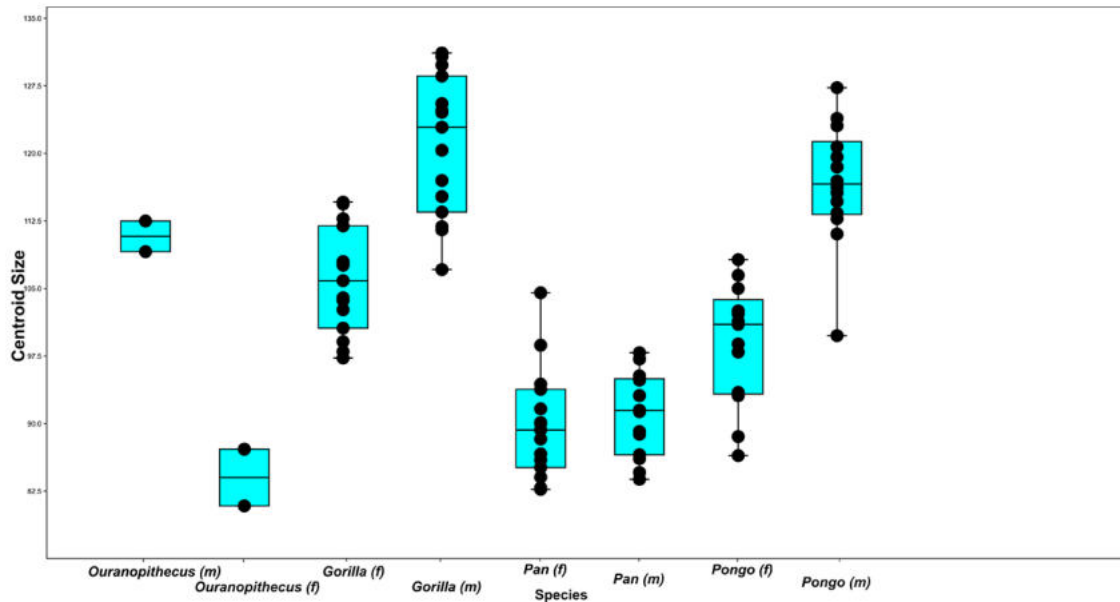


Fig. S2: Boxplots of the male-female centroid size differences in *Ouranopithecus*, *Gorilla*, *Pan*, and *Pongo* (hemimandible analysis).

Table S1: Values within the 95 % probability interval – bilateral analysis.

Curve	<i>G. gorilla</i>	<i>P. troglodytes</i>	<i>P. pygmaeus</i>
Mean	0.12	0.09	0.10
SD	0.03	0.02	0.02
SD*2	0.05	0.04	0.04
Mean-(SD*2)	0.06	0.05	0.06
Mean+(SD*2)	0.17	0.13	0.14

Table S2: Values within the 95 % probability interval – hemimandible.

Curve	<i>G. gorilla</i>	<i>P. troglodytes</i>	<i>P. pygmaeus</i>
Mean	0.12	0.10	0.11
SD	0.03	0.02	0.02
SD*2	0.05	0.05	0.04
Mean-(SD*2)	0.07	0.05	0.06
Mean+(SD*2)	0.17	0.15	0.14

Table S3: Procrustes distances between RPI-391 and the extant great apes used in this study – ramal analysis.

	RPI-391
RPI-391	0
Gorilla_g_2674	0.185034
Gorilla_g_7465	0.120879
Gorilla_g_38230	0.178846
Gorilla_g_38972	0.210297
Gorilla_g_USNM-174720	0.15097
Gorilla_g_USNM-220380	0.146077
Gorilla_g_USNM-252575	0.199351
Gorilla_g_USNM-252576	0.211291
Gorilla_g_USNM-252579	0.122284
Gorilla_g_7464	0.162596
Gorilla_g_32010	0.151481
Gorilla_g_USNM-174712	0.160571
Gorilla_g_USNM-174714	0.192459
Gorilla_g_USNM-174715	0.140817
Gorilla_g_USNM-174716	0.129199
Gorilla_g_USNM-176216	0.156624
Gorilla_g_USNM-176225	0.164322
Pan_7475	0.12069
Pan_SMF-50	0.156473
Pan_SMF-100	0.137967
Pan_ZMB-7872	0.160509
Pan_ZMB-11638	0.1475
Pan_ZMB-15847	0.165533
Pan_ZMB-27054	0.16363
Pan_ZMB-45130	0.161184

Pan_ZMB-83654	0.135157
Pan_1797	0.123381
Pan_7531	0.165098
Pan_ZMB-15846	0.157043
Pan_ZMB-19071	0.118018
Pan_ZMB-29472	0.158939
Pan_ZMB-30846	0.143689
Pan_ZMB-83602	0.124594
Pan_ZMB-83636	0.128801
Pan_ZMB-83642	0.185627
Pan_ZMB-83664	0.153104
Pongo_p_7460	0.132414
Pongo_p_USNM-142169	0.136409
Pongo_p_USNM-142184	0.134098
Pongo_p_USNM-142191	0.170551
Pongo_p_USNM-153828	0.181162
Pongo_p_USNM-197664	0.177162
Pongo_p_ZMB-6948	0.099905
Pongo_p_ZMB-6957	0.166311
Pongo_p_1687	0.124959
Pongo_p_7459	0.123452
Pongo_p_USNM-142188	0.126881
Pongo_p_USNM-142189	0.118132
Pongo_p_USNM-142194	0.132357
Pongo_p_USNM-122196	0.134184
Pongo_p_USNM-142198	0.116151
Pongo_p_USNM-145319	0.152391
Pongo_p_ZMB-15850	0.122275

Table S4: Number of pairwise M/F centroid size comparisons in the extant species that exceed the values in *Ouranopithecus*.

Analysis	<i>G. gorilla</i>	<i>P. troglodytes</i>	<i>P. pygmaeus</i>
Bilateral	4/72	0/90	20/72
Hemimandible	0/72	0/90	3/72

CHAPTER 5

Study 3

Text and analyses incorporated in this chapter are a manuscript that is ready for submission in the American Journal of Physical Anthropology.

Ioannidou M., Koufos G. D., de Bonis L. & Harvati K. 3D mandibular dental analysis of *Ouranopithecus macedoniensis*. (ready for submission, *American Journal of Physical Anthropology*)

The original idea for this study was developed in collaboration with Prof. Dr. Harvati, Prof. Koufos and Prof. de Bonis. Regarding the data presented in this chapter, I was the main conductor and collected the data.

Author	Author position	Scientific ideas %	Data generation %	Analysis & interpretation %	Paper writing %
Ioannidou, M.	1	40	100	80	80
Koufos, G.	2	10	-	-	-
de Bonis, L.	3	10	-	-	-
Harvati, K.	4	40	-	20	20
Title of the paper		3D mandibular dental analysis of <i>Ouranopithecus macedoniensis</i>			
Status in Publication Process		Ready for submission in <i>American Journal of Physical Anthropology</i>			

3D mandibular dental analysis of *Ouranopithecus macedoniensis*

Abstract

Objectives: First, to observe and characterize the root length and morphology in the lower post-canine dentition of *Ouranopithecus macedoniensis* and to compare it to extant and extinct taxa. Second, to explore the possibility of using root and pulp canal morphology to clarify the controversial phylogenetic position of *Ouranopithecus macedoniensis*.

Materials and methods: We measure the root length and characterize the root morphology in the premolars and molars of two original mandibular fragments and an isolated tooth from *Ouranopithecus macedoniensis*, and we compare our results with published data on extant great apes, humans, and a few extinct hominoid taxa, including the much-discussed *Graecopithecus freybergi*.

Results: *Ouranopithecus macedoniensis* has relatively shorter root lengths than the extant great apes, and the two mandibular fragments show a similar root and pulp canal configuration. *Ouranopithecus* shares the following with the African apes, *Gorilla* and *Pan*, but also *Pongo*: three pulp canals in P₃; four pulp canals in P₄; three roots and four canals in M₁; and four pulp canals in M₂. Moreover, our results indicate that *O. macedoniensis* differs from *G. freybergi* in the root and pulp canal configuration.

Discussion: *Ouranopithecus* specimens show a similar pattern to their mandibular root morphology, implying that the configuration shown was not uncommon in this species. *Ouranopithecus* resembles the internal tooth morphology of the African apes and *Pongo*. Our results, however, did not indicate a clear relationship between *O. macedoniensis* and any of the great apes in particular. Therefore, additional research in lower dentition is needed to clarify this issue further. Lastly, our results do not reject the hypothesis that *Ouranopithecus* is taxonomically distinct from *G. freybergi*.

Keywords: Miocene hominoids, dentition, dental roots, Geometric morphometrics

5.1 Introduction

Ouranopithecus macedoniensis is a hominoid known from the late Miocene deposits of Northern Greece (Macedonia). Since 1974, it has been documented from three localities (Koufos, 2006): Ravin de la Pluie (RPI) and Xirochori (XIR) in the Axios Valley; and Nikiti-1 (NKT) in Chalkidiki Peninsula. Material from RPI is plentiful and includes maxillary and mandibular remains multiple isolated teeth and just two postcranial elements (de Bonis, 1974; de Bonis and Melentis, 1977, 1978; Koufos and de Bonis 2006; de Bonis et al., 1990; 1998; Koufos et al., 2016). Several other specimens were also discovered in the other two localities, XIR and NKT, including XIR-1, an almost entire face (de Bonis et al., 1990; de Bonis and Melentis, 1977, 1978; Koufos, 1993, 1995). Faunal correlation and magnetostratigraphic evidence at these three localities place the chronostratigraphic range of *O. macedoniensis* between 9.6 and 8.7 Ma (Koufos et al., 2016; Sen et al., 2000).

Despite 40 years of research, the phylogenetic position of *O. macedoniensis* is still under discussion, and diverse hypotheses have been proposed. It has been hypothesized to represent a member either of the *Gorilla-Pan-Homo* clade (meaning African apes and humans) (de Bonis and Koufos, 2004; Begun, 2009; Kunimatsu et al., 2007), of the pongine clade (Köhler et al., 2001), or the gorilline clade (Dean and Delson, 1992). These hypotheses have been based on the comparative investigation of external craniodental anatomical features, using mostly cladistic analyses or traditional morphometric techniques.

Recent methodological advances allow not only the reconstruction of incomplete or distorted specimens (see e.g., Spoor et al., 2015; Ioannidou et al., 2019; Harvati et al., 2019), but also the in-depth quantitative investigation of complex features, including internal traits previously difficult to assess, providing additional valuable information in reconstructing phylogeny (e.g., Harvati, 2003; Baab et al., 2012; Gamarra et al., 2016). In this framework, dental features have emerged as particularly useful (Tafforeau and Smith, 2008; Kupczik and Hublin, 2010; Smith et al., 2015). Although teeth are relatively frequently recovered in the fossil record due to their dense and cohesive structure, it is only with the establishment of virtual anthropology methods and the wide use of micro CT-scans in recent years that an easier, non-destructive exploration of the inner structure of dental remains could be

achieved (e.g., Kupczik, 2003; Emonet et al., 2012; Zanolli and Mazurier, 2013; Moore et al., 2015; Zanolli et al., 2018).

Dental features have been used to assess the phylogenetic affinities of Miocene apes, suggesting a promising avenue for research (Emonet et al., 2012; 2014; Fuss et al., 2017; Smith et al., 2019). Post-canine (premolar and molar) dental root structures in extant and extinct hominoid taxa can differ in form, size, and root and canal number. These characteristics have been used in a variety of studies on taxonomy, phylogeny, sexual dimorphism, as well as tooth function (Wood et al., 1988; Brunet et al., 1996; Shields, 2005; Emonet et al., 2012; Emonet and Kullmer, 2014; Moore et al., 2015). Three-dimensional techniques are increasingly used to explore the internal morphology of dental roots belonging to extant and extinct taxa (e.g., Kupczik, 2003; Tafforeau and Smith, 2008; Emonet et al., 2012; Moore et al., 2013; 2015). The information that has been evaluated includes the number and morphology of the dental roots, characteristics that have been proposed to carry a phylogenetic signal (Kovacs, 1971; Wood et al., 1988; Kupczik, 2003; Kupczik et al., 2005). Post-canine dental roots are proposed to preserve low degrees of homoplasy (Tobias, 1995; Kupczik et al., 2005; but see Spencer, 2003). Therefore, they can possibly qualify as informative indicators of hominoid evolution and taxonomy (e.g., Emonet et al., 2014; Fuss et al., 2017).

Here, we use two original mandibular fragments and an isolated tooth from the RPI locality belonging to *Ouranopithecus macedoniensis*, a taxon whose internal tooth morphology is poorly known. First, we aim to observe and characterize the root length and morphology in the lower premolars and molars of this sample. We then compare our results with published data on extant great apes and extinct hominoid taxa, including the much-discussed single specimen of *G. freybergi* (type specimen; Fuss et al., 2017; Table 1). Our second aim is to explore the possibility of using root and pulp canal morphology to clarify the phylogenetic position of *Ouranopithecus macedoniensis*. Although our sample is limited, this study is the first that focuses on characterizing the internal tooth structure of *Ouranopithecus*, revealing characteristics of its root and pulp canal morphology. Our results can contribute new data for evaluating conflicting hypotheses on the phylogenetic position of this still enigmatic Miocene ape.

5.2 Materials and Methods

Sample

The *Ouranopithecus* sample used in this study was micro-CT scanned at the Paleoanthropology High Resolution Computed Tomography Laboratory, University of Tübingen (Phoenix X-Ray, v/tomex/s GE). The scanning parameters were as follows: tube voltage 220 kV, tube current 210 mA, and 0.6 mm copper filter. This sample consists of two partial mandibles and an isolated lower molar, all coming from the RPI fossiliferous locality (Table 1).

Table 1: *Ouranopithecus macedoniensis* and other Miocene extinct species used in the study.

Species	Specimen	Sex	Description	Age (MA)	Analysis used	Source
<i>Ouranopithecus macedoniensis</i>	RPI-54	female	mandible	9.6-8.7	root length, pulp canal number	de Bonis, 1974; de Bonis and Melentis, 1977
<i>Ouranopithecus macedoniensis</i>	RPI-75	male	mandible	9.6-8.7	root length, pulp canal number	de Bonis, 1974; de Bonis and Melentis, 1977
<i>Ouranopithecus macedoniensis</i>	RPI-237	male	isolated tooth	9.6-8.7	root length	Koufos et al., 2016
<i>Graecopithecus freibergi</i>	type specimen	male?	mandible	7.25-7.15	root length, pulp canal number	von Koenigswald 1972; Böhme et al., 2017
<i>Sahelanthropus tchadensis</i>	TM 266-02-154-1, TM 292-02-01	?	mandible	7-6	root length, pulp canal number	Emonet et al., 2014

Description of the *Ouranopithecus* specimens

RPI-54 (mandibular corpus and symphysis, holotype): This specimen belongs to a late juvenile/young adult female individual preserving its entire dentition, except for the left M₃. The right M₃ is not yet erupted but preserved in the crypt. The teeth are well preserved and little worn (de Bonis, 1974; de Bonis and Melentis, 1977; Fig. 1).

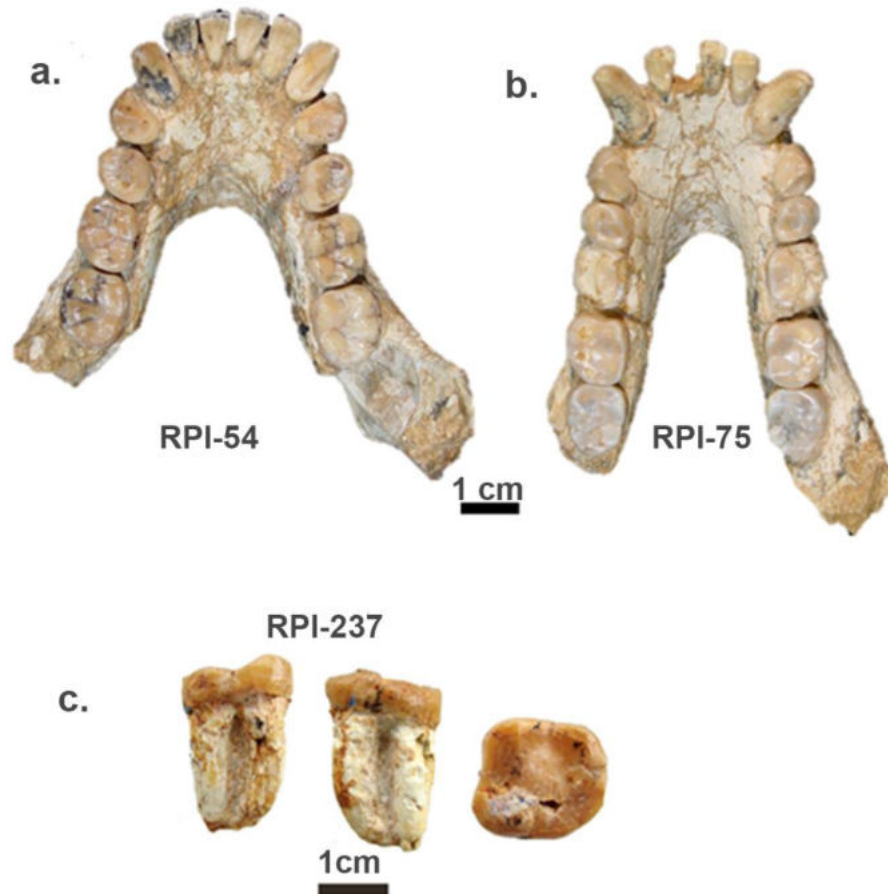


Fig.1: a. Partial mandible of the young adult female holotype of *O. macedoniensis* (RPI-54), b. Partial mandible of the male adult *O. macedoniensis* (RPI-75), and c. isolated first lower molar of *O. macedoniensis* (RPI-237). Photographs by G. D. Koufos.

RPI-75 (mandibular corpus and symphysis): This mandibular specimen preserves the entire dentition (I₁ to M₃ right and left), and it belongs to an adult male individual. The teeth are well preserved, however more worn than the holotype (de Bonis, 1974; de Bonis and Melentis, 1977; Fig. 1).

RPI-237: isolated lower M₁ (left side) with well-preserved crown and roots, belonging to an adult male individual (Koufos et al., 2016; Fig. 1).

Methodology

For this analysis, only the lower post-canine dentition was used. Furthermore, we have chosen the right side teeth, as they were complete in both mandibles. However, if the right side's internal structure was not suitable for our study purposes, we substituted it with the left side. As both mandibles are highly fossilized, automatic virtual segmentation of the teeth was not applicable. Instead, the teeth were virtually segmented from the mandible using manual or semi-automatic segmentation in Avizo software (©FEI Visualization Sciences Group, version 9.1). We assessed root length, as well as root morphology classification. We used comparative samples from the literature (Moore et al., 2013; 2015; Emonet, 2009; Emonet et al., 2014; Fuss et al., 2017); therefore, we followed the protocols provided in these studies for our results to be comparable. To measure and later compare our results to the available literature, we followed the protocol from Moore et al. (2013), where root length is measured from the root apex to the surface of the cervical plane (linearly). This linear measurement also corresponds to the area where the pulp canal intersects with the cervical plane (Moore et al., 2013). The comparative data include root length measurements from extant great apes (*Gorilla gorilla*, *Pan troglodytes*, *Pongo pygmaeus*) and humans (Abbott, 1984). We followed the Emonet (2009) protocol to assess the dental root and pulp canal classification for the *Ouranopithecus* teeth. Here, the number of roots (fused and unfused) was counted, and the dental root and pulp canal configuration was evaluated using the formula given by Emonet (2009). For multi-rooted teeth, the formula is the following: $X_a M + Y_\beta D$, where: X/Y is the mesial/distal root number; a/β is the mesial/distal pulp canals number; while M/D stands for mesial/distal surface of the tooth.

5.3 Results

Dental root lengths

In RPI-54, all roots were reliably measured from the right-sided post-canine dentition (P₃ to M₂, Table 2), except for the P₄. Due to massive mineralization, it was impossible to virtually extract the entire root of this tooth; thus, its maximum root lengths can only be estimated.

As for RPI-75, the maximum root lengths were measured from the premolars (P₃ right side, P₄ left side) and M₂ (right side), while the dental roots of the isolated M₁ (RPI-237) were also successfully measured (Table 2).

Table 2: Dental root measurements of the lower dentition of the *Ouranopithecus macedoniensis* specimens used in this study.

	length in mm (mean)
RPI-54	
P ₃	13,40
P ₄	13,41
M ₁	15,12
M ₂	13,68
RPI-75	
P ₃	17,87
P ₄	15,95
M ₁	-
M ₂	20,60
RPI-237	
M ₁	16,04

Fig. 2 and 3 show the root lengths of the lower post-canine dentition of *O. macedoniensis* compared with the extinct species *S. tchadensis* (Emonet et al., 2014) and *G. freybergi* (Fuss et al., 2017), and extant great apes and humans. The premolar root lengths of *O. macedoniensis* are relatively short compared to the great apes (Fig. 2): both the female and male P₃ roots of *O. macedoniensis* fall in the range of *Pan* and *Homo*, but outside the range of *Pongo* or *Gorilla* females/males, respectively - although the male overlaps with the range of the *Gorilla* females. The P₃ roots of *S. tchadensis* and *G. freybergi* are also short and have similar lengths to the male *O. macedoniensis* specimen. Among extant great apes, *Pongo* (both sexes) have the longest P₃ roots. P₄ root lengths show a similar pattern, with the female *O. macedoniensis* being the shortest and falling just below the range of *Pan* and *Homo*. The male P₄ root lengths of *O. macedoniensis*, but also *S. tchadensis* and *G. freybergi*, overlap with female *Pongo* and *Gorilla*, as well as *Pan* and *Homo*. Again *Pongo* (both sexes) have the longest P₄ roots.

Fig. 3 shows the root lengths of the lower molars (M₁ and M₂). The female and male M₁ roots of *O. macedoniensis* have similar lengths and fall in the range of *Pan*, *Homo*, and *Pongo*

(female). *G. freybergi* has shorter M₁ root lengths and falls in the range of *Pan* and *Homo*. *S. tchadensis* has longer roots and falls in the range of *Gorilla* and *Pongo*. Male *Gorilla* and *Pongo* show the longest M₁ roots among the great apes. As for the M₂ roots, the female root length of *O. macedoniensis* is shorter than the male one, and overlaps with *Pan* and *Homo*. The male M₂ root of *O. macedoniensis* is longer and falls in the range of *Pongo* and *Gorilla* (only male) and outside that of *Pan* or *Pongo*. The *G. freybergi* M₂ root is shorter than the male *O. macedoniensis*, but also falls in the range of *Pongo* and *Gorilla*. Among the great apes, *Pongo* and female *Gorilla* show the longest M₂ roots.

Dental root and pulp canal morphology

Virtual isolation and segmentation of the pulp canals were challenging, as in many teeth, there was a growth of secondary dentine layers in the pulp chamber. For that reason, it was impossible to extract the pulp canals from RPI-54 virtually; however, based on the micro CT-scan, we observed the number of pulp canals of each tooth (Table 3; Fig. 4 and 5). Unfortunately, that was not possible for the isolated RPI-237 M₁ due to extreme fossilization and bad preservation. As for the RPI-75, we could trace and segment the pulp canals from P₃, P₄, and M₂ (Fig. 4 and 6), while the pulp canals of the M₁ were also observed via the CT-scan (Fig. S1).

The premolars of *Ouranopithecus macedoniensis* have three roots and three or four pulp canals, while the molars are two- or three-rooted and have four pulp canals (Table 4). These results agree with those of Emonet (2009) and Emonet et al. (2012), where two different *O. macedoniensis* mandibles (male and female RPI-89 and RPI-117, respectively) were examined. The P₃ in RPI-75 (Fig. 6a) and RPI-54 presents three roots; one mesial with a single pulp canal and two distal roots (partially in contact with each other) with two pulp canals. This pattern is also observed to some extent in *Gorilla* and *Pan* (Emonet et al., 2012; Moore et al., 2015). However, *Gorilla* and *Pan* mostly have two rooted P₃ with three pulp canals, which is also the case for australopiths (three or four pulp canals; Woods et al., 1988; Moore et al., 2016) and the early hominin *S. tchadensis* (Emonet et al., 2014).

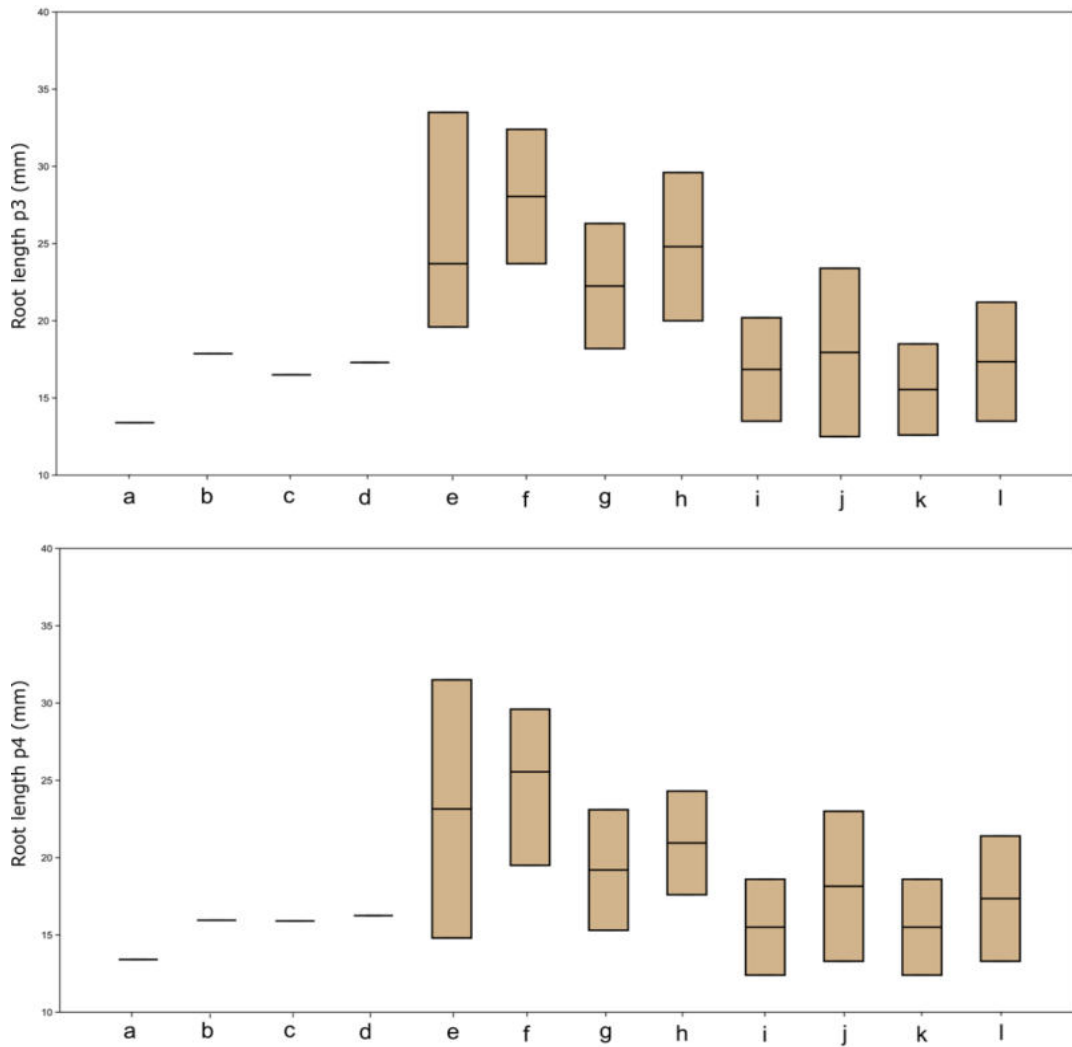


Fig. 2: Box-plot diagrams comparing the absolute root lengths of the lower premolars (P₃ and P₄) of *Ouranopithecus macedoniensis*, extant great apes (*Gorilla gorilla*, *Pan troglodytes*, *Pongo pygmaeus*), *Homo sapiens*, and a few other Miocene hominoids/hominids: *Sahelanthropus tchadensis* (Emonet et al., 2014) and *Graecopithecus freybergi* (Fuss et al., 2017). a: *O. macedoniensis* – female, b: *O. macedoniensis* – male, c: *G. freybergi* – male, d: *S. tchadensis* – male, e: *P. pygmaeus* – female, f: *P. pygmaeus* – male, g: *G. gorilla* – female, h: *G. gorilla* – male, i: *P. troglodytes* – female, j: *P. troglodytes* – male, k: *H. sapiens* – female, l: *H. sapiens* – male.

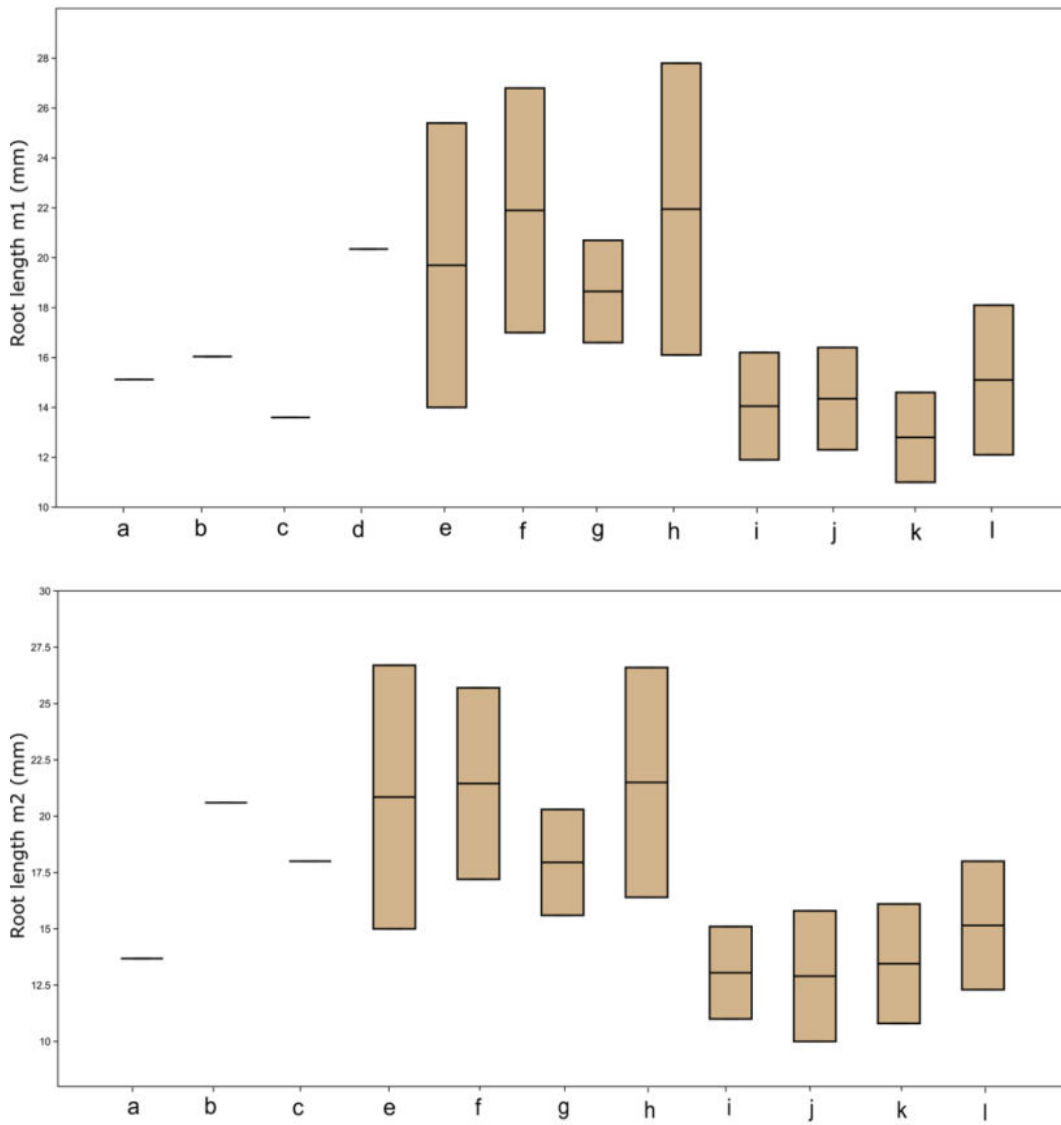


Fig. 3: Box-plot diagrams comparing the absolute root lengths of the lower molars (M₁ and M₂) of *Ouranopithecus macedoniensis*, extant great apes (*Gorilla gorilla*, *Pan troglodytes*, *Pongo pygmaeus*), *Homo sapiens*, and a few other Miocene hominoids/hominids: *Sahelanthropus tchadensis* (only M₁; Emonet et al., 2014) and *Graecopithecus freybergi* (Fuss et al., 2017). a: *O. macedoniensis* – female, b: *O. macedoniensis* – male, c: *G. freybergi* – male, d: *S. tchadensis* – male, e: *P. pygmaeus* – female, f: *P. pygmaeus* – male, g: *G. gorilla* – female, h: *G. gorilla* – male, i: *P. troglodytes* – female, j: *P. troglodytes* – male, k: *H. sapiens* – female, l: *H. sapiens* – male.

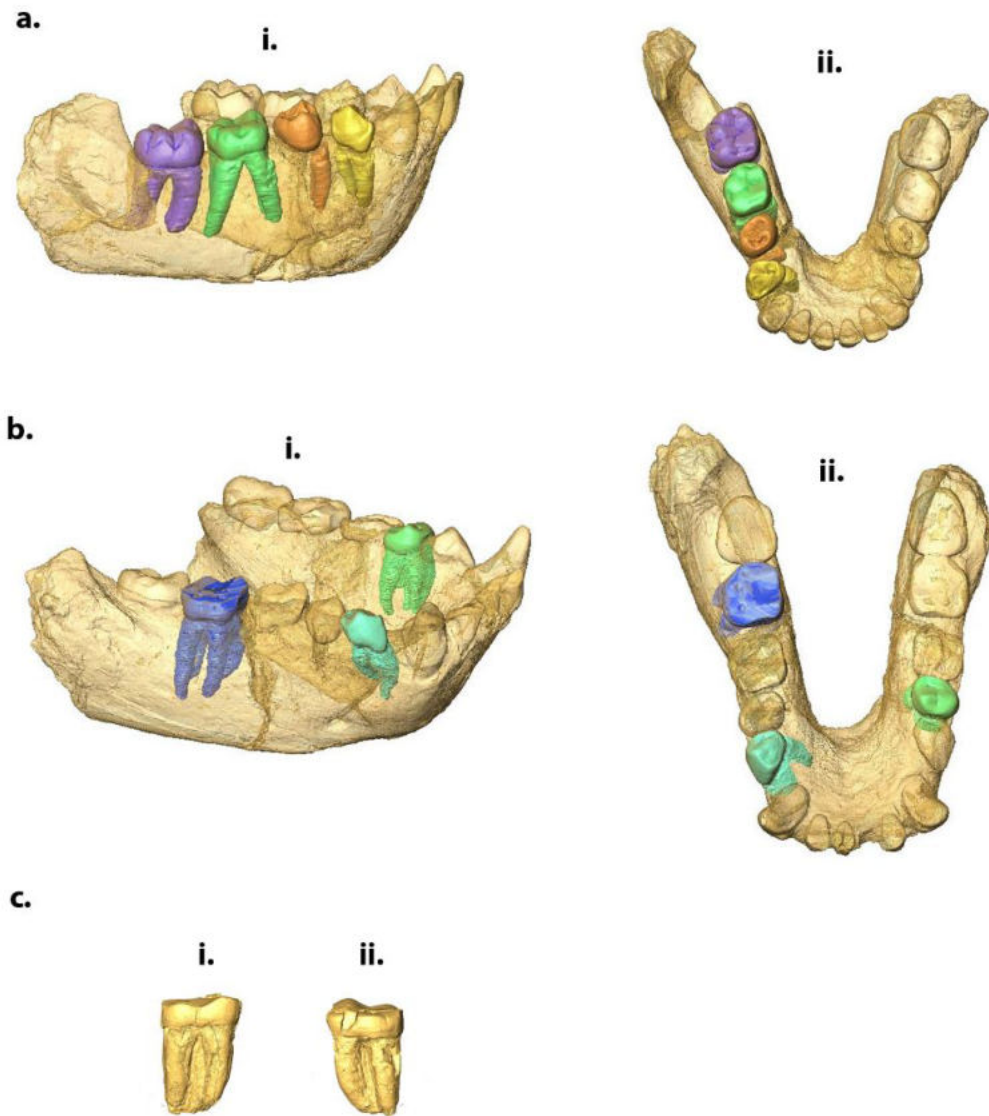


Fig. 4: Virtual reconstructions of the *Ouranopithecus macedoniensis* specimens used in this study. a. RPI-54 (i. buccal view, ii. occlusal view), b. RPI-75 (i. buccal view, ii. occlusal view), and c. RPI-237 (i. buccal and ii. lingual view).

Table 3: RPl-54 - root and pulp canal configuration.

P ₃	1 ₁ M + 2 ₂ D	single mesial root and partially fused distal roots - observation
P ₄	1 ₂ M + ? ₂ D	fused mesial roots and distal roots are missing - observation
M ₁	2 ₂ M + 1 ₂ D	partially fused mesial roots and fused distal roots - observation
M ₂	1 ₂ M + 1 ₂ D	fused roots (mesial and distal) - observation

Table 4: RPl-75 - root and pulp canal configuration.

P ₃	1 ₁ M + 2 ₂ D	single mesial root and fused distal roots - virtually segmented
P ₄	1 ₂ M + 2 ₂ D	fused mesial and partially fused distal roots - virtually segmented
M ₁	2 ₂ M + 1 ₂ D	partially fused mesial and fused distal roots - observation
M ₂	2 ₂ M + 1 ₂ D	partially fused mesial and fused distal roots - virtually segmented

The P₄ in both RPl-54 (although partially preserved) and RPl-75 (Fig. 6b) have three roots: one mesial with two pulp canals and two distal with two pulp canals. In both specimens, the mesial pulp canals are entirely connected with a secondary dentine layer, making the distinction between them harder (Fig. S2; S3). Moreover, the distal roots of RPl-75 are connected to each other for two-thirds of their length. *Gorilla* and *Pan*, and *Pongo* are mostly two rooted with three pulp canals, but some also have four pulp canals (Emonet et al., 2012; Moore et al., 2015).

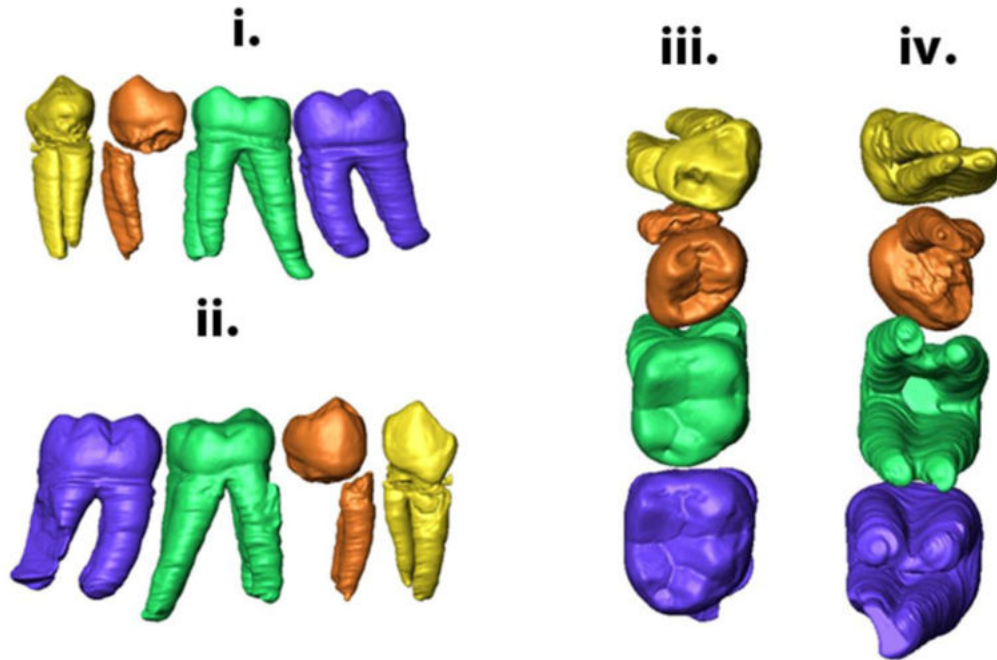


Fig. 5: Result of the virtual segmentation of the lower dentition of RPI-54 (right P₃ to M₂). i. lingual view, ii. buccal view, iii. occlusal view, and iv. ventral view.

In humans, the most common number of roots is one with one pulp canal (Shields, 2005), while in australopiths, two roots with four pulp canals, similar to the African apes (Wood et al., 1988; Moore et al., 2016). *S. tchadensis* also has two P₄ roots with four pulp canals (Emonet et al., 2014). *G. freybergi* is similar to our *O. macedoniensis* specimens in having three P₄ roots; however, its mesial root has only one pulp canal rather than two in *O. macedoniensis*, while its partially fused two distal roots also show two pulp canals (Fuss et al., 2017). The M₁ in both RPI-54 and RPI-75 exhibit three roots, two mesial and one distal root. However, the mesial and distal roots are in contact through a thin layer (or blade as defined by Kupczik, 2003) for at least half of their length. M₁ also has four pulp canals (although the mesial canals are connected to each other with a secondary dentine layer as in P₄).

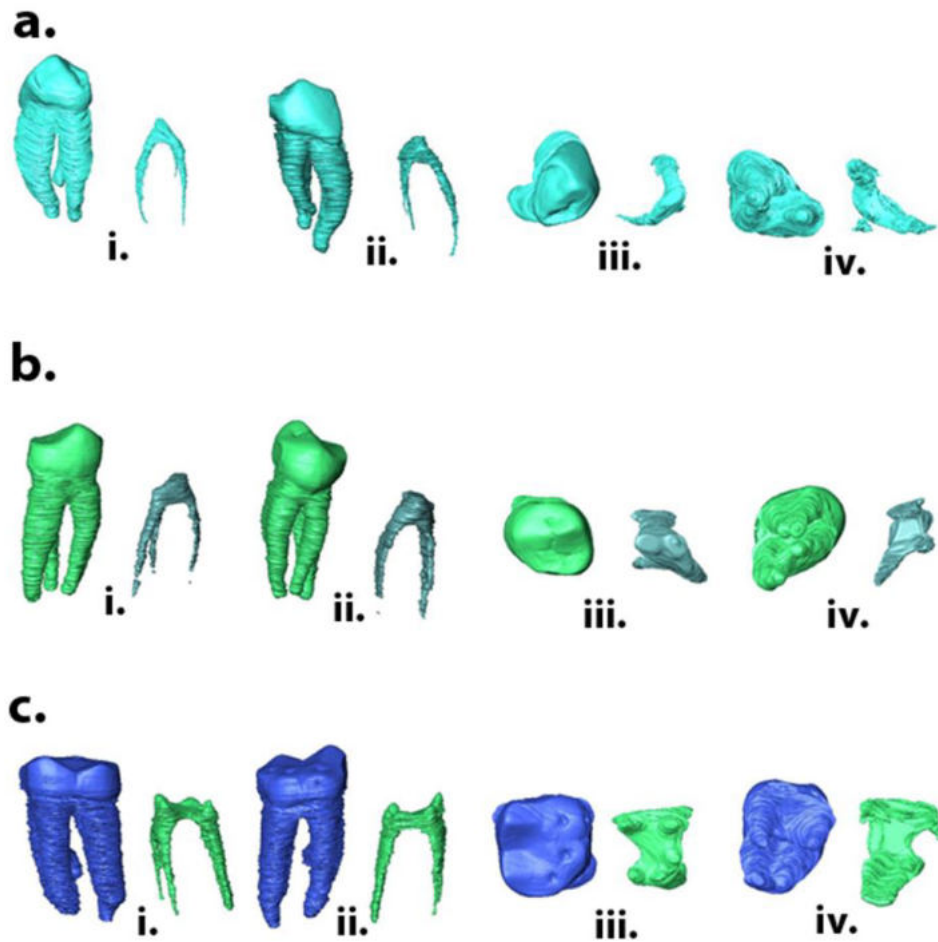


Fig. 6: Result of the virtual segmentation of the lower dentition of RPI-75 (right P₃ and M₂, and left P₄) including the whole teeth and the subsequent isolation of the pulp canal. a. right P₃ b. left P₄ and c. right M₂. In all, a to c: i. lingual view, ii. buccal view, iii. occlusal view, and iv. ventral view.

Gorilla, *Pan*, and *Pongo* mostly display three M₁ roots and four pulp canals (Emonet et al., 2012), while humans two roots and four pulp canals (Shields, 2005). *S. tchadensis* displays three M₁ roots with four pulp canals (Emonet et al., 2014), while *G. freybergi* exhibits three roots; one mesial with two pulp canals and two distal roots with one or two pulp canals (Fuss et al., 2017).

Table 5: root and pulp canal number in *Ouranopithecus macedoniensis* and comparative sample.

	P₃	P₄	M₁	M₂	Source
<i>O. macedoniensis</i> (n=4)	1 ₁ M + 2 ₂ D	1 ₂ M + ?-2 ₂ D	2 ₂ M + 1 ₂ D	1-2 ₂ M + 1 ₂ D	This study, Emonet et al., 2009
<i>G. freybergi</i> (n=1)	1 ₁ M + 1 ₂ D	1 ₁ M + 1 ₂ D	2 ₂ M + 1 ₁₋₂ D	1-2 ₂ M + 1 ₁ D	Fuss et al., 2017
<i>Gorilla</i> (n=94)	1 ₁ M + 1-2 ₂ D	1 ₂ M + 1 ₁₋₂ D	2 ₂ M + 1 ₂ D	2 ₂ M + 1 ₂ D	Emonet et al., 2012;2014, Moore et al., 2015
<i>Pan</i> (n=166)	1 ₁ M + 1-2 ₂ D	1 ₂ M + 1 ₁₋₂ D	2 ₂ M + 1 ₂ D	2 ₂ M + 1 ₂ D	Emonet et al., 2012;2014, Moore et al., 2015
<i>Pongo</i> (n=50)	1 ₁₋₂ M + 1 ₁₋₂ D	1 ₂ M + 1 ₁₋₂ D	2 ₂ M + 1 ₂ D	2 ₂ M + 1 ₂ D	Emonet et al., 2012;2014, Moore et al., 2015
<i>H. sapiens</i> (n=1615)	1 ₁	1 ₁	1 ₂ M + 1 ₂ D	1 ₂ M + 1 ₂ D	Shields, 2005
<i>S. tchadensis</i> (n=2)	1 ₁ M + 1 ₂ D	1 ₁ M + 1 ₂ D	1 ₂ M + 1 ₂ D	1 ₂ M + 1 ₂ D	Emonet et al., 2014
<i>Australopiths</i> (n=95)	1 ₁ M + 1 ₁₋₂ D	1 ₁₋₂ M + 1 ₂ D	N/A	N/A	Wood et al., 1988; Moore et al., 2016

The M₂ in RPI-54 and RPI-75 displays two or three roots, one or two mesial and one distal root. Part of the distal roots in RPI-54 is missing, while the mesial and distal roots are either fused or in contact with each other through a thin layer for most if not all their length. In RPI-75, the mesial roots are free of contact for half of their length, while the distal root is fused (Fig. 6c). Both specimens have four pulp canals (although the mesial canals are connected to each other with a secondary dentine layer as in P₄).

As with the M₁, *Gorilla*, *Pan* and *Pongo* mostly display three M₂ roots and four pulp canals (Emonet et al., 2012; 2014), while humans have two roots and four pulp canals (Shields, 2005). *S. tchadensis* displays three M₂ roots with four pulp canals (Emonet et al., 2014). Like the *O. macedoniensis* examined here, *G. freybergi* displays one or two mesial M₂ roots with two pulp canals and one distal root with one pulp canal (Fuss et al., 2017).

5.4 Discussion

Dental root morphology and phylogenetic affinities of *Ouranopithecus macedoniensis*

Our preliminary results indicate that the female specimen RPI-54 and the male RPI-75 display almost the same number of roots and the same number of pulp canals. The same pattern was also observed in the male and female specimens RPI-89 and RPI-117, respectively, in previous studies (Emonet, 2009; Emonet et al., 2012), suggesting that this morphology may have been typical in *Ouranopithecus macedoniensis*. The root lengths of the *Ouranopithecus* premolars are relatively shorter than the great apes, while the molars are either within the range of most great apes. The male (RPI-237) and female (RPI-54) specimens have similar P₄ and M₁ root lengths, while P₃ and M₂ roots differ in their length.

Ouranopithecus dental root morphology resembles the great apes' morphology based on our comparisons with current published data (Table 5). *Ouranopithecus* shares the following with the African apes and *Pongo*: three pulp canals in P₃; four pulp canals in P₄; three roots and four canals in M₁; and four pulp canals in M₂. However, our preliminary results did not indicate any special relationship with either the African apes or *Pongo*. If the internal tooth morphology of *O. macedoniensis* is similar to all great apes, then that makes *O. macedoniensis* likely stem hominid. It is necessary to conduct additional research to corroborate or reject this hypothesis. In the study by Emonet et al. (2012), the 3D analysis of mandibular dental root morphology showed that *Ouranopithecus* (specimens RPI-89 and RPI-117) resemble the root morphology of *Gorilla* and *Pan* than of *Pongo*. In this study, however, apart from 3D landmarks, a cladistic analysis of eight dental morphological characters was used. It also indicated a closer relationship (phylogenetic or size-related) of *Ouranopithecus* and *Gorilla*, based on the morphology of the P₄ roots. Moreover, other studies (e.g., de Bonis and Koufos, 1990; 2004; Koufos et al., 2016) have also supported the hypothesis that *Ouranopithecus* can be related to African apes and humans. However, these morphological similarities might correspond to homoplasies or shared ancestry of primitive characters and may not reflect close phylogenetic relationships.

Comparison with other extinct species

Our results confirm Fuss et al. (2017) observations in that the two *O. macedoniensis* specimens examined here differ from *G. freybergi* in their dental roots and pulp canal configuration/number (Table 5). The premolars in *G. freybergi* are two-rooted with three pulp canals, while the molars are two- or three-rooted with two to four pulp canals (Fuss et al., 2017). This might be taken to support the view that *G. freybergi* is taxonomically distinct from *O. macedoniensis* (see also Koufos and de Bonis, 2005), however more material from both *G. freybergi* and *O. macedoniensis* is needed for a definitive conclusion, primarily since *G. freybergi* is only known from one specimen. Moreover, Fuss et al. (2017) also argued that the reduction in the root and pulp chamber configuration shown by the *G. freybergi* specimen links it with later hominins, who also show this condition at high frequencies (Brunet et al., 2005; Emonet et al., 2014). However, variability of this feature in both extinct Miocene hominoids or among extant taxa should be investigated before its validity as a phylogenetic marker can be accepted. *Sahelanthropus tchadensis*, a possible early hominin, has a combination of primitive and derived dental root characters (Emonet et al., 2014), resembling the root morphology of the African apes in some traits (e.g., number of P₃ roots) and australopiths and *Homo* in other (e.g., incisor roots). This mosaic of characteristics can perhaps indicate an early hominin root morphology (Emonet et al., 2014). Compared to *Ouranopithecus*, australopiths have a reduced premolar root number, two-rooted P₃ and P₄, while they mostly have three to four pulp canals (Wood et al., 1988; Table 5). However, a recent study by Moore et al. (2016) has demonstrated a variation in the number of the pulp canals in *A. africanus* and *P. robustus*, varying between one to four. As for the post-canine root lengths, the *Ouranopithecus* premolars (in particular) and molars are similar to the root lengths of *S. tchadensis* and *G. freybergi*. Of great interest, however, would be the inclusion of the canine roots of the mandibular fragments (especially the male individual), as canine reduction is proposed to be a hominin trait (Jungers, 1978; White et al., 2009)

Premolar roots show the greatest variability within the hominoids (Emonet et al., 2012). The derived condition of root and pulp canal reduction in the maxillary and mandibular dentition is characteristic of the hominin clade (Moore et al., 2016 and references therein). On the other hand, the so-called "ancestral" great ape type for the mandible indicates a two rooted

P₃ with three pulp canals, while P₄ has two roots and four pulp canals (Abbott 1984; Wood et al., 1988; Kupczik et al., 2005; Emonet, 2009; Emonet et al., 2014). A partial fusion on the buccal side of the lower P₄ has been proposed by some as an exclusive hominin character, as it is present in some australopiths (Haile-Selassie and Melillo, 2015; Moore et al., 2016). Many late Miocene hominoids, including *Ouranopithecus macedoniensis*, do not have this potentially derived character. The P₄ partial root fusion found in *G. freybergi* is an integral part of the argument put forth by Fuss et al. (2017) that *G. freybergi* is a potential hominin. However, this hypothesis has been questioned by Benoit and Thackeray (2017), while several studies (Moore et al., 2013; 2015; Emonet and Kullmer, 2014) have shown that this pattern of a P₄ root fusion is also present in *Pan*, but at a low frequency (2-5 %). This indicates that this character is not exclusive to hominins, raising doubts about the interpretation of Fuss et al. (2017).

Conclusion

Our study has contributed new data about the internal mandibular tooth morphology obtained from three previously not investigated specimens of *Ouranopithecus macedoniensis* from the RPI fossiliferous locality. These individuals exhibit similar mandibular root morphology, implying that the configuration shown was not uncommon in this species. Our results do not reject the hypothesis that *O. macedoniensis* is taxonomically distinct from *G. freybergi*. However, firm conclusions cannot be reached based on the very limited sample of the latter. *Ouranopithecus* resembles the morphology of the African apes, *Gorilla* and *Pan*, but also *Pongo*. Our results did not indicate a clear relationship of the *O. macedoniensis* with any of the great apes in particular. Therefore, additional research in the lower dentition (including canines) of other *O. macedoniensis* teeth is needed to clarify this issue further. The variation of these features in both extinct and extant hominoids must be further evaluated before they can be ascertained. However, this study can serve as a pilot framework for analyzing the internal tooth morphology of *Ouranopithecus macedoniensis*.

ACKNOWLEDGMENTS

This work was supported by the Senckenberg Gesellschaft für Naturforschung, the Leventis Foundation, and the Deutsche Forschungsgemeinschaft (DFG INST 37/706-1). Special

thanks to C. Röding and A. Lockey for providing useful tips on the virtual teeth segmentation and to Dr. Katerina Tsarava for proofreading the manuscript.

REFERENCES

- Baab, K. L., McNulty, K. P., & Rohlf, F. J. (2012). The shape of human evolution: a geometric morphometrics perspective. *Evolutionary Anthropology: Issues, News, and Reviews*, 21(4), 151-165.
- Begun, D. R. (2009). Dryopithecins, Darwin, de Bonis, and the European origin of the African apes and human clade. *Geodiversitas*, 31(4), 789-816.
- Benoit, J., & Thackeray, F. J. (2017). A cladistic analysis of Graecopithecus. *South African Journal of Science*, 113(11-12), 1-2.
- de Bonis, L. (1974). Première découverte d'un primates hominoïde dans le Miocène supérieur de Macédoine (Grèce). *Comptes rendus de l'Académie des Sciences, Paris, série D*, 278, 3063-3066.
- de Bonis, L., & Melentis, J. (1977). Les Primates hominoïdes du Vallésien de Macédoine (Grèce). Étude de la mâchoire inférieure. *Geobios*, 10(6), 849-885.
- de Bonis, L., & Melentis, J. (1978). Les Primates hominoïdes du Miocène supérieur de Macédoine—Étude de la mâchoire supérieure. In *Annales de Paléontologie (vertébrés)*, 64, 185-202.
- de Bonis, L., & Koufos, G. D. (2004). Ouranopithecus et la date de séparation des hominoïdes modernes. *Comptes Rendus Palevol*, 3(4), 257-264.
- de Bonis, L., Bouvrain, G., Geraads, D., & Koufos, G. (1990). New hominid skull material from the late Miocene of Macedonia in Northern Greece. *Nature*, 345(6277), 712.
- de Bonis, L., Koufos, G. D., Guy, F., Peigné, S., & Sylvestrou, I. (1998). Nouveaux restes du primate hominoïde *Ouranopithecus* dans les dépôts du Miocène supérieur de Macédoine (Grèce). *Comptes Rendus de l'Académie des Sciences-Series IIA-Earth and Planetary Science*, 327(2), 141-146.
- Dean, D., & Delson, E. (1992). Second gorilla or third chimp?. *Nature*, 359(6397), 676.

- Emonet E.G. (2009). *Khoratpithecus* et la radiation des hominoides en Asie du Sud-Est au Miocène. Doctoral dissertation. Université de Poitiers
- Emonet, E. G., & Kullmer, O. (2014). Variability in Premolar and Molar Root Number in a Modern Population of *Pan troglodytes* versus. *The Anatomical Record*, 297(10), 1927-1934.
- Emonet, E. G., Tafforeau, P., Chaimanee, Y., Guy, F., De Bonis, L., Koufos, G., & Jaeger, J. J. (2012). Three-dimensional analysis of mandibular dental root morphology in hominoids. *Journal of Human Evolution*, 62(1), 146-154.
- Emonet, E. G., Andossa, L., Taisso Mackaye, H., & Brunet, M. (2014). Subocclusal dental morphology of *Sahelanthropus tchadensis* and the evolution of teeth in hominins. *American Journal of Physical Anthropology*, 153(1), 116-123.
- Fuss, J., Spassov, N., Begun, D. R., & Böhme, M. (2017). Potential hominin affinities of *Graecopithecus* from the Late Miocene of Europe. *PloS one*, 12(5), e0177127.
- Gamarra, B., Delgado, M. N., Romero, A., Galbany, J., & Pérez-Pérez, A. (2016). Phylogenetic signal in molar dental shape of extant and fossil catarrhine primates. *Journal of Human Evolution*, 94, 13-27.
- Harvati, K. (2003). Quantitative analysis of Neanderthal temporal bone morphology using three-dimensional geometric morphometrics. *American Journal of Physical Anthropology*, 120(4), 323-338.
- Harvati, K., Röding, C., Bosman, A. M., Karakostis, F. A., Grün, R., Stringer, C., ... & Kouloukoussa, M. (2019). Apidima Cave fossils provide earliest evidence of *Homo sapiens* in Eurasia. *Nature*, 571(7766), 500-504.
- Ioannidou, M., Koufos, G. D., de Bonis, L., & Harvati, K. (2019). A new three-dimensional geometric morphometrics analysis of the *Ouranopithecus macedoniensis* cranium (Late Miocene, Central Macedonia, Greece). *American Journal of Physical Anthropology*, 170(2), 295-307.
- Jungers, W. L. (1978). On canine reduction in early hominids. *Current Anthropology*, 19, 155-156.
- Köhler, M., Solà, S. M., & Alba, D. M. (2001). Eurasian hominoid evolution in the light of recent *Dryopithecus* findings. In *Hominoid evolution and climatic change in Europe, volume 2:*

phylogeny of the Neogene hominoid primates of Eurasia (pp. 193-212). Cambridge University Press.

Koufos, G. D. (1993). Mandible of *Ouranopithecus macedoniensis* (Hominidae, Primates) from a new late Miocene locality of Macedonia (Greece). *American Journal of Physical Anthropology*, 91(2), 225-234.

Koufos, G. D. (1995). The first female maxilla of the hominoid *Ouranopithecus macedoniensis* from the late Miocene of Macedonia, Greece. *Journal of Human Evolution*, 29(4), 385-399.

Koufos, G. D. (2006). The Neogene mammal localities of Greece: faunas, chronology and biostratigraphy. *Hellenic Journal of Geosciences*, 41(1), 183-214.

Koufos, G. D., & de Bonis, L. (2005). The Late Miocene hominoids *Ouranopithecus* and *Graecopithecus*. Implications about their relationships and taxonomy. *Annales de Paléontologie*, 91(3), 227-240

Koufos, G. D., & de Bonis, L. (2006). New material of *Ouranopithecus macedoniensis* from late Miocene of Macedonia (Greece) and study of its dental attrition. *Geobios*, 39(2), 223-243.

Koufos, G. D., Kostopoulos, D. S., & Vlachou, T. D. (2016). Revision of the Nikiti 1 (NKT) fauna with description of new material. *Geobios*, 49(1-2), 11-22.

Kovacs, I. (1971). A systematic description of dental roots. *Dental Morphology and Evolution*, 211-256.

Kunimatsu, Y., Nakatsukasa, M., Sawada, Y., Sakai, T., Hyodo, M., Hyodo, H., Itaya, T., Nakaya, H., Saegusa, H., Mazurier, A. & Saneyoshi, M. (2007). A new Late Miocene great ape from Kenya and its implications for the origins of African great apes and humans. *Proceedings of the National Academy of Sciences*, 104(49), 19220-19225.

Kupczik, K. (2003). Tooth root morphology in primates and *carnivores* (Doctoral dissertation, Ph. D. Thesis, University of London).

Kupczik, K., & Hublin, J. J. (2010). Mandibular molar root morphology in Neanderthals and Late Pleistocene and recent *Homo sapiens*. *Journal of Human Evolution*, 59(5), 525-541.

- Kupczik, K., Spoor, F., Pommert, A., & Dean, C. (2005). Premolar root number variation in hominoids: genetic polymorphism vs. functional significance. *Current Trends in Dental Morphology Research. University of Lodz Press, Lodz*, 257-268.
- Moore, N. C., Skinner, M. M., & Hublin, J. J. (2013). Premolar root morphology and metric variation in *Pan troglodytes verus*. *American Journal of Physical Anthropology*, 150(4), 632-646.
- Moore, N. C., Hublin, J. J., & Skinner, M. M. (2015). Premolar root and canal variation in extant non-human hominoidea. *American Journal of Physical Anthropology*, 158(2), 209-226.
- Moore, N. C., Thackeray, J. F., Hublin, J. J., & Skinner, M. M. (2016). Premolar root and canal variation in South African Plio-Pleistocene specimens attributed to *Australopithecus africanus* and *Paranthropus robustus*. *Journal of Human Evolution*, 93, 46-62.
- Sen, S., Koufos, G. D., Kondopoulou, D., & de Bonis, L. (2000). Magnetostratigraphy of the late Miocene continental deposits of the lower Axios valley, Macedonia, Greece. *Geological Society Greece Special Publications*, 9, 197-206.
- Shields ED. (2005). Mandibular premolar and second molar root morphological variation in modern humans: what root number can tell us about tooth morphogenesis. *American Journal of Physical Anthropology*, 128, 299-311.
- Smith, T. M., Tafforeau, P., Pouech, J., & Begun, D. R. (2019). Enamel thickness and dental development in *Rudapithecus hungaricus*. *Journal of human evolution*, 136, 102649.
- Smith, T. M., Tafforeau, P., Le Cabec, A., Bonnin, A., Houssaye, A., Pouech, J., ... & Menter, C. G. (2015). Dental ontogeny in Pliocene and early Pleistocene hominins. *PLoS one*, 10(2), e0118118.
- Spencer, M. A. (2003). Tooth-root form and function in platyrrhine seed-eaters. *American Journal of Physical Anthropology: The Official Publication of the American Association of Physical Anthropologists*, 122(4), 325-335.
- Spoor, F., Gunz, P., Neubauer, S., Stelzer, S., Scott, N., Kwekason, A., & Dean, M. C. (2015). Reconstructed *Homo habilis* type OH 7 suggests deep-rooted species diversity in early *Homo*. *Nature*, 519(7541), 83-86.

- Tafforeau, P., & Smith, T. M. (2008). Nondestructive imaging of hominoid dental microstructure using phase contrast X-ray synchrotron microtomography. *Journal of Human Evolution*, 54(2), 272-278.
- Tobias, P. V. (1995). Root number in the maxillary third premolars: a very ancient polymorphism. *Aspects of Dental Biology: Palaeontology, Anthropology and Evolution*, 283-290
- White, T. D., Asfaw, B., Beyene, Y., Haile-Selassie, Y., Lovejoy, C. O., Suwa, G., & WoldeGabriel, G. (2009). *Ardipithecus ramidus* and the paleobiology of early hominids. *Science*, 326(5949), 64-86.
- Wood B, Abbott SA, Uytterschaut H. (1988). Analysis of the dental morphology of Plio-Pleistocene hominids IV. Mandibular postcanine root morphology. *Journal of Anatomy*, 156, 107-139.
- Zanolli, C., & Mazurier, A. (2013). Endostructural characterization of the *H. heidelbergensis* dental remains from the early Middle Pleistocene site of Tighenif, Algeria. *Comptes Rendus Palevol*, 12(5), 293-304.
- Zanolli, C., Pan, L., Dumoncel, J., Kullmer, O., Kundrat, M., Liu, W., ... & Tuniz, C. (2018). Inner tooth morphology of *Homo erectus* from Zhoukoudian. New evidence from an old collection housed at Uppsala University, Sweden. *Journal of Human Evolution*, 116, 1-13.

Supplementary Material



Fig. S1: Cross-sectional depiction of the four canals present in the M_1 of RPl-75.



Fig. S2: Cross-sectional depiction of the P₄ of RPI-54, where it can be observed that the mesial pulp canals are entirely connected with a secondary dentine layer.

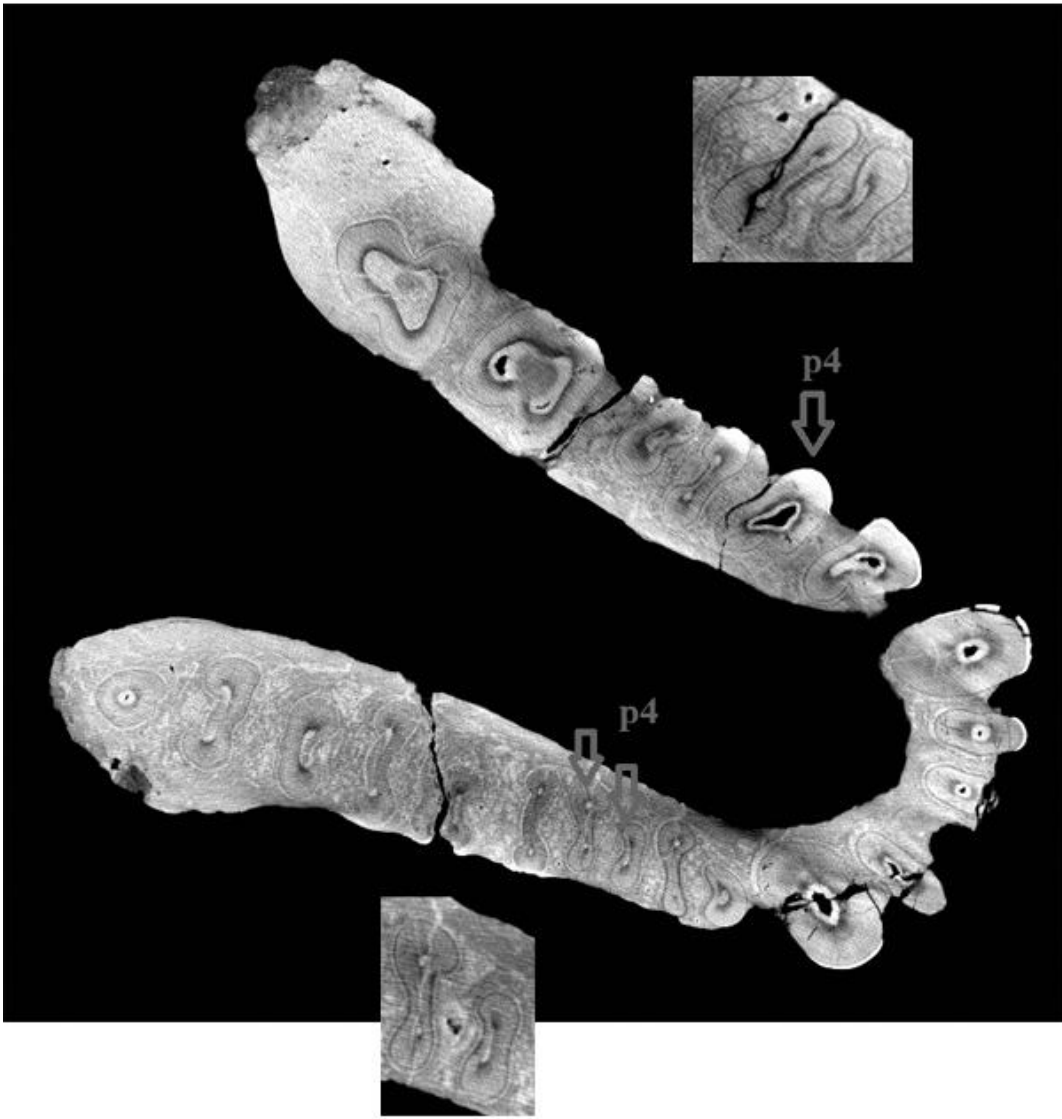


Fig. S3: Cross-sectional depiction of the P₄ of RPI-75, where it can be observed that the mesial pulp canals are entirely connected with a secondary dentine layer.

CHAPTER 6

6 General discussion

This section summarizes the key results of the three studies included in this dissertation, followed by an elaborated discussion on how these results can contribute to the ongoing discussion about *O. macedoniensis*. Lastly, the concluding remarks and future outlook for further research on the *O. macedoniensis* material are provided.

6.1 Key results and discussion

6.1.1 Study 1

In the first study (Chapter 3), two virtual cranial reconstructions of *O. macedoniensis* (XIR-1 cranium and RPI-128 maxilla) and their analyses via the application of 3D geometric morphometrics were conducted. The results showed that *O. macedoniensis* groups phenetically with *Gorilla*, than *Pan*, *Pongo*, or *Homo*. In the PCA *O. macedoniensis* falls within or close to the *Gorilla* convex hull. Thus, it is closer to the mean Procrustes shape distance of primarily *Gorilla*. Both specimens, face and maxilla, are classified as *Gorilla* based on DFA.

Traditionally traits used to infer phylogeny in the Miocene hominoids focus on dental (e.g., canine and post-canine tooth morphology, canine reduction, and enamel thickness); cranial (e.g., cranial vault size, and position of the foramen magnum); and facial features (e.g., orbital shape, supraorbital torus morphology, and zygomatic bones). Cladistics are predominately based on the presence of shared derived characters on cranial and postcranial elements used to taxonomically and phylogenetically group extant and extinct organisms. However, the way cladistics are used to infer hominin evolution has been questioned over the years (e.g., Smith, 2005; Ackermann and Smith, 2007; Haile-Selassie et al., 2016). It has been suggested that several factors, such as sexual dimorphism and inter- and intra-specific variation, shall be taken into account when identifying groups (Haile-Selassie et al., 2016; Ackermann and Smith, 2007).

The 3D shape analyses of this study included an area of potential phylogenetic interest, the face. The landmarks used were limited to the maxillofacial area, a combination of what is preserved on the two *O. macedoniensis* specimens. Nevertheless, these landmarks captured morphological areas with phylogenetic interest (e.g., the supraorbital region and the orbital shape). The PCA analyses showed that *O. macedoniensis* falls either within or closest to the

Gorilla convex hulls, while both specimens are classified as a *Gorilla* in the DFA. The results may suggest a close phenetic relationship between *Ouranopithecus* and *Gorilla*. Still, the phylogenetic connection could only be made if the former shares derived characters with the latter. *Ouranopithecus* and *Gorilla* share similarities in their orbital shape and their supraorbital torus morphology, traits that are proposed to be derived (de Bonis and Koufos, 1996; 1997; 2001). Moreover, the similarity between *Ouranopithecus* (XIR-1) and *Gorilla* is influenced by a similar shape of the nasoalveolar area, a feature considered primitive (Begun, 1992; de Bonis and Koufos, 1997; 2001).

The polarity of these features is subject of disagreements. One good example is the supraorbital torus, which, although it is recognized as a derived character, is connected to different groups by different authors. De Bonis and Koufos (2001) suggest that features on the *O. macedoniensis* supraorbital torus are similar to hominins, Begun (1992) to African apes and humans, Dean and Delson (1992) to *Gorilla*, and Köhler et al., (2001) to *Pongo*. What is more, facial morphology has been used to infer phylogeny (Lahr, 1996; Lockwood et al., 2004), however other studies in recent humans indicate that this anatomical area can be influenced by a variety of factors, such as dietary and environmental adaptations (Harvati and Weaver, 2006; Noback and Harvati, 2015; Reyes-Centeno et al., 2017). Hence, the value of these characters for reconstructing phylogeny is unclear and may not be the most reliable indicator of phylogenetic relationships.

Overall, the present study was a first step in quantifying the facial morphology of *O. macedoniensis* and placing it in the context of hominoid morphological variation. Further, this study formed the first attempt to restore deformities in the *O. macedoniensis* cranial fossil specimens virtually. Nevertheless, the results of the virtual reconstruction and comparative analysis of the XIR-1 cranium and RPI-128 maxilla are purely based on phenetic analyses. As morphology does not necessarily reflect phylogeny, no direct phylogenetic implications can be drawn at this point. Further interdisciplinary work is needed, e.g., on mechanisms driving facial morphology.

6.1.2 Study 2

In the second study (Chapter 4), 3D geometric morphometrics and multivariate statistical analyses were utilized to study mandibular fragments of *O. macedoniensis* and a comparative sample of extant great apes. The results showed that mandibular shape could differentiate *O. macedoniensis* from the extant great apes, although it showed some shape similarities to the larger great apes (*Gorilla* and *Pongo*). The PCA results suggested that the male and female specimens of *O. macedoniensis* have mandibular shapes that are quite similar, besides differences in mandibular length and symphysis height. The analyses of the Procrustes distances suggested, however, that there is more shape variation in *O. macedoniensis* than in the extant great apes. Moreover, the degree of sexual dimorphism in *O. macedoniensis* was found to be greater than in any of the great apes. Lastly, based on the correlation analyses, some principal components (PCs) are significantly correlated with size, with correlation varying from moderate to substantial. This suggests that size at least partly determines the morphology of these taxa, including *Ouranopithecus*, and contributes to the greater similarity in mandibular shape between *Ouranopithecus* and the larger great apes than compared to the smaller *Pan*. However, these results could be influenced by the small sample sizes and lack of extinct comparative samples (see below). Nonetheless, they indicated a high level of sexual dimorphism in the *O. macedoniensis* mandibles. *O. macedoniensis* shows a relatively elevated degree of morphological variation and, in particular, sexual dimorphism in mandibular size compared to *Gorilla* and *Pongo*.

In general, mandibular variation in primates reflects a combination of rather complex factors, such as phylogeny, diet and masticatory mechanisms, and sexual dimorphism/size. The latter was the focus of the 3D mandibular analyses in this study, however as the shape of the *O. macedoniensis* mandibles is controlled by all these factors, each of them will be discussed below:

Phylogeny: If we assume that the mandible preserves a low phylogenetic signal, as several studies suggest (Raveloson et al., 2005; Nicholson and Harvati, 2006; Schmittbuhl et al., 2007), then the mandibular similarities (if any) of *O. macedoniensis* to the great apes would reflect shared morphology. However, the 3D mandibular analyses in this study did not show any apparent similarities, rather than the fact that the *O. macedoniensis* mandibles are more

similar in shape to the larger great apes than they are to *Pan*. These mandibular similarities of the *O. macedoniensis* and the larger great apes could then be homoplasies or primitive retentions from the common ancestor of all three great apes.

Diet and masticatory mechanisms: As mentioned in the introduction, it is suggested that *O. macedoniensis* was consuming hard food items during dry periods but also fruits, fresh branches, and leaves during rainy periods. It seems plausible, therefore, that the alternation of hard and soft objects in the diet of *O. macedoniensis* may have influenced its mandibular morphology. However, it is also possible that hard object fallback foods may have been more impactful on morphology, as they lead to greater selective pressure. In some other hominoids, such as *Gigantopithecus*, characterized by a thick, large, and robust mandibular corpus, this morphology was also interpreted as an indication of a hard-object diet (Woo, 1962). The latter assumption is based on functional and biomechanical interpretations of food mastication in extant primates' mandibles, suggesting that a hard-object diet can alter the mandibular shape (e.g., Beecher 1977; Ravosa and Hylander; 1994; Daegling, 2001). Among these changes could be the fusion of the mandibular symphysis or the increase of the mandibular corpus thickness (Miller et al., 2008, and references therein). The mandibular body of *Ouranopithecus* is thick and robust, even if it is not as extreme as *Gigantopithecus*. Nevertheless, if these hypothetical models are reliable, this could suggest that the diet of *Ouranopithecus* may have influenced its mandibular morphology. However, some studies on primate skulls suggest that dietary functional adaptations alone cannot alter the development of the mandible, for instance, in such a great way. Following these great morphological changes would rather involve an interplay of size, diet, and phylogeny (e.g., Perez et al., 2011; Baab et al., 2014; Meloro et al., 2015).

Sexual dimorphism/size: Among great apes, *Pongo* is the most dimorphic, followed by *Gorilla*, and the least dimorphic being *Pan*. As for the mandibles, studies demonstrate that sexual size and shape dimorphism is present only in the larger great apes (Chamberlain and Wood, 1985; Taylor and Grooves, 2003; Taylor, 2006; Schmittbuhl et al., 2007; Robinson 2003; 2012; Singh, 2014). The high level of dental size variation in *O. macedoniensis* led some researchers to propose a two-species hypothesis in the past (Kay, 1982; Kay and Simons; 1983). However, it is indicated by later works (Koufos, 1995; Schrein, 2006; Scott et al., 2009;

Koufos et al., 2016a) that this variation is related to a high degree of sexual dimorphism, as *O. macedoniensis* is characterized by morphological homogeneity in the dentition. Moreover, a high degree of dental variation that exceeds the ranges expressed by the larger extant great apes is also present within other Miocene species, such as *Lufengpithecus lufengensis* (Kelley and Xu, 1991; Kelley and Plavcan, 1998; Scott et al., 2009). Results of Study 2 indicated that the degree of sexual dimorphism in the mandibles of *Ouranopithecus* exceeds that of *Pongo*, an interpretation that is in line with results from previous studies on the dentition (Scott et al., 2009; Koufos et al., 2016a).

To conclude, the results of Study 2 showed that mandibular shape could differentiate *Ouranopithecus macedoniensis* from the extant great apes. However, *O. macedoniensis* displays some shape similarities to the larger great apes, *Gorilla* and *Pongo*, probably partly due to a similar size. The limited *Ouranopithecus* sample also indicated that compared to *Gorilla* and *Pongo*, *O. macedoniensis* shows a relatively elevated degree of morphological variation and, in particular, sexual dimorphism in mandibular size to the latter taxon.

6.1.3 Study 3

In the third study enclosed in this dissertation (Chapter 5), a 3D analysis of the mandibular dentition of *O. macedoniensis* provided new data about its internal mandibular tooth morphology. The results showed that the lower dentition of the two mandibular specimens used exhibits a similar mandibular root morphology to each other, implying homogeneity in this species. *O. macedoniensis* shares several dental traits with the African apes and *Pongo*: three pulp canals in P₃; four pulp canals in P₄; three roots and four canals in M₁; and four pulp canals in M₂. However, the results did not indicate a clear relationship of *O. macedoniensis* with any of the great apes in particular. In relation to the great apes, the root lengths of the *Ouranopithecus* premolars are shorter, while the molars are within the range of most great apes. The male (RPI-237) and female (RPI-54) specimens have similar P₄ and M₁ root lengths, while their P₃ and M₂ roots differ in their length. Moreover, the results indicated that *O. macedoniensis* differs from *G. freybergi* in the root and pulp canal configuration. This supports the hypothesis that *O. macedoniensis* is taxonomically distinct from *G. freybergi*. These results are preliminary but have revealed new data about the lower

dental morphology of *O. macedoniensis*. Additional research in the lower dentition (including canines) of other *O. macedoniensis* teeth is needed to clarify this finding further.

The results indicated that the female specimen RPI-54 and the male RPI-75 display almost the same pattern in regard to the number of roots and pulp canals. The male (RPI-89) and female (RPI-117) specimens also match this pattern (Emonet, 2009; Emonet et al., 2012), suggesting that this morphology may have been typical in *O. macedoniensis*. *Ouranopithecus* dental root morphology and length (partly) resembles the great apes' based on our comparisons with current published data. However, the results did not indicate any specific relationship with either the African apes or *Pongo*. If the internal tooth morphology of *O. macedoniensis* is similar to all great apes, then that makes *O. macedoniensis* likely a stem hominid. Therefore, it is necessary to conduct additional research to confirm or reject this hypothesis. In contrast, the 3D analysis of mandibular dental root morphology by Emonet et al. (2012) showed that *Ouranopithecus* (specimens RPI-89 and RPI-117) resemble the root morphology of *Gorilla* and *Pan*, rather than the morphology of *Pongo*. However, in this study, apart from 3D landmarks, a cladistic analysis of eight dental morphological characters was used. This study also indicated a closer relationship (phylogenetic or size-related) of *Ouranopithecus* and *Gorilla*, based on the morphology of the P₄ roots. Other studies (e.g., de Bonis et al., 1990; Koufos et al., 2016a) have also supported the hypothesis that *Ouranopithecus* could be the sister group of the *Gorilla-Pan-Homo* clade. However, it is debated whether these observed morphological similarities are phylogenetically meaningful or correspond to homoplasies or shared ancestry of primitive characters and, thereby, may not reflect close phylogenetic relationships.

A reduction in the root and pulp chamber configuration is proposed to be a trait characteristic for hominins, as they display this condition at high frequencies (Brunet et al., 2005; Emonet et al., 2014). Fuss et al. (2017) argued that the reduction in the root and pulp chamber configuration shown by the *G. freybergi* specimen links it with later hominins. However, variability of this feature in both extinct Miocene hominoids or among extant taxa should be investigated before its validity as a phylogenetic marker can be accepted. *Sahelanthropus tchadensis* has a combination of primitive and derived dental root characters (Emonet et al., 2014), resembling the root morphology of the African apes in some traits (e.g.,

number of P₃ roots) and australopiths and *Homo* in other (e.g., incisor roots). This mosaic of characteristics could be typical in an early hominin root morphology (Emonet et al., 2014). Compared to *Ouranopithecus*, australopiths have a reduced premolar root number, with two-rooted P₃ and P₄, while they mostly show three to four pulp canals (Wood et al., 1988). However, a recent study by Moore et al. (2016) has demonstrated a variation in the number of the pulp canals in *A. africanus* and *P. robustus*, varying between one to four. As for the post-canine root lengths, the *Ouranopithecus* premolars (in particular) and molars are similar to the root lengths of *S. tchadensis* and *G. freybergi*. Of great interest, however, would be the inclusion of the canine roots of the mandibular fragments (especially the male individual), as canine reduction is proposed to be a hominin trait (Jungers, 1978; White et al., 2009).

Premolar roots show the greatest variability within the hominoids (Emonet et al., 2012). The derived condition of root and pulp canal reduction in the maxillary and mandibular dentition is characteristic of the hominin clade (Moore et al., 2016 and references therein). Nonetheless, the so-called "ancestral" great ape type for the lower dentition indicates a two-rooted P₃ with three pulp canals, while P₄ has two roots and four pulp canals (Abbott, 1984; Wood et al., 1988; Kupczik et al., 2005; Emonet, 2009; Emonet et al., 2014). A partial fusion on the buccal side of the lower P₄ has been proposed by some as an exclusive hominin character, as it is present in some australopiths (Haile-Selassie and Melillo, 2015; Moore et al., 2016). Many late Miocene hominoids, including *Ouranopithecus macedoniensis*, do not have this potentially derived character. The P₄ partial root fusion found in *G. freybergi* is an integral part of the argument put forth by Fuss et al. (2017) that *G. freybergi* is a potential hominin. However, this hypothesis has been questioned by Benoit and Thackeray (2017), while several studies (Moore et al., 2013; 2015; Emonet and Kullmer, 2014) have shown that this pattern of a P₄ root fusion is also present in *Pan*, but at a low frequency (2-5 %). This indicates that this character is not exclusive to hominins, raising doubts about the interpretation of Fuss et al. (2017).

Regarding the comparison of *O. macedoniensis* and *G. freybergi*, the results confirmed the observation by Fuss et al. (2017) that they differ in their dental root and pulp canal configuration/number. The premolars in *G. freybergi* are two-rooted with three pulp canals, while the molars are two- or three-rooted with two to four pulp canals (Fuss et al., 2017).

This might support the view that *G. freybergi* is taxonomically distinct from *O. macedoniensis*, as Koufos and de Bonis (2005) have previously suggested. However, more material from both *G. freybergi* and *O. macedoniensis* is needed for a definitive conclusion, primarily since *G. freybergi* is only known from one mandibular specimen.

Overall, this study contributed new data about the internal mandibular tooth morphology obtained from three previously not investigated specimens of *Ouranopithecus macedoniensis* from the RPI fossiliferous locality. Although preliminary, this study can serve as a pilot framework for analyzing the internal tooth morphology of *Ouranopithecus macedoniensis*.

6.2 Concluding remarks and future perspectives

Using advanced techniques, such as VA and GM, to study fossil material is an interesting venture, with many potential applications to paleontological and paleoanthropological projects. The findings of the doctoral research disclosed in this dissertation provided new insights on the phenetic and possible phylogenetic affinities of *O. macedoniensis*, as well as the variability and sexual dimorphism exhibited within the species and in comparison to the extant great apes. Finally, potential factors influencing morphology across great apes were also indicated.

The research questions outlined at the beginning of this dissertation were: (1) What are the morphological affinities of the reconstructed facial area of *O. macedoniensis* in relation to the extant great apes? (Study 1), (2) Does male-female mandibular shape vary within *O. macedoniensis*? (Study 2), (3) How do mandibular shape, size, and sexual dimorphism in *O. macedoniensis* compare to the extant great apes? (Study 2) and (4) Is the study of the internal root morphology the key to resolving the debatable phylogenetic position of *O. macedoniensis*? (Study 3). In response, findings of this dissertation suggest:

(1) The two *O. macedoniensis* specimens (XIR-1 and RPI-128) suggest a closer phenetic relationship of *Ouranopithecus* and *Gorilla* compared to the other great apes. *Ouranopithecus* and *Gorilla* share similarities in the orbital shape and supraorbital torus morphology, characters which are proposed to be derived. As these results are based on similarity analyses, direct phylogenetic implications cannot be drawn. Nonetheless, the study forms

the first attempt to restore deformities in the *O. macedoniensis* cranial fossil specimens virtually.

(2) Findings suggest that the male and female specimens of *O. macedoniensis* have mandibular shapes that are quite similar, although differences exist (mandibular length and symphysis height). Additional findings indicate that there is more shape variation in the small *O. macedoniensis* sample than in the extant great apes.

(3) Findings suggest that *O. macedoniensis* shows some mandibular shape similarities to the larger great apes, *Gorilla* and *Pongo*, probably partly due to a similar size. Moreover, *O. macedoniensis* shows a relatively elevated degree of morphological variation and, especially, sexual dimorphism in mandibular size compared to *Gorilla* and *Pongo*.

(4) The preliminary findings suggest that the internal root morphology in *O. macedoniensis* resembles the morphology of the African apes, but also *Pongo*. Since no direct relationship of *O. macedoniensis* with either the African great apes or *Pongo* was found, additional research in the lower dentition is needed to clarify this further.

The small sample size of fossil hominoids, and in this case of craniodental elements of *O. macedoniensis*, is a major impediment in the validity of its phylogenetic position. Variation within and between species is an essential factor that many times is not well-understood nor reported. When working with fossils, the sample size is almost always limited due to the nature of the fragmentary fossil record. For instance, *O. macedoniensis* is only represented by one almost complete face of a male individual and one maxilla of another male. *How can we determine the phylogeny of this species based solely on such a small sample size? How do we know that it is representative of this species?* Nonetheless, as long as the fossil samples of the Miocene are scarce, even the smallest piece of information is important. For instance, findings from Study 2 have revealed information about the mandibular within-species variation, despite the fact that only 3 or 4 mandibular fragments were available. Apart from the small fossil sample size, the size of the comparative sample is also an important component. More great apes shall be added, but more importantly, other Miocene hominoids. In particular, the hominoids from the Eastern Mediterranean are essential,

although access to this fossil material was not granted and will remain challenging in the future.

Moreover, despite the efforts to avoid distorted anatomical regions in the cranium or mandibles, the *O. macedoniensis* specimens might also be affected by taphonomic processes resulting in slight distortions and asymmetries. This is common in the fossil record, and it may affect the registration of the 3D landmarks (Study 1 and 2) or in the elevated mandibular variation observed in Study 2. As for the virtual reconstruction in Study 1, although established protocols were followed, every reconstruction that is at least partially manual is subjective to a certain degree depending on the amount of preserved anatomy and state of preservation. Approaches such as reference-based reconstructions (Gunz et al., 2009; Senck et al., 2015) try to limit this source of bias. However, these reconstructions rely on an appropriate reference sample to guide the reconstruction. Such a reference sample is not available for *O. macedoniensis*.

As mentioned before, using only extant great apes as models might restrict our image of the possible extent of variability in the past. As observed in Study 2, where only extant great apes were used, sexual dimorphism in *O. macedoniensis* exceeds the "standards", as it shows a greater degree than the dimorphic *Gorilla* and *Pongo*. But perhaps if mandibles of other Miocene hominoids could have been included, the results may differ. Nevertheless, comparisons of dental sexual dimorphism helped to build a framework for this result. Some researchers question the necessity to connect the fossil record with the extant living species, as it may restrict our view and hypotheses of what else was present during the Miocene and later epochs (e.g., Taylor 2006; Fleagle and Liebermann, 2015; Macchiarelli et al., 2020). The golden mean is proposed here: extant great apes must continue to be used as a comparative sample (without underestimating existing variation), and if possible, adding extinct species into the samples, even if their data derives from the literature. Besides the limitation that 3D analyses require the use of scans and therefore full access to extinct material, studies 1-3 show the importance of using VA and GM in studying fossil materials. Traditional methods cannot reach the full potential of analyzing these materials compared to VA and GM techniques.

Altogether, the first study attempted to restore symmetry and investigate the phenetic similarities of *O. macedoniensis* with extant great apes and humans. The facial analysis of the XIR-1 cranium and RPI- maxilla provided interesting results, as the facial/maxillary area was analyzed for the first time using VA and GM. The second study revealed information about mandibular variation within this Miocene ape species, mandibular morphology, and sexual dimorphism. Inferring phylogeny was beyond the scope of this study, as it focused on intra-specific variation. In this analysis, the *Ouranopithecus* sample was limited to the available fossils, two males and two females, deriving from the same locality. This study was informative as it filled a gap from previous research by focusing on the mandibular morphology of *Ouranopithecus* with state-of-the-art techniques. Nonetheless, as mentioned before, both facial and mandibular areas are subject to many influencing factors, which prevent drawing a definite conclusion for *O. macedoniensis*'s phylogenetic position purely based on this morphology. Lastly, the 3D dental analysis, although preliminary at this stage, is promising. Based on the current literature and research, it seems that the most reliable way to follow when working with highly fossilized/damaged fossils is the internal morphology of the upper and lower dentition. Since dental remains of *O. macedoniensis* are plentiful, future research focusing on them could be very informative. Overall, findings from these three studies can be used as a supportive and informative basis when evaluating the existing phylogenetic hypotheses of *O. macedoniensis* or when referring to sexual dimorphism and homogeneity in its mandibular and dental traits.

Different researchers have different ideas about the Miocene hominoids, and *how(/if)* they connect to the human lineage. Apart from a thorough and vigorous examination of morphology, cladistics, molecular analyses, a re-consideration of the characters seen as primitive or derived is required. In my point of view *O. macedoniensis*, along with the other late Miocene taxa found in Eurasia, belong to the hominids (great apes and humans). However, their placement to the evolution of the hominid lineage is not straightforward, as this doctoral dissertation has partially supported. Although we always urge to connect every specimen with what is present today, this is not always optimal. It is possible that there are missing species whose fossils may not have been found until today. Also, it might be the case that there are areas of potential excavations, which for several reasons (political issues,

geology, etc.), cannot be excavated. *Shall this stop us from continuing research on the Miocene hominoids? No*, but while reporting such findings, one shall not also forget to report the aforementioned issues.

Last but of great importance is the **unity missing among people working on Miocene materials**. This would allow for collaborations and data exchanges between scientists, which would enhance more robust comparative analyses and offer more decisive findings on very debated specimens. An open science mentality in our field is more than necessary since we urge to conclude about a very complex past based on fragmentary and scarce fossil findings.

REFERENCES

- Abbott, S. A. (1984). A comparative study of tooth root morphology in the great apes, modern man and early hominids. Doctoral dissertation. University of London.
- Abel, O. (1903). Zwei neue Menschenaffen aus den Leithakalkbildungen des wiener Beckens. E. Scweiz. Verlags.
- Ackermann, R. R., & Smith, R. J. (2007). The macroevolution of our ancient lineage: what we know (or think we know) about early hominin diversity. *Evolutionary Biology*, *34*(1), 72-85.
- Adams, D. C., Rohlf, F. J., & Slice, D. E. (2004). Geometric morphometrics: ten years of progress following the 'revolution'. *Italian Journal of Zoology*, *71*(1), 5-16.
- Alba, D. M. (2012). Fossil apes from the vallès-enedès basin. *Evolutionary Anthropology: Issues, News, and Reviews*, *21*(6), 254-269.
- Almécija, S., Hammond, A. S., Thompson, N. E., Pugh, K. D., Moyà-Solà, S., & Alba, D. M. (2021). Fossil apes and human evolution. *Science*, *372*(6542).
- Alpagut, B., Andrews, P., Fortelius, M., Kappelman, J., Temizsoy, I., Çelebi, H., & Lindsay, W. (1996). A new specimen of *Ankarapithecus meteai* from the Sinap Formation of central Anatolia. *Nature*, *382*(6589), 349-351.
- Andrews, W. C. (1918). Note on some fossil mammals from Salonica and Imbros. *Geological Magazine*, London, *5*, 540-543.
- Andrews, P. (2020). Last Common Ancestor of Apes and Humans: Morphology and Environment. *Folia Primatologica*, *91*(2), 122-148.
- Andrews, P., & Bernor, R. L. (1999). Vicariance biogeography and paleoecology of Eurasian Miocene hominoid primates. In: Agustí, J., Rook, L., Andrews, P. (Eds.), *Hominid Evolution and Climatic Change in Europe*. In: *Climatic and Environmental Change in the Neogene of Europe*, vol. 1. (pp. 454-487). Cambridge University Press.
- Arambourg, C., & Piveteau, J. (1929). Les Vertébrés du Pontien de Salonique. *Annales de Paléontologie*, *18*, 59-138.
- Ataabadi, M. (2010). The Miocene of Western Asia; fossil mammals at the crossroads of faunal provinces and climate regimes. PhD thesis, University of Helsinki, Helsinki University Print, Helsinki.

- Baab, K. L., Perry, J. M., Rohlf, F. J., & Jungers, W. L. (2014). Phylogenetic, ecological, and allometric correlates of cranial shape in Malagasy lemuriforms. *Evolution*, 68(5), 1450-1468.
- Beecher, R. M. (1977). Function and fusion at the mandibular symphysis. *American Journal of Physical Anthropology*, 47(2), 325-335.
- Begun, D. R. (1992). Miocene fossil hominids and the chimp-human clade. *Science*, 257(5078), 1929-1933.
- Begun, D. R. (1994). Relations among the great apes and humans: new interpretations based on the fossil great ape *Dryopithecus*. *American Journal of Physical Anthropology*, 37(S19), 11-63.
- Begun, D. R. (2000). Middle Miocene hominoid origins. *Science*, 287(5462), 2375-2375.
- Begun, D. R. (2003). Planet of the apes. *Scientific American*, 289(2), 74-83.
- Begun, D. R. (2009). Dryopithecins, Darwin, de Bonis, and the European origin of the African apes and human clade. *Geodiversitas*, 31(4), 789-816
- Begun, D. R. (2015). Fossil record of Miocene hominoids. In W. Henke & I. Tattersall (Eds.), *Handbook of Paleoanthropology*, 1261-1332. Berlin, Springer
- Begun, D. R., & Kordos, L. (1997). Phyletic affinities and functional convergence in *Dryopithecus* and other Miocene and living hominids. In *Function, Phylogeny, and Fossils* (pp. 291-316). Springer, Boston, MA.
- Benoit, J., & Thackeray, F. J. (2017). A cladistic analysis of *Graecopithecus*. *South African Journal of Science*, 113(11-12), 1-2.
- Böhme, M., Spassov, N., Fuss, J., Tröscher, A., Deane, A. S., Prieto, J., ... & Begun, D. R. (2019). A new Miocene ape and locomotion in the ancestor of great apes and humans. *Nature*, 575(7783), 489-493.
- Bookstein, F. L. (1991). *Morphometric tools for landmark data: geometry and biology*. Cambridge University Press.
- Bookstein, F. L. (1997). Landmark methods for forms without landmarks: morphometrics of group differences in outline shape. *Medical Image Analysis*, 1(3), 225-243.
- Bookstein, F.L., Slice, D.E., Gunz, P., & Mitteroecker, P. (2004). Anthropology takes control of morphometrics. *Collegium Antropologicum*, 28(2), 121-132.

- Brooks, D. R., & McLennan, D. A. (2003). Extending phylogenetic studies of coevolution: secondary Brooks parsimony analysis, parasites, and the Great Apes. *Cladistics*, *19*(2), 104-119.
- Brunet, M., Guy, F., Pilbeam, D., Mackaye, H. T., Likius, A., Ahounda, D., ... & Zollikofer, C. (2002). A new hominid from the Upper Miocene of Chad, Central Africa. *Nature*, *418*(6894), 145-151.
- Brunet, M., Guy, F., Pilbeam, D., Lieberman, D. E., Likius, A., Mackaye, H. T., ... & Vignaud, P. (2005). New material of the earliest hominid from the Upper Miocene of Chad. *Nature*, *434*(7034), 752-755.
- Cachel, S. (2015). Fossil primates. Cambridge University Press.
- Casnovas-Vilar, I., Alba, D. M., Garcés, M., Robles, J. M., & Moyà-Solà, S. (2011). Updated chronology for the Miocene hominoid radiation in Western Eurasia. *Proceedings of the National Academy of Sciences*, *108*(14), 5554-5559.
- Chaimanee, Y., Yamee, C., Tian, P., Khaowiset, K., Marandat, B., Tafforeau, P., Christian Nemoz, & Jaeger, J. J. (2006). Khoratpithecus piriyai, a late Miocene hominoid of Thailand. *American Journal of Physical Anthropology*, *131*(3), 311-323.
- Chaimanee, Y., Lazzari, V., Chaivanich, K., & Jaeger, J. J. (2019). First maxilla of a late Miocene hominid from Thailand and the evolution of pongine derived characters. *Journal of Human Evolution*, *134*, 102636.
- Chamberlain, A. T., & Wood, B. A. (1985). A reappraisal of variation in hominid mandibular corpus dimensions. *American Journal of Physical Anthropology*, *66*(4), 399-405.
- Coppens, Y. (1994). East side story: the origin of humankind. *Scientific American*, *270*(5), 88-95.
- Daegling, D. J. (2001). Biomechanical scaling of the hominoid mandibular symphysis. *Journal of Morphology*, *250*(1), 12-23.
- Dean, D., & Delson, E. (1992). Second gorilla or third chimp?. *Nature*, *359*(6397), 676-677.
- de Bonis, L. (1974). Première découverte d'un primates hominoïde dans le Miocène supérieur de Macédoine (Grèce). *Comptes rendus de l'Académie des Sciences, série D*, *278*, 3063-3066.
- de Bonis, L., Bouvrain, G., Geraads, D., & Koufos, G. D. (1990). New hominid skull material from the late Miocene of Macedonia in Northern Greece. *Nature*, *345*(6277), 712-714.

- de Bonis, L., Bouvrain, G., Geraads, D., & Koufos, G. D. (1992). Diversity and paleoecology of Greek late Miocene mammalian faunas. *Palaeogeography, Palaeoclimatology, Palaeoecology*, 91(1), 99-121.
- de Bonis, L., & Koufos, G. D. (1993). The face and the mandible of *Ouranopithecus macedoniensis*: Description of new specimens and comparisons. *Journal of Human Evolution*, 24(6), 469-491.
- de Bonis, L., & Koufos, G. D. (1994). Our ancestors' ancestor: *Ouranopithecus* is a Greek link in human ancestry. *Evolutionary Anthropology: Issues, News, and Reviews*, 3(3), 75-83.
- de Bonis, L., & Koufos, G. D. (1996). Phyletic relationships and taxonomic assessment of *Ouranopithecus macedoniensis* (Primates, Mammalia). *Current Primatology Ecology and Evolution*, 13, 295-301.
- de Bonis, L., & Koufos, G. D. (1997). The phylogenetic and functional implications of *Ouranopithecus macedoniensis*. In D. R. Begun, C. V. Ward, & M. D. Rose (Eds.), *Function, phylogeny, and fossils: Miocene hominoid evolution and adaptations* (pp. 317-326). New York: Plenum.
- de Bonis, L., & Koufos, G. D. (2001). Phylogenetic relationships of *Ouranopithecus macedoniensis* (Mammalia, Primates, Hominoidea, Hominidae) of the late Miocene deposits of Central Macedonia (Greece). In L. Bonis, G. D. Koufos, & P. Andrews (Eds.), *Phylogeny of the neogene hominoid primates of Eurasia* (pp. 254-268). Cambridge, UK: Cambridge University Press.
- de Bonis, L., & Koufos, G. D. (2004). *Ouranopithecus* et la date de séparation des hominoïdes modernes. *Comptes Rendus Palevol*, 3(4), 257-264.
- de Bonis, L., & Koufos, G. D. (2014). First discovery of postcranial bones of *Ouranopithecus macedoniensis* (Primates, Hominoidea) from the late Miocene of Macedonia (Greece). *Journal of Human Evolution*, 74, 21-36.
- de Bonis, L., Koufos, G. D., Guy, F., Peigné, S., & Sylvestrou, I. (1998). Nouveaux restes du primate hominoïde *Ouranopithecus* dans les dépôts du Miocène supérieur de Macédoine (Grèce). *Comptes Rendus de l'Académie des Sciences-Series IIA-Earth and Planetary Science*, 327 (2), 141-146.
- de Bonis, L., & Melentis, J. (1977). Les Primates hominoïdes du Vallésien de Macédoine (Grèce). Étude de la mâchoire inférieure. *Geobios*, 10(6), 849-885.

- de Bonis, L., & Melentis, J. (1978). Les Primates hominoïdes du Miocène supérieur de Macédoine—Étude de la mâchoire supérieure. *Annales de Paléontologie (vertébrés)*, 64, 185-202.
- Diogo, R., Molnar, J. L., & Wood, B. (2017). Bonobo anatomy reveals stasis and mosaicism in chimpanzee evolution, and supports bonobos as the most appropriate extant model for the common ancestor of chimpanzees and humans. *Scientific Reports*, 7(1), 1-8.
- Easteal, S., & Herbert, G. (1997). Molecular evidence from the nuclear genome for the time frame of human evolution. *Journal of Molecular Evolution*, 44(1), S121-S132.
- Emonet E.G. (2009). *Khoratpithecus* et la radiation des hominoïdes en Asie du Sud-Est au Miocène: Université de Poitiers
- Emonet, E. G., & Kullmer, O. (2014). Variability in Premolar and Molar Root Number in a Modern Population of *Pan troglodytes* versus. *The Anatomical Record*, 297(10), 1927-1934.
- Emonet, E. G., Tafforeau, P., Chaimanee, Y., Guy, F., De Bonis, L., Koufos, G., & Jaeger, J. J. (2012). Three-dimensional analysis of mandibular dental root morphology in hominoids. *Journal of Human Evolution*, 62(1), 146-154.
- Emonet, E. G., Andossa, L., Taïso Mackaye, H., & Brunet, M. (2014). Subocclusal dental morphology of *Sahelanthropus tchadensis* and the evolution of teeth in hominins. *American Journal of Physical Anthropology*, 153(1), 116-123.
- Fleagle, J. G. (2013). *Primate adaptation and evolution*. Academic press.
- Fleagle, J. G., & Lieberman, D. E. (2021). 15 Major Transformations in the Evolution of Primate Locomotion. In *Great transformations in vertebrate evolution* (pp. 257-280). University of Chicago Press.
- Fortelius, M., Werdelin, L., Andrews, P., Bernor, R. L., Gentry, A., Humphrey, L., H-W. Mittmann & Viranta, S. (1996). Provinciality, diversity, turnover, and paleoecology in land mammal faunas of the later Miocene of western Eurasia. In: Bernor, R.L., Fahlbusch, V., Mittmann, H. V. (Eds.), *The Evolution of Western Eurasian Neogene Mammal Faunas*. Columbia University Press, New York, 414-448.
- Fuss, J., Spassov, N., Begun, D. R., & Böhme, M. (2017). Potential hominin affinities of *Graecopithecus* from the Late Miocene of Europe. *PloS One*, 12(5), e0177127.

- Gilbert, C. C., Pugh, K. D., & Fleagle, J. G. (2020). Dispersal of Miocene hominoids (and Pliopithecoids) from Africa to Eurasia in light of changing tectonics and climate. In *Biological Consequences of Plate Tectonics* (pp. 393-412). Springer, Cham.
- Glazko, G. V., & Nei, M. (2003). Estimation of divergence times for major lineages of primate species. *Molecular Biology and Evolution*, *20*(3), 424-434.
- Gower, J. C. (1975). Generalized Procrustes analysis. *Psychometrika*, *40*(1), 33-51.
- Groves, C. (2001). Primate taxonomy. Smithsonian Institution Press, Washington, DC.
- Güleç, E. S., Sevim, A., Pehlevan, C., & Kaya, F. (2007). A new great ape from the late Miocene of Turkey. *Anthropological Science*, *115*(2), 153-158.
- Gunz, P., Mitteroecker, P., Neubauer, S., Weber, G. W., & Bookstein, F. L. (2009). Principles for the virtual reconstruction of hominin crania. *Journal of Human Evolution*, *57*(1), 48-62.
- Haile-Selassie, Y., & Melillo, S. M. (2015). Middle Pliocene hominin mandibular fourth premolars from Woranso-Mille (Central Afar, Ethiopia). *Journal of Human Evolution*, *78*, 44-59.
- Haile-Selassie, Y., Melillo, S. M., & Su, D. F. (2016). The Pliocene hominin diversity conundrum: Do more fossils mean less clarity?. *Proceedings of the National Academy of Sciences*, *113*(23), 6364-6371.
- Hara, Y., Imanishi, T., & Satta, Y. (2012). Reconstructing the demographic history of the human lineage using whole-genome sequences from human and three great apes. *Genome Biology and Evolution*, *4*(11), 1133-1145.
- Harrison, T. (2010a). Dendropithecoidea, Proconsuloidea, and Hominoidea. In L. Werdelin & W. J. Sanders (Eds.), *Cenozoic mammals of Africa* (pp. 429-469). Berkeley: University of California Press.
- Harrison, T. (2010b). Apes among the tangled branches of human origins. *Science*, *327*(5965), 532-534.
- Harrison, T., Jin, C., Zhang, Y., Wang, Y., & Zhu, M. (2014). Fossil Pongo from the Early Pleistocene Gigantopithecus fauna of Chongzuo, Guangxi, southern China. *Quaternary International*, *354*, 59-67.

- Harvati, K., Röding, C., Bosman, A. M., Karakostis, F. A., Grün, R., Stringer, C., ... & Kouloukoussa, M. (2019). Apidima Cave fossils provide earliest evidence of *Homo sapiens* in Eurasia. *Nature*, *571*(7766), 500-504.
- Harvati, K., & Weaver, T. D. (2006). Human cranial anatomy and the differential preservation of population history and climate signatures. *The Anatomical Record Part A: Discoveries in Molecular, Cellular, and Evolutionary Biology: An Official Publication of the American Association of Anatomists*, *288*(12), 1225-1233.
- Hobolth, A., Dutheil, J. Y., Hawks, J., Schierup, M. H., & Mailund, T. (2011). Incomplete lineage sorting patterns among human, chimpanzee, and orangutan suggest recent orangutan speciation and widespread selection. *Genome research*, *21*(3), 349-356.
- Ishida, H., & Pickford, M. (1997). A new Late Miocene hominoid from Kenya: *Samburupithecus kiptalami* gen. et sp. nov. *Comptes Rendus de l'Académie des Sciences-Series IIA-Earth and Planetary Science*, *325*(10), 823-829.
- Jungers, W. L. (1978). On canine reduction in early hominids. *Current Anthropology*, *19*, 155-156.
- Kay, R. F. (1982). Sexual dimorphism in Ramapithecinae. *Proceedings of the National Academy of Sciences*, *79*(2), 209-212.
- Kay, R. F., & Simons, E. L. (1983). A reassessment of the relationship between later Miocene and subsequent Hominoidea. In *New Interpretations of Ape and Human Ancestry* (pp. 577-624). Springer, Boston, MA.
- Karakostis, F. A., Hotz, G., Tournloukis, V., & Harvati, K. (2018). Evidence for precision grasping in Neandertal daily activities. *Science Advances*, *4*(9), eaat2369.
- Kelley, J., & Gao, F. (2012). Juvenile hominoid cranium from the late Miocene of southern China and hominoid diversity in Asia. *Proceedings of the National Academy of Sciences*, *109*(18), 6882-6885.
- Kelley, J., & Plavcan, J. M. (1998). A simulation test of hominoid species number at Lufeng, China: implications for the use of the coefficient of variation in paleotaxonomy. *Journal of Human Evolution*, *35*(6), 577-596.
- Kelley, J. & Xu, Q. (1991). Extreme sexual dimorphism in a Miocene hominoid. *Nature*, *352*(6331), 151-153.

- King, T. (2001). Dental microwear and diet in Eurasian Miocene catarrhines. In *Hominoid Evolution and Climatic Change in Europe, Volume 2: Phylogeny of the Neogene Hominoid Primates of Eurasia* (pp. 102-117). Cambridge University Press Cambridge.
- Köhler, M., Solà, S. M., & Alba, D. M. (2001). Eurasian hominoid evolution in the light of recent *Dryopithecus* findings. In *Hominoid evolution and climatic change in Europe, Vol. 2: phylogeny of the Neogene hominoid primates of Eurasia* (pp. 193-212). Cambridge: Cambridge University Press.
- Kordos, L., & Begun, D. R. (2002). Rudabánya: a Late Miocene subtropical swamp deposit with evidence of the origin of the African apes and humans. *Evolutionary Anthropology: Issues, News, and Reviews: Issues, News, and Reviews*, 11(2), 45-57.
- Koufos, G. D. (1993). Mandible of *Ouranopithecus macedoniensis* (Hominidae, Primates) from a new late Miocene locality of Macedonia (Greece). *American Journal of Physical Anthropology*, 91(2), 225-234.
- Koufos, G. D. (1995). The first female maxilla of the hominoid *Ouranopithecus macedoniensis* from the late Miocene of Macedonia, Greece. *Journal of Human Evolution*, 29(4), 385-399.
- Koufos, G. D. (2006). The Neogene mammal localities of Greece: faunas, chronology and biostratigraphy. *Hellenic Journal of Geosciences*, 41(1), 183-214.
- Koufos G. D. (2013). Neogene mammal biostratigraphy and chronology of Greece. In: Wang X., Flynn L.J., Fortelius M., editor. *Asian neogene mammal biostratigraphy and chronology* (pp. 595-628). New York: Columbia University Press.
- Koufos, G. D. (2016). Primates. *Geobios*, 49(1-2), 45-51.
- Koufos, G. D., & de Bonis, L. (2004). The deciduous lower dentition of *Ouranopithecus macedoniensis* (Primates, Hominoidea) from the late Miocene deposits of Macedonia, Greece. *Journal of Human Evolution*, 46(6), 699-718.
- Koufos, G. D., & de Bonis, L. (2005). The Late Miocene hominoids *Ouranopithecus* and *Graecopithecus*. Implications about their relationships and taxonomy. In *Annales de Paléontologie*, 91(3), 227-240.
- Koufos, G. D., & de Bonis, L. (2006). New material of *Ouranopithecus macedoniensis* from late Miocene of Macedonia (Greece) and study of its dental attrition. *Geobios*, 39(2), 223-243.

- Koufos, G. D., & Vasileiadou, K. (2015). Miocene/Pliocene mammal faunas of southern Balkans: implications for biostratigraphy and palaeoecology. *Palaeobiodiversity and Palaeoenvironments*, 95(3), 285-303.
- Koufos, G. D., de Bonis, L., & Kugiumtzis, D. (2016a). New material of the hominoid *Ouranopithecus macedoniensis* from the Late Miocene of the Axios Valley (Macedonia, Greece) with some remarks on its sexual dimorphism. *Folia Primatologica*, 87(2), 94-122.
- Koufos, G. D., Kostopoulos, D. S., & Vlachou, T. D. (2016b). Revision of the Nikiti 1 (NKT) fauna with description of new material. *Geobios*, 49 (1-2), 11-22.
- Kuhlwilm, M., De Manuel, M., Nater, A., Greminger, M. P., Krützen, M., & Marques-Bonet, T. (2016). Evolution and demography of the great apes. *Current Opinion in Genetics & Development*, 41, 124-129.
- Kunimatsu, Y., Nakatsukasa, M., Sawada, Y., Sakai, T., Hyodo, M., Hyodo, H., ... & Mbua, E. (2007). A new Late Miocene great ape from Kenya and its implications for the origins of African great apes and humans. *Proceedings of the National Academy of Sciences*, 104(49), 19220-19225.
- Kupczik, K., Spoor, F., Pommert, A., & Dean, C. (2005). Premolar root number variation in hominoids: genetic polymorphism vs. functional significance. *Current Trends in Dental Morphology Research. University of Lodz Press, Lodz*, 257-268.
- Lahr, M. M. (1996). The evolution of modern human diversity: A study of cranial variation (Vol. 18). Cambridge: Cambridge University Press.
- Langergraber, K. E., Prüfer, K., Rowney, C., Boesch, C., Crockford, C., Fawcett, K., Inoue, E., Inoue-Muruyama, M., Mitani, J.C., Muller, M.N. & Robbins, M. M. (2012). Generation times in wild chimpanzees and gorillas suggest earlier divergence times in great ape and human evolution. *Proceedings of the National Academy of Sciences*, 109(39), 15716-15721.
- Le Gros Clark, W.E., & Leakey, L.S.B. (1950). Diagnoses of East African Miocene Hominoidea. *Quarterly Journal of the Geological Society*, 105(1-4), 260-264.
- Locke, D. P., Hillier, L. W., Warren, W. C., Worley, K. C., Nazareth, L. V., Muzny, D. M., ... & Wilson, R. K. (2011). Comparative and demographic analysis of orang-utan genomes. *Nature*, 469(7331), 529-533.

- Lockwood, C. A., Lynch, J. M., & Kimbel, W. H. (2002). Quantifying temporal bone morphology of great apes and humans: an approach using geometric morphometrics. *Journal of Anatomy*, 201(6), 447-464.
- Lockwood, C. A., Kimbel, W. H., & Lynch, J. M. (2004). Morphometrics and hominoid phylogeny: Support for a chimpanzee–human clade and differentiation among great ape subspecies. *Proceedings of the National Academy of Sciences of the United States of America*, 101(13), 4356-4360.
- Macchiarelli, R., Bergeret-Medina, A., Marchi, D., & Wood, B. (2020). Nature and relationships of Sahelanthropus tchadensis. *Journal of Human Evolution*, 149, 102898.
- McBrearty, S., & Jablonski, N. G. (2005). First fossil chimpanzee. *Nature*, 437(7055), 105-108.
- McNulty, K. P., Begun, D. R., Kelley, J., Manthi, F. K., & Mbua, E. N. (2015). A systematic revision of Proconsul with the description of a new genus of early Miocene hominoid. *Journal of Human Evolution*, 84, 42-61.
- Meloro, C., Cáceres, N. C., Carotenuto, F., Sponchiado, J., Melo, G. L., Passaro, F., & Raia, P. (2015). Chewing on the trees: Constraints and adaptation in the evolution of the primate mandible. *Evolution*, 69(7), 1690-1700.
- Merceron, G., Blondel, C., De Bonis, L., Koufos, G. D., & Viriot, L. (2005). A new method of dental microwear analysis: application to extant primates and *Ouranopithecus macedoniensis* (Late Miocene of Greece). *Palaios*, 20(6), 551-561.
- Merceron, G., Blondel, C., Viriot, L., Koufos, G. D., & de Bonis, L. (2007). Dental microwear analysis of bovids from the Vallesian (late Miocene) of Axios Valley in Greece: reconstruction of the habitat of *Ouranopithecus macedoniensis* (Primates, Hominoidea). *Geodiversitas*, 29(3), 421-433.
- Mercier, J. (1973). Etude géologique des zones internes des Hellenides en Macedoine Centrale. *Annales Géologiques des Pays Helleniques*, 20, 1-596.
- Miller, S. F., White, J. L., & Ciochon, R. L. (2008). Assessing mandibular shape variation within Gigantopithecus using a geometric morphometric approach. *American Journal of Physical Anthropology*, 137(2), 201-212.
- Mitteroecker, P., & Gunz, P. (2009). Advances in geometric morphometrics. *Evolutionary Biology*, 36(2), 235-247.

- Mongle, C. S., Strait, D. S., & Grine, F. E. (2019). Expanded character sampling underscores phylogenetic stability of *Ardipithecus ramidus* as a basal hominin. *Journal of Human Evolution*, *131*, 28-39.
- Moore, N. C., Skinner, M. M., & Hublin, J. J. (2013). Premolar root morphology and metric variation in Pan troglodytes verus. *American Journal of Physical Anthropology*, *150*(4), 632-646.
- Moore, N. C., Hublin, J. J., & Skinner, M. M. (2015). Premolar root and canal variation in extant non-human hominoidea. *American Journal of Physical Anthropology*, *158*(2), 209-226.
- Moore, N. C., Thackeray, J. F., Hublin, J. J., & Skinner, M. M. (2016). Premolar root and canal variation in South African Plio-Pleistocene specimens attributed to *Australopithecus africanus* and *Paranthropus robustus*. *Journal of Human Evolution*, *93*, 46-62.
- Moorjani, P., Amorim, C. E. G., Arndt, P. F., & Przeworski, M. (2016). Variation in the molecular clock of primates. *Proceedings of the National Academy of Sciences*, *113*(38), 10607-10612.
- Moyà-Solà, S. M., & Köhler, M. (1993). Recent discoveries of *Dryopithecus* shed new light on evolution of great apes. *Nature*, *365*(6446), 543-545.
- Moyà-Solà, S., Köhler, M., Alba, D. M., Casanovas-Vilar, I., & Galindo, J. (2004). *Pierolapithecus catalaunicus*, a new Middle Miocene great ape from Spain. *Science*, *306*(5700), 1339-1344.
- Nengo, I., Tafforeau, P., Gilbert, C. C., Fleagle, J. G., Miller, E. R., Feibel, C., ... & Spoor, F. (2017). New infant cranium from the African Miocene sheds light on ape evolution. *Nature*, *548*(7666), 169-174.
- Nicholson, E., & Harvati, K. (2006). Quantitative analysis of human mandibular shape using three-dimensional geometric morphometrics. *American Journal of Physical Anthropology*, *131*(3), 368-383.
- Noback, M., & Harvati, K. (2015). The contribution of diet to global human cranial variation. *Journal of Human Evolution*, *80*, 34-50.
- Perelman, P., Johnson, W. E., Roos, C., Seuáñez, H. N., Horvath, J. E., Moreira, M. A., Perelman, P., Johnson, W.E., Roos, C., Seuáñez, H.N., Horvath, J.E., Moreira, M.A., Kessing, B., Pontius, J., Roelke, M., Rumpler, Y. & Schneider, M. P. C. (2011). A molecular phylogeny of living primates. *PLoS Genet*, *7*(3), e1001342.

- Perez, S. I., Kłaczko, J., Rocatti, G., & Dos Reis, S. F. (2011). Patterns of cranial shape diversification during the phylogenetic branching process of New World monkeys (Primates: Platyrrhini). *Journal of Evolutionary Biology*, 24(8), 1826-1835.
- Pickford, M. (1985). A new look at Kenyapithecus based on recent discoveries in western Kenya. *Journal of Human Evolution*, 14(2), 113-143.
- Pilbeam, D. (1982a). Hominoid evolution and hominid origins. In *Recent Advances in the Evolution of the Primates* (pp. 43-61).
- Pilbeam, D. (1982b). New hominoid skull material from the Miocene of Pakistan. *Nature*, 295(5846), 232-234.
- Pilbeam, D. (1996). Genetic and morphological records of the Hominoidea and hominid origins: a synthesis. *Molecular Phylogenetics and Evolution*, 5(1), 155-168.
- Pilbeam, D. 2002. Perspectives on the Miocene Hominoidea. In: Hartwig WC, editor. The primate fossil record. Cambridge: Cambridge University Press. p 301-310.
- Pilgrim, G. E. (1915). New Siwalik primates and their bearing on the question of the evolution of man and the Anthropoidea. *Rec. Geol Surv. India*, 45, plates-I.
- Prüfer, K., Munch, K., Hellmann, I., Akagi, K., Miller, J. R., Walenz, B., Koren, S., Sutton, G., Kodira, C., Winer, R & Knight, J. R. (2012). The bonobo genome compared with the chimpanzee and human genomes. *Nature*, 486(7404), 527-531.
- Raveloson, H., Le Minor, J. M., Rumpler, Y., & Schmittbuhl, M. (2005). Shape of the lateral mandibular outline in Lemuridae: a quantitative analysis of variability using elliptical Fourier analysis. *Folia Primatologica*, 76(5), 245-261.
- Ravosa, M. J., & Hylander, W. L. (1994). Function and fusion of the mandibular symphysis in primates. In *Anthropoid origins* (pp. 447-468). Springer, Boston, MA.
- Reyes-Centeno, H., Ghirotto, S., & Harvati, K. (2017). Genomic validation of the differential preservation of population history in the human cranium. *American Journal of Physical Anthropology*, 162, 170-179.
- Robinson, C. (2003). Extant hominoid and Australopith mandibular morphology; assessing alpha taxonomy and phylogeny in hominoids using mandibular characters. Ph.D. Dissertation, New York University.
- Robinson, C. (2012). Geometric morphometric analysis of mandibular shape diversity in Pan. *Journal of Human Evolution*, 63(1), 191-204.

- Rohlf, F. J. (1999). Shape statistics: Procrustes superimpositions and tangent spaces. *Journal of classification*, 16(2), 197-223.
- Rohlf, F. J., & Marcus, L. F. (1993). A revolution morphometrics. *Trends in Ecology & Evolution*, 8(4), 129-132.
- Rohlf, F. J., & Slice, D. (1990). Extensions of the Procrustes method for the optimal superimposition of landmarks. *Systematic Biology*, 39(1), 40-59.
- Ruvolo, M. (1997). Molecular phylogeny of the hominoids: inferences from multiple independent DNA sequence data sets. *Molecular Biology and Evolution*, 14(3), 248-265.
- Scally, A., Dutheil, J. Y., Hillier, L. W., Jordan, G. E., Goodhead, I., Herrero, J., Scally, A., Dutheil, J.Y., Hillier, L.W., Jordan, G.E., Goodhead, I., Herrero, J., Hobolth, A., Lappalainen, T., Mailund, T., Marques-Bonet, T. & McCarthy, S. (2012). Insights into hominid evolution from the gorilla genome sequence. *Nature*, 483(7388), 169-175
- Schaller, G.B. (1963). *The Mountain Gorilla: Ecology & Behavior*. University of Chicago Press, Chicago.
- Scherf, H. (2013). Computed tomography in paleoanthropology—an overview. *Archaeological and Anthropological Sciences*, 5(3), 205-214.
- Schmittbuhl, M., Rieger, J., Le Minor, J. M., Schaaf, A., & Guy, F. (2007). Variations of the mandibular shape in extant hominoids: generic, specific, and subspecific quantification using elliptical Fourier analysis in lateral view. *American Journal of Physical Anthropology*, 132(1), 119-131.
- Schrager, C. G., & Voloch, C. M. (2013). The precision of the hominid timescale estimated by relaxed clock methods. *Journal of Evolutionary Biology*, 26(4), 746-755.
- Schrein, C. M. (2006). Metric variation and sexual dimorphism in the dentition of *Ouranopithecus macedoniensis*. *Journal of Human Evolution*, 50(4), 460-468.
- Scott, J. E., Schrein, C. M., & Kelley, J. (2009). Beyond Gorilla and Pongo: alternative models for evaluating variation and sexual dimorphism in fossil hominoid samples. *American Journal of Physical Anthropology*, 140(2), 253-264.
- Sen, S., Koufos, G. D., Kondopoulou, D., & de Bonis, L. (2000). Magnetostratigraphy of the Late Miocene continental deposits of the lower Axios valley, Macedonia, Greece. *Geological Society Greece Special Publications*, 9, 197-206.

- Senck, S., Bookstein, F. L., Benazzi, S., Kastner, J., & Weber, G. W. (2015). Virtual reconstruction of modern and fossil hominoid crania: consequences of reference sample choice. *The Anatomical Record*, 298(5), 827-841.
- Senut, B., Pickford, M., Gommery, D., Mein, P., Cheboi, K., & Coppens, Y. (2001). First hominid from the Miocene (Lukeino formation, Kenya). *Comptes Rendus de l'Académie des Sciences-Series IIA-Earth and Planetary Science*, 332(2), 137-144.
- Simons, E. L., & Pilbeam, D. R. (1965). Preliminary revision of the Dryopithecinae (pongidae, anthropoidea). *Folia Primatologica*, 3, 81-152.
- Singh, N. (2014). Ontogenetic study of allometric variation in Homo and Pan mandibles. *The Anatomical Record*, 297(2), 261-272.
- Smith, R. J. (2005). Species recognition in paleoanthropology: implications of small sample sizes. *Interpreting the past: essays on human, primate, and mammal evolution in honor of David Pilbeam* (pp. 207-219). Boston: Brill Academic Publishers.
- Stevens, N. J., Seiffert, E. R., O'Connor, P. M., Roberts, E. M., Schmitz, M. D., Krause, C., Stevens, N.J., Seiffert, E.R., O'Connor, P.M., Roberts, E.M., Schmitz, M.D., Krause, C., Gorscak, E., Ngasala, S., Hieronymus, T.L. & Temu, J. (2013). Palaeontological evidence for an Oligocene divergence between Old World monkeys and apes. *Nature*, 497(7451), 611-614.
- Suwa, G., Kono, R. T., Katoh, S., Asfaw, B., & Beyene, Y. (2007). A new species of great ape from the late Miocene epoch in Ethiopia. *Nature*, 448 (7156), 921-924.
- Syrides, G. (1990). Lithostratigraphic, biostratigraphic and palaeogeographic study of the neogene-quaternary sedimentary deposits of Chalkidiki Peninsula, Macedonia, Greece. *Scientific Annals of the School of Geology, University of Thessaloniki*, 1(11), 1-243.
- Taylor, A. B. (2006). Size and shape dimorphism in great ape mandibles and implications for fossil species recognition. *American Journal of Physical Anthropology*, 129(1), 82-98.
- Taylor, A. B., & Groves, C. P. (2003). Patterns of mandibular variation in Pan and Gorilla and implications for African ape taxonomy. *Journal of Human Evolution*, 44(5), 529-561.
- Tekkaya, I. (1974). A new species of Tortonian anthropoid (Primates, Mammalia) from Anatolia. *Maden Tetkik ve Arama Dergisi*, 83(83), 1-21.

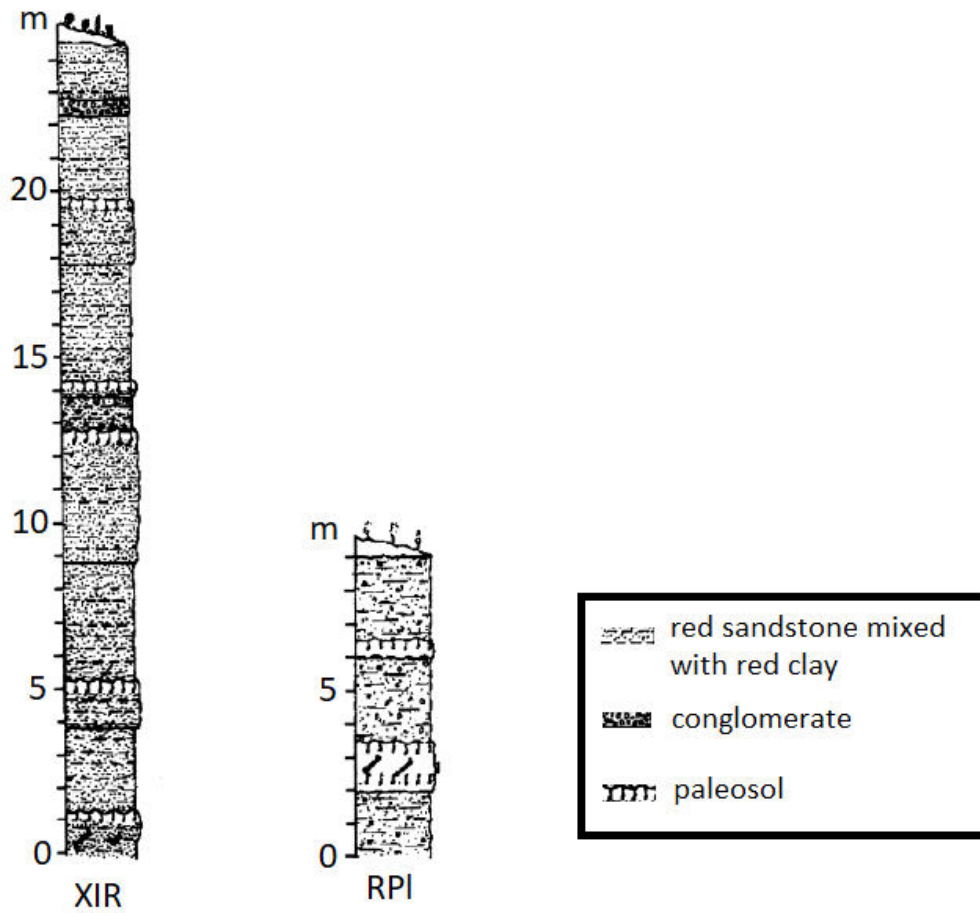
- Ungar, P.S. (1996). Dental microwear of European Miocene catarrhines: evidence for diets and tooth use. *Journal of Human Evolution*, 31(4), 335-366.
- Venn, O., Turner, I., Mathieson, I., de Groot, N., Bontrop, R., & McVean, G. (2014). Strong male bias drives germline mutation in chimpanzees. *Science*, 344(6189), 1272-1275.
- von Cramon-Taubadel, N., Frazier, B. C., & Lahr, M. M. (2007). The problem of assessing landmark error in geometric morphometrics: theory, methods, and modifications. *American Journal of Physical Anthropology*, 134(1), 24-35.
- von Freyberg, B. (1951). Die Pikermi-fauna von tour la Reine (Attika). *Ann. Geol. Pays Helleniques (Ser. 1)*, 3, 7-10.
- von Koenigswald, G. H. R. (1952). *Gigantopithecus blacki* von Koenigswald, a giant fossil hominoid from the Pleistocene of Southern China. *Anthropol. Papers Am. Mus. Nat. Hist.*, 43(4), 1-325.
- von Koenigswald, G. V. (1972). Ein unterkiefer eines fossilen hominoiden aus dem Unterpliozan Greichenlands. *Proc. Kon. Nederlands Akad. Wet.(Ser. B.)*, 75, 386-394.
- Weber, G. W. (2015). Virtual anthropology. *American Journal of Physical Anthropology*, 156, 22-42.
- Weber, G. W., & Bookstein, F. L. (2011). Virtual anthropology: a guide to a new interdisciplinary field. Springer Verlag.
- Weber, G. W., Schäfer, K., Prossinger, H., Gunz, P., Mitteröcker, P., & Seidler, H. (2001). Virtual anthropology: the digital evolution in anthropological sciences. *Journal of Physiological Anthropology and Applied Human Science*, 20(2), 69-80.
- White, T. D., Asfaw, B., Beyene, Y., Haile-Selassie, Y., Lovejoy, C. O., Suwa, G., & WoldeGabriel, G. (2009). *Ardipithecus ramidus* and the paleobiology of early hominids. *Science*, 326(5949), 64-86.
- White, T. D., Suwa, G., & Asfaw, B. (1994). *Australopithecus ramidus*, a new species of early hominid from Aramis, Ethiopia. *Nature*, 371(6495), 306-312.
- Wilkinson, R. D., Steiper, M. E., Soligo, C., Martin, R. D., Yang, Z., & Tavaré, S. (2011). Dating primate divergences through an integrated analysis of palaeontological and molecular data. *Systematic Biology*, 60(1), 16-31.
- Woo, J. (1962). The mandibles and dentitions of *Gigantopithecus*. *Paleontologica Sinica*, 11, 65-94.

- Wood, B., Abbott, S. A., & Uytterschaut, H. (1988). Analysis of the dental morphology of Pliocene hominids IV. Mandibular post-canine root morphology. *Journal of Anatomy*, 156, 107-139.
- Xu, Q. H., Lu, Q. W., Pan, Y. R., Qi, G. Q., Zhang, X. Y., & Zheng, L. (1978). The fossil mandible of *Ramapithecus lufengensis*. *Kexue Tongbao*, 23(9), 554-556.
- Zelditch, M. L., Swiderski, D. L., & Sheets, H. D. (2012). Geometric morphometrics for biologists: a primer. Academic Press.
- Zhang, Y., & Harrison, T. (2017). *Gigantopithecus blacki*: a giant ape from the Pleistocene of Asia revisited. *American Journal of Physical Anthropology*, 162, 153-177.

APPENDICES

Appendix I – Stratigraphic columns showing the lithologies of the XIR and RPI localities.

Modified from Sen et al., 2000.




Appendix II – External samples permits

Permits for external specimens used in this dissertation were obtained before any data collection. For each study, information is given in the "Acknowledgments" section. Below, a summary table with the institution/type of agreement is provided.

External sample	Type	Institution	Type of agreement
<i>H. laietanus</i>	Surface scan	University of Toronto	Written (e-mail)
<i>S. tchadensis</i>	3D landmarks	University of Poitiers	Written (e-mail)
Great apes	Surface and CT scans	Senckenberg Museum of Natural History, Frankfurt	Written
Great apes	3D landmarks/surface scans	State Museum of Natural History, Stuttgart	Written (e-mail)
Great apes	Surface scans	Museum of Natural History, Berlin	Written
<i>Homo sapiens</i>	CT scans	University of Copenhagen	Written (e-mail)
Great apes	Surface scans	Smithsonian National Museum of Natural History in Washington, D.C.	Written (e-mail)
<i>Australopithecus africanus</i>	Surface scan	University of Vienna	Written (e-mail)

DECLARATION

I hereby declare that I have conducted the present work independently and without the use of any aids other than those indicated. All passages that have been adopted verbatim or mutatis mutandis from published or unpublished resources are appropriately referenced as such. I also declare that I am the sole author of this dissertation. This work has not yet been submitted in the same, in a similar form, or in excerpts in another examination, nor has it been part of any other PhD thesis.



Tübingen, 07.06.2021

Melania Ioannidou

